

Identification-aware Markov Chain Monte Carlo*

Toru Kitagawa¹ and Yizhou Kuang²

¹Brown University

²University of Manchester

This Version: December 18th, 2025

Abstract

Leaving posterior sensitivity concerns aside, non-identifiability of the parameters does not raise a difficulty for Bayesian inference as far as the posterior is proper, but multi-modality or flat regions of the posterior induced by the lack of identification leaves a challenge for modern Bayesian computation. Sampling methods often struggle with slow or non-convergence when dealing with multiple modes or flat regions of the target distributions. This paper develops a novel Markov chain Monte Carlo (MCMC) approach for non-identified models, leveraging the knowledge of observationally equivalent sets of parameters, and highlights an important role that identification plays in modern Bayesian analysis. We show that our identification-aware proposal eliminates mode entrapment, achieving a convergence rate uniformly bounded away from zero, in sharp contrast to the exponentially decaying rates characterizing standard Random Walk Metropolis and Hamiltonian Monte Carlo. Simulation studies show its superior performance compared to other popular computational methods including Hamiltonian Monte Carlo and sequential Monte Carlo. We also demonstrate that our method uncovers non-trivial modes in the target distribution in a structural vector moving-average (SVMA) application.

KEYWORDS: Markov chain Monte Carlo, Bayesian inference, identified set, observational equivalence

*We would like to thank Donald Andrews, Ben Deaner, Raffaella Giacomini, Frank Kleibergen, Yuan Liao, José Luis Montiel Olea, Kristoffer Nimark, Andriy Norets, Alexei Onatski, Mikkel Plagborg-Møller, Anna Simoni, Tomasz Woźniak, and Andrei Zeleneev for useful discussions. We also thank seminar participants at the University of Cambridge and conference participants at CFE-CMStatistics, Aarhus Econometrics Workshop, and SETA for their valuable feedback. All remaining errors are our own.

1 Introduction

Many Bayesian economists and statisticians are inclined to adopt [Lindley \(1972\)](#)’s assertion that “unidentifiability causes no real difficulty in the Bayesian approach,” a view further supported by [Gelman \(2014\)](#), who argues in his blog that “the concept of identification is less important in the Bayesian world than elsewhere.” In theory, if a well-defined prior and likelihood yield a proper posterior, Bayesian inference can proceed without fundamental obstruction. However, in practice, modern applications often involve structural models with large parameter spaces, incomplete data, or weak identifying assumptions, leading to multi-modal or flat posterior regions. Applied economists often proceed under the assumption that a chosen sampler, such as Metropolis–Hastings (MH), Hamiltonian Monte Carlo (HMC) or sequential Monte Carlo (SMC), will eventually reveal the relevant features of the posterior, as is guaranteed asymptotically under certain strong regularity conditions. However, real data sets are finite, computational budgets are limited, and posteriors are often analytically intractable, so the conditions required for fast convergence are difficult to verify and frequently fail. As a result, even a “proper” posterior can pose significant practical challenges for effective sampling.

Despite their widespread use in econometrics, popular algorithms such as MH, HMC, and SMC¹ often struggle to explore complex posterior surfaces thoroughly. These methods can fail to traverse low-density regions separating multiple modes, can suffer from slow mixing in high-dimensional spaces, provide little guidance in flat or weakly identified regions. Several strategies have been proposed to alleviate these issues, including *tempering* methods that flatten the target distribution to facilitate movement between modes, and *mode-jumping* techniques that rely on either prior knowledge of mode locations or extensive presampling. Both approaches come with substantial costs: tempering often requires careful tuning of intermediate distributions and can remain computationally expensive in large-scale problems, while mode-jumping typically depends on substantial a priori information. Moreover, the challenges of multi-modality, high dimensionality, and flat or ill-conditioned likelihood regions compound one another, making it even harder to design robust, general-purpose samplers. As a result, determining how best to navigate unknown distributions that combine these features remains an open and active area of research.

This paper argues that identification analysis is crucial even for Bayesians, and shows that explicit knowledge of observationally equivalent parameter values can be used to overcome the

¹Although SMC is not technically an MCMC method, the implementation by [Herbst and Schorfheide \(2014\)](#) applies a local MCMC step to each particle, integrating MCMC techniques into the SMC framework.

challenges of sampling from complex multi-modal posteriors. We propose a new “identification-aware” MCMC approach that exploits the knowledge or computability of the set of observationally equivalent parameters and can attain faster convergence than widely used MCMC algorithms. The key innovation is a *teleportation* step: the chain moves directly to an observationally equivalent point in the state space, bypassing low-probability regions or distant valleys that incremental updates struggle to cross. By construction, this teleportation step preserves the target posterior while ensuring efficient exploration of flat regions, multiple modes, or disconnected neighborhoods. Our approach treats teleportation as a modular component that can be integrated into any Markov chain-based method, including MH, HMC, or the mutation steps in SMC. Our method combines teleportation with a standard MCMC-type transition (e.g., MH or HMC updates) to refine the position locally. This scheme leverages both directed global jumps and fine-tuned local adjustments, allowing the algorithm to balance global exploration with local optimization and to sample effectively from high-dimensional, multi-modal posteriors without requiring an exponentially increasing number of evaluations as dimension grows. The specific implementation depends on the structure of the observationally equivalent set, which may be finite, of varying cardinality, or a low-dimensional manifold. We provide theoretical guarantees that, in such settings, our identification-aware sampler improves convergence rates relative to standard MCMC approaches.

Simulation studies validate the superior performance of our proposal against popular computational methods. In multimodal mixture Gaussian settings, our algorithm successfully teleports across isolated modes where standard Random Walk Metropolis (RWM) consistently becomes trapped. Similarly, in set-identified scenarios, it achieves a more diffuse and representative exploration of the parameter space compared to SMC, which can exhibit clustering around initialization points. We further demonstrate the method’s practical utility in Bayesian estimation for SVMA models as considered in [Plagborg-Møller \(2019\)](#). As shown in [Lippi and Reichlin \(1994\)](#), SVMA models are not globally identified, with no closed-form expression for the impulse response identified-set. It makes the standard MCMC difficult to capture all the modes of the posterior distribution. In the complex environment with the number of parameters as many as 153, we demonstrate implementation of identification aware HMC algorithms and show that they can recover the dominant marginal modes found by the standard HMC, but also uncovers non-trivial high-density regions that remain elusive to the standard HMC. This suggests that incorporating teleportation step exploiting analytical characterization of identification of the model can help characterize the posterior landscape and provide a more robust and reliable numerical approximation for it.

Related Literature: There is a well-established literature in economics applying MCMC methods for Bayesian estimation and inference, including Chib and Greenberg (1996), An and Schorfheide (2007), Flury and Shephard (2011), Herbst and Schorfheide (2014), Kline and Tamer (2016), Plagborg-Møller (2019), Meager (2022), and Müller and Norets (2023). Beyond the Bayesian framework, these methods are also employed in frequentist settings. For example, Chernozhukov and Hong (2003) uses standard MCMC to obtain minimizers of criterion functions for point-identified models, and Chen et al. (2018) applies SMC to construct confidence sets for identified sets defined by either likelihood-based conditions or moment equalities and inequalities, following approaches similar to Herbst and Schorfheide (2014) and Durham and Geweke (2014).

Most of the literature mentioned above treats these computational methods primarily as tools for estimation and inference rather than focusing on their theoretical properties such as convergence rates, central limit theorems (CLT), or laws of large numbers (LLN). One notable exception is Herbst and Schorfheide (2014), which provides some formal results, demonstrating that LLN and CLT can hold under certain conditions in their proposed SMC.

Outside of economics, a substantial literature has established theoretical guarantees for MCMC algorithms, but these results often rest on restrictive conditions that rarely hold in the complex settings typical of economic models. For example, classical mixing and convergence analyses for RWM (e.g. Mengerson and Tweedie (1996); Roberts and Tweedie (1996); Roberts and Rosenthal (2004)) typically assume log-concave or strongly unimodal targets, compact support, and uniform minorization, conditions that do not capture high-dimensional, multi-modal, or weakly identified likelihoods. Although a few exceptions can tackle more complicated cases, including multimodality (e.g., Guan and Krone (2007); Mangoubi et al. (2018)), the general applicability of these results to empirical economic problems remains unknown.

Similar issues arise in the theoretical treatment of more sophisticated methods, such as SMC and HMC. While several works (Chopin, 2004; Del Moral et al., 2012; Huggins and Roy, 2015; Durmus et al., 2017, 2020; Mangoubi and Smith, 2021) offer insights into convergence rates, central limit theorems, and stability, they too rely on assumptions such as smoothness (e.g. Lipschitz-continuous gradients or bounded higher-order derivatives) and well-behaved high-dimensional scaling (e.g. controlled deterioration of error rates with dimension), assumptions that often fail in the heavily parameterized, data-driven models typical in econometrics.

For advanced algorithms explicitly designed to tackle multimodality, such as tempering-based samplers (Woodard et al., 2009) and mode-jumping methods (Zhou, 2011; Pompe et al., 2020), the

theoretical underpinnings are even sparser. [Woodard et al. \(2009\)](#) demonstrates that tempering can still mix slowly in certain multi-modal regimes. Meanwhile, mode-jumping approaches often rely on heuristics or prior knowledge, or on computationally expensive approximations of mode locations, providing little theoretical guarantee beyond basic ergodicity. As a result, despite significant progress in algorithm development and analysis, sampling efficiently and reliably from complex, unknown distributions, especially those with multiple modes, high dimensionality, or flat identified sets, remains a major open challenge.

To the best of our knowledge, only a handful of studies exploit identification information directly during sampling. For Bayesian estimation of finite mixture models, [Frühwirth-Schnatter \(2006\)](#) and [Geweke \(2007\)](#) handle multimodality of the posterior by permuting or augmenting the observationally equivalent parameter values in a standard MCMC run. Our identification-aware MCMC proposal includes their augmentation trick as a special case, while ours can cover more general cases in which cardinality of the observationally equivalent parameter values is infinite or varies over the parameter space.

Bayesian estimation for non-identified models has been studied extensively in the literature of structural vector autoregressions (SVAR). [Uhlig \(2005\)](#) and [Rubio-Ramirez et al. \(2010\)](#) propose a Gibbs sampling algorithm with uniform draws of a non-identified orthonormal matrix. The step of drawing an orthonormal matrix can be viewed as a certain teleportation step in our framework. In the SVAR context, our proposal of identification-aware MCMC can accommodate a non-uniform prior for the orthonormal matrix implied by a prior on the structural parameters along the proposal of [Baumeister and Hamilton \(2015\)](#). Our analytical results on fast convergence of the identification-aware MCMC to the target posterior highlight a benefit of having a step of drawing the orthonormal matrix instead of performing standard MCMC procedures directly on the structural parameter space. For locally-identified SVAR, [Bacchicocchi and Kitagawa \(2025\)](#) considers a transportation step in their Bayesian approach, while they do not investigate the convergence rate for approximating the posterior distribution.

The identification-aware proposal is designed to improve sampling efficiency in Bayesian inference, and should be viewed as complementary to the Bayesian sensitivity analysis to set-identified models. Relying on computability of the mapping between reduced-form and structural parameters, [Kline and Tamer \(2016\)](#) and [Giacomini and Kitagawa \(2021\)](#) study how to draw Bayesian inference for the identified set. [Chen et al. \(2018\)](#) develops criterion-based quasi-Bayesian procedures for frequentist-valid inference in partially identified models. Their implementation

builds on MCMC draws from the quasi-posterior that can have multiple modes or flat regions due to set-identification. Our identification-aware MCMC can contribute to their inference approach by better approximating the flat quasi-posterior. The method discussed in this paper also shares key structural similarities with Algorithm 1 in [Kuang \(2025\)](#), while its focus is on Bayesian robustness and inference on the identified set.

Roadmap The rest of the paper is organized as follows: In Section 2, we review standard MCMC methods (including MH and HMC) and SMC. We then introduce our algorithm and compare it against RWM and HMC in both multimodal and set-identified settings. Section 3 presents two main simulation exercises comparing the sampling efficiency of our method with standard RWM, HMC and SMC. Section 4 presents Bayesian analyses of an MA(1) process, and a 3-variable, 17-lag structural vector moving average model (SVMA), showing that our method delivers superior performance in large models.

2 Markov Chain Monte Carlo and Mixing Time

2.1 MCMC Methods

Markov chain Monte Carlo methods are a class of algorithms used to sample from a target probability distribution π over a state space Ω , which can be either finite or general (e.g., \mathbb{R}^d). The goal of MCMC is to construct a Markov chain with a stationary distribution equal to π , ensuring that, as the chain evolves, its samples approximate the desired target distribution.

When Ω is finite, the Markov chain can be described by a transition matrix $P(x, y)$, where $P(x, y)$ represents the probability of transitioning from state x to state y conditional on that the current state is at x . In the case of a general state space, Ω is often a subset of \mathbb{R}^d , and the Markov chain is defined through a transition kernel $P(x, \cdot)$, which specifies a conditional probability measure given the current state x . Popular MCMC algorithms, such as MH and HMC, operate as Markov chains with transition kernels constructed to preserve the target distribution and satisfy the necessary conditions for convergence.

Metropolis–Hastings. In MH, one proposes candidate states from a distribution $q(x'|x)$ and either accepts or rejects these proposals based on an acceptance probability that ensures detailed

balance. A simple version of the MH procedure is shown in Algorithm 1. MH is appealing for its generality: any proposal distribution $q(\theta'|\theta)$ that adequately explores the parameter space produces a Markov chain with $\pi(\theta)$ as its stationary distribution. Common proposals include δ -ball random walks, Gaussian random walks, and adaptive schemes that adjust proposal scales to target appropriate acceptance rates. The efficiency of MH depends on balancing exploration against excessive rejections, with optimal asymptotic acceptance rates around 0.234 (Gelman et al., 1997).

Algorithm 1 (MH). 1. *Given target distribution $\pi(\theta)$, proposal distribution $q(\theta'|\theta)$, set initial state*

θ_0 and number of iterations N .

2. *For $t = 1$ to N ,*

(a) Sample $\theta' \sim q(\cdot|\theta_{t-1})$.

(b) Compute the acceptance probability:

$$\alpha := \min \left\{ 1, \frac{\pi(\theta')q(\theta_{t-1}|\theta')}{\pi(\theta_{t-1})q(\theta'|\theta_{t-1})} \right\}.$$

(c) Accept $\theta_t = \theta'$ with probability α , otherwise, $\theta_t = \theta_{t-1}$.

3. *Return $\{\theta_t\}_{t=1}^N$.*

An important special case of the MH framework is the Gibbs sampler, which samples directly from conditional distributions when available, thereby avoiding acceptance steps. Gibbs can be efficient in hierarchical or conjugate settings but may be infeasible when conditionals lack convenient closed forms.

Hamiltonian Monte Carlo. Despite its generality, MH often suffers from slow random-walk behavior in high-dimensional spaces. HMC addresses this limitation by incorporating gradient information to make longer, directed moves through the parameter space. By introducing auxiliary momentum variables and simulating Hamiltonian dynamics, HMC proposals reduce random walks and achieve better mixing, particularly for correlated or high-dimensional targets (Neal, 2011). A standard version of HMC is given in Algorithm 2.

Algorithm 2 (HMC). 1. *Input: target density $\pi(\theta) \propto e^{-U(\theta)}$, step size ϵ , number of leapfrog steps L ,*

initial state θ_0 , number of iterations N .

2. For $t = 1, \dots, N$:

(a) Sample momentum $p^{(0)} \sim \mathcal{N}(0, I)$.

(b) Initialize $(\theta^{(0)}, p^{(0)}) = (\theta_{t-1}, p^{(0)})$.

(c) Perform L leapfrog steps:

i. Half-step momentum update:

$$p^{(0)} \leftarrow p^{(0)} - \frac{\epsilon}{2} \nabla_{\theta} U(\theta^{(0)}).$$

ii. For $i = 1, \dots, L$:

A. Position update:

$$\theta^{(i)} = \theta^{(i-1)} + \epsilon p^{(i-1)}.$$

B. If $i < L$, full momentum update:

$$p^{(i)} = p^{(i-1)} - \epsilon \nabla_{\theta} U(\theta^{(i)}).$$

iii. Final half-step momentum update:

$$p^{(L)} = p^{(L-1)} - \frac{\epsilon}{2} \nabla_{\theta} U(\theta^{(L)}).$$

(d) Denote the proposal as $(\theta^*, p^*) = (\theta^{(L)}, p^{(L)})$, compute the acceptance probability:

$$\alpha = \min \left\{ 1, \exp \left(-U(\theta^*) - \frac{1}{2} \|p^*\|^2 + U(\theta_{t-1}) + \frac{1}{2} \|p^{(0)}\|^2 \right) \right\}.$$

Set $\theta_t = \theta^*$ with probability α , and θ_{t-1} otherwise.

3. Return $\{\theta_t\}_{t=1}^N$.

In practice, performance depends on the choice of step size ϵ and the number of leapfrog steps L , often tuned adaptively or with algorithms such as NUTS (Hoffman et al., 2014). Well-tuned HMC typically achieves acceptance rates of 60–80% (Betancourt, 2017), offering substantial efficiency gains relative to random-walk MH.

Although both MH and HMC are powerful, they remain local in nature, relying on proposals that stay reasonably close to the current state. This can be problematic in multi-modal settings

where local moves risk becoming trapped in a single mode. SMC methods, discussed in Appendix B.1, take a more global approach using populations of particles to explore the state space in parallel, thereby providing a complementary alternative to standard MCMC.

2.2 Identification-aware MCMC

Denote the target distribution $\pi(\theta)$, such as a posterior distribution of the form $p(\theta|Y)$ in Bayesian analysis. We define an associated partition $K : \Omega \rightarrow 2^\Omega$ which maps each parameter $\theta \in \Omega$ to the set of parameters θ' that are observationally equivalent to θ . Specifically, this equivalence relationship is characterized by $L(\cdot|\theta) = L(\cdot|\theta')$ for all $\theta' \in K(\theta)$ and possible data outcomes y , where $L(\cdot|\theta)$ denotes the likelihood function of the observed data given θ . In the case of a mixture of two Gaussian distributions, with parameters $\theta = (p, (1-p), \mu_1, \mu_2, \sigma_1^2, \sigma_2^2)$, each equivalence class $K(\theta)$ captures the inherent label-switching problem: swapping the component labels does not affect the likelihood. Thus, for this mixture Gaussian case, each $K(\theta)$ comprises exactly two elements: $(p, (1-p), \mu_1, \mu_2, \sigma_1^2, \sigma_2^2)$ and $((1-p), p, \mu_2, \mu_1, \sigma_2^2, \sigma_1^2)$. However, unlike the setting in [Geweke \(2007\)](#), our $K(\theta)$ is not necessarily a finite set, nor does it need to have a fixed number of elements for all θ . This flexibility allows for more general equivalence relationships.

When the parameters θ are not identified, the shape of the posterior for θ over $K(\theta)$ is fully determined by the prior for θ along $K(\theta)$ since the likelihood is flat on $K(\theta)$. A uniform prior on $K(\theta)$ can be a benchmark analysis if the researcher wishes to summarize the shape of the likelihood or put an unbiased belief for θ . An alternative scenario is to specify a non-uniform prior on $K(\theta)$ to reflect an available prior knowledge for θ . Our identification-aware MCMC algorithms can accommodate either cases so that it is useful no matter whether the purpose of posterior analysis is to perform subjective Bayesian inference or summarize the shape of likelihood.

The *teleport kernel* is the posterior conditional law restricted to the observationally equivalent set $K(\theta)$:

$$T(\theta, A) = \frac{\int_{A \cap K(\theta)} \pi(u) \nu(du)}{\int_{K(\theta)} \pi(u) \nu(du)}, \quad 0 < \int_{K(\theta)} \pi(u) \nu(du) < \infty, \pi - a.e. \quad (1)$$

The reference measure ν is the natural one for the geometry of $K(\theta)$: counting measure if $K(\theta)$ is finite, Lebesgue measure if it has full dimension, and r -dimensional Hausdorff measure if it is an r -dimensional manifold. We can interpret the posterior π restricted to $K(\theta)$ as the conditional prior over observationally equivalent parameters given they belongs to identified set $K(\theta)$. Since the likelihood $L(y|\cdot)$ is constant on $K(\theta)$, it is uniform only if this conditional prior density is constant

along $K(\theta)$. When π is constant on each $K(\theta)$, $T(\theta, \cdot)$ reduces to:

$$T(\theta, A) = \frac{\nu(A \cap K(\theta))}{\nu(K(\theta))}, \quad 0 < \nu(K(\theta)) < \infty, \pi - a.e. \quad (2)$$

Note that for the teleport kernel to preserve the target distribution, $K(\theta)$ in (1) does not strictly need to be the identified set for θ and suffices to be any subset of the identified set of θ . That is, the teleportation kernel T need not be supported on the full observationally equivalent set $K(\theta)$ and one can restrict the teleport move to a known or computationally convenient subset of the identified set.

All invariance and reversibility statements given below hold for any target π . For quantitative mixing bounds we will later impose a mild regularity condition on the restriction of π to each $K(\theta)$. See Assumption 2(iv) in Section 2.3.2.

To motivate and illustrate our proposal, consider the following toy example with 4 states.

Example 1. Consider two parameters θ_1 and θ_2 , each taking binary values 0 and 1. The parameters have the following joint posterior distribution (we obscure its dependence on data Y for simplicity, and write it as $p(\theta_1, \theta_2)$):

$$p(\theta_1, \theta_2) = \begin{cases} p_{00}, & (\theta_1, \theta_2) = (0, 0), \\ p_{01}, & (\theta_1, \theta_2) = (0, 1), \\ p_{10}, & (\theta_1, \theta_2) = (1, 0), \\ p_{11}, & (\theta_1, \theta_2) = (1, 1). \end{cases}$$

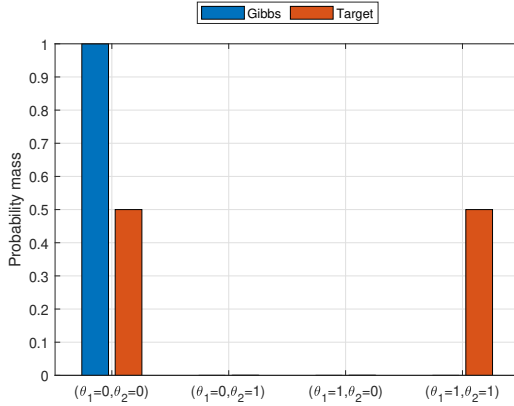
In this setup, assume the target distribution depends only on θ_1 and θ_2 through their difference $\theta_1 - \theta_2$. Therefore, $(\theta_1, \theta_2) = (1, 1)$ is observationally equivalent to $(\theta_1, \theta_2) = (0, 0)$, that is, under uniform prior,

$$p_{00} = p_{11} \quad \text{for any realization of data.}$$

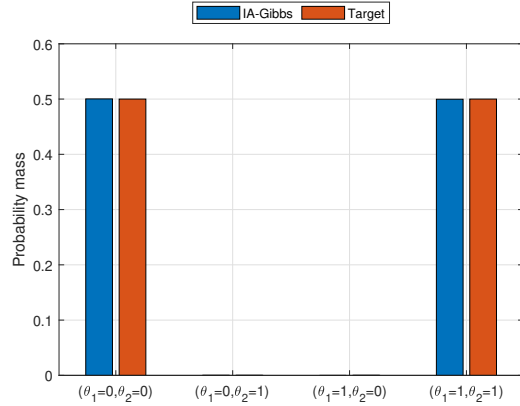
We construct a Markov transition matrix P based on Gibbs sampler over the four possible states $\{(0, 0), (0, 1), (1, 0), (1, 1)\}$, listed in that order. Starting from $(0, 0)$, we run 100,000 Gibbs iterations under the setting $p_{11} = p_{00} = 0.49999$ and $p_{10} = p_{01} = 0.00001$ to simulate an extremely bimodal scenario.² As shown in Figure 1a, the sampler is stuck at $(0, 0)$ for the entire run and never visits $(1, 1)$.³

²The equality $p_{11} = p_{00}$ follows from recognized observational equivalences and is assumed to be known to the researcher. In contrast, the choice $p_{10} = p_{01}$ is introduced purely for computational simplicity and does not stem from any observational equivalence. Breaking this equality will not affect our results.

³Extending the chain length to 1,000,000 increases the ratio of visits to $(1, 1)$ to 0.53, but it still fails to



(a) Gibbs-sampled distribution.



(b) identification-aware Gibbs.

Figure 1: Comparison of Gibbs vs. identification-aware Gibbs, 100,000 samples.

A natural remedy is to make the Gibbs sampler *identification-aware*. Before each round of update, we first teleport to an observationally equivalent point, chosen uniformly from $K(\theta)$. This ensures that, in Example 1, the chain moves freely between $(0, 0)$ and $(1, 1)$ according to their posterior probabilities, rather than remaining stuck in whichever state it started.

The same idea extends beyond Gibbs to any MCMC method. Let $P(\theta, \cdot)$ denote the transition kernel of a standard algorithm such as MH, HMC, or Gibbs. We compose the teleportation kernel $T(\theta, \cdot)$ in (1) with P to obtain an identification-aware kernel $\tilde{P} = PT$.⁴

Concretely, here is one approach we recommend for implementing identification-aware MH:

Algorithm 3 (Identification-aware MH).

- Given target distribution $\pi(\theta)$, identification structure $K(\cdot)$, symmetric proposal distribution $q(\theta'|\theta)$, set initial state θ_0 and number of iterations N .

2. For $t = 1$ to N :

- Draw $\theta' \sim T(\theta_{t-1}, \cdot)$.
- Sample $\theta'' \sim q(\cdot|\theta')$.

accurately reflect the true ratio implied by the target distribution. Additionally, this resulting ratio varies significantly across different simulations, indicating instability in Gibbs's performance.

⁴We write kernel composition by

$$(PT)(x, A) := \int P(y, A) T(x, dy),$$

so $PT = P \circ T$ and $PTf = P(Tf)$. Order can also matter: in general PT and TP need not have the same mixing rate unless the kernels commute.

(c) The acceptance probability should be defined as:

$$\alpha(\theta', \theta'') = \min \left\{ 1, \frac{\pi(\theta'')}{\pi(\theta')} \right\}$$

where:

(d) Accept $\theta_t = \theta''$ with probability α , otherwise $\theta_t = \theta'$.

3. Return $\{\theta_t\}_{t=1}^N$.

Our algorithm blends two elements: a global move that draws a point from the observationally-equivalent class $K(\theta)$, step 2 (a), and a standard local transition, steps 2 (b) - (d). The teleport step in Algorithm 3 can be introduced also to the HMC algorithms shown in Algorithm 2. Specifically, before step 2 in Algorithm 2, we teleport θ_{t-1} within $K(\theta_{t-1})$ to obtain θ' as done in step 2 of Algorithm 3, and run Algorithm 2 step 2 (a) onward with θ' in place of θ_{t-1} .

By construction, \tilde{P} inherits the advantages of the original MCMC method, and it preserves the stationary distribution, formalized below.

Proposition 1 (Stationary Distribution of the Composite Kernel). *Let π be the target probability distribution. If the transition kernel $P(\theta, A)$ is π -invariant, then the teleportation kernel $T(\theta, A)$ is π -preserving (i.e., $\int T(\theta, A)\pi(d\theta) = \pi(A)$), and the composite kernel $\tilde{P} = PT$ is also π -invariant.*

However, the π -invariance in Proposition 1 does not, by itself, imply detailed balance⁵ for the composed kernel $\tilde{P} = PT$. In this paper, reversibility is needed only as a technical device for deriving mixing-rate bounds. When reversibility is required, we replace \tilde{P} by the order-randomized envelope $\bar{P} = \frac{1}{2}(PT) + \frac{1}{2}(TP)$, which is π -reversible. See Proposition 5 in Appendix C.

The same principle generates a family of identification-aware samplers. One may replace T by a finite-group label-switch operator, embed T in a single Metropolis step via an exact or pseudo-marginal mixture proposal, or post-process a stored chain with conditional draws on each $K(\theta)$ (as in [Geweke \(2007\)](#)), which is particularly helpful in high dimensions when likelihood evaluation is costly. Another option is the convex mixture $\tilde{P}_H = (1 - \varepsilon)P + \varepsilon T$. Implementation details, advantages, and limitations of these variants are collected in Appendix B.2. Empirically, no single variant dominates across settings. In our simulations and applications we select among \tilde{P} , the order-randomized \bar{P} , batch augmentation and the convex mixture \tilde{P}_H according to computational

⁵A Markov kernel P is reversible (or satisfies detailed balance) with respect to a measure π if it fulfills the condition $\pi(d\theta)P(\theta, d\theta') = \pi(d\theta')P(\theta', d\theta)$.

cost and problem structure. For theoretical mixing bounds we analyze \tilde{P} , which is π -reversible by construction. The convergence arguments in Section 2.3 extend to all reversible variants with at most constant-factor changes in the conductance and hence the spectral-gap bounds. See Proposition 6 in Appendix C for details.

From a computational perspective, the identification-aware samplers add a fixed cost. Each sample from $T(\theta, \cdot)$ must (i) identify the observationally-equivalent set $K(\theta)$ and (ii) draw from the conditional distribution $\pi(\cdot | K(\theta))$. When $K(\theta)$ is obtained by simple algebra, such as label permutations, sign flips, or orthogonal rotations, the overhead is trivial relative to one likelihood call, yet it eliminates the spectral bottlenecks that stall purely local chains, a gain most visible for highly multi-modal or high-dimensional posteriors.

If $K(\theta)$ can be computed only through expensive numerics (e.g., solving a high-dimensional nonlinear system), that gain may be partly offset by run time. Two compromises are then useful. One is to run several inexpensive local updates per teleport: perform one T move then apply P for m consecutive iterations. This periodic schedule is time-inhomogeneous but remains π -stationary because both P and T leave π invariant.⁶ Alternatively, the convex combination $\tilde{P}_H = (1-\varepsilon)P + \varepsilon T$ keeps the kernel time-homogeneous. If we further let $\varepsilon \approx \frac{1}{m+1}$, this matches the average teleport frequency of the periodic schedule while keeping a fixed kernel each iteration. In either case, they preserve improvements on mixing rate while holding down the cost of computing $K(\theta)$.

The practical rule is therefore to engage more identification-aware moves whenever $K(\theta)$ is algebraic and the likelihood dominates computation. Otherwise, adopt a sparse or hybrid schedule that balances the mixing benefit against the price of constructing $K(\theta)$.

Example 1 (Continued). Define an identification-aware transition kernel $\tilde{P} = T \cdot P$, where

$$T = \begin{pmatrix} 1/2 & 0 & 0 & 1/2 \\ 0 & 1 & 0 & 0 \\ 0 & 0 & 1 & 0 \\ 1/2 & 0 & 0 & 1/2 \end{pmatrix},$$

and P is the original Gibbs transition. As shown in Figure 1b, the identification-aware Markov chain mixes much better.

⁶When T is much cheaper than P , one may instead apply m successive teleports followed by one local update, i.e. PT^m , optionally retaining the m intermediate teleport states. This also preserves π . See the batch augmentation in Appendix B.2.4.

2.3 Convergence and Mixing rate

In general, we are interested in multiple aspects of the performance of these samplers. First, we would like to have convergence between the sample distribution and target distribution, either in total variation distance, Kullback-Leibler divergence, or other discrepancy measures, which may or may not depend on the initial point/distribution. Then, we would like to understand how fast they converge. Although other asymptotic properties such as the law of large numbers (LLN) and central limit theorems (CLT) can be of primary interest in their own right, particularly because most applications focus on the performance of a mean estimator of the form $\frac{1}{N} \sum_{i=1}^N f(\theta_i)$ for a given function f , these results are consequences of the convergence of the sample distribution.

In this paper, we measure convergence with the total-variation norm⁷

$$\|\mu_1 - \mu_2\|_{\text{TV}} = \sup_{A \in \mathcal{F}} |\mu_1(A) - \mu_2(A)|,$$

where μ_1 and μ_2 are probability measures on the same measurable space (Ω, \mathcal{F}) . For a Markov kernel P with stationary distribution π and any initial law μ_0 , we monitor $\|\mu_0 P^n - \pi\|_{\text{TV}}$ to quantify convergence. The chain is called *geometrically ergodic* if there exists $0 < \gamma < 1$ such that

$$\|\mu_0 P^n - \pi\|_{\text{TV}} \leq (1 - \gamma)^n \|\mu_0 - \pi\|_{\text{TV}},$$

implying an exponential decay of rate $1 - \gamma$ in TV distance.

In a finite state space, assume P is irreducible, aperiodic, and π -reversible. Then 1 is a simple eigenvalue of P and all other eigenvalues lie strictly inside the unit circle. Let λ_2 be the second-largest eigenvalue in absolute value. The *spectral gap* is $\gamma(P) = 1 - |\lambda_2|$, and the spectral theorem yields

$$\|\mu_0 P^n - \pi\|_{\text{TV}} \leq C(1 - \gamma(P))^n$$

for a constant C depending only on μ_0 and π .

⁷If the chain has a unique stationary law π and $P^n(\theta, \cdot) \rightarrow \pi$ in total variation for every start θ , then the ergodic theorem gives: for any $f \in L^1(\pi)$, the sample mean $\bar{f}_N := \frac{1}{N} \sum_{t=1}^N f(\theta_t)$ satisfies $\bar{f}_N \rightarrow \mathbb{E}_\pi[f]$ almost surely. If, in addition, the chain is geometrically ergodic (defined below) and $f \in L^{2+\delta}(\pi)$ for some $\delta > 0$, then a CLT holds: $\sqrt{N}(\bar{f}_N - \mathbb{E}_\pi[f]) \Rightarrow \mathcal{N}(0, \sigma_f^2)$ with $\sigma_f^2 = \text{Var}_\pi(f(\theta_0)) + 2 \sum_{k \geq 1} \text{Cov}_\pi(f(\theta_0), f(\theta_k))$. Here $\theta_0 \sim \pi$, and all expectations/covariances are taken under π . See, e.g., [Meyn and Tweedie \(2009\)](#); [Jones \(2004\)](#); [Roberts and Rosenthal \(2004\)](#).

This finite-state characterization extends to general state spaces when P is reversible. Let

$$L_2(\pi) = \left\{ f : \Omega \rightarrow \mathbb{R} : \int f^2 d\pi < \infty \right\}, \quad \langle f, g \rangle = \int f g d\pi, \quad L_2^0(\pi) = \{f \in L_2(\pi) : \langle f, 1 \rangle = 0\}.$$

Reversibility makes the Markov operator $(Pf)(x) = \int f(y)P(x, dy)$ self-adjoint on $L_2(\pi)$ and a contraction on $L_2^0(\pi)$. Its (*absolute*) *spectral gap* is

$$\gamma(P) = 1 - \sup_{\substack{f \in L_2^0(\pi) \\ \|f\|=1}} |\langle Pf, f \rangle| = 1 - \sup_{\substack{f \in L_2^0(\pi) \\ \|f\|=1}} \frac{\|Pf\|}{\|f\|}.$$

In finite state spaces this coincides with $1 - |\lambda_2|$. For the rest of the paper we use this spectral-gap viewpoint to compare convergence rates. Our theoretical results cover three settings: (i) a finite state space with m^2 states and m modes; (ii) a general state space where π is a mixture of m log-concave components; and (iii) a general state space with local non-identification. The finite state space case is attractive by its simplicity and clear intuition, while it is less common in practice, so we place the results for that case in the Appendix C.

2.3.1 Multi-modality

Multimodal posteriors arise frequently in applied econometrics, even beyond the mixture models that have been extensively discussed in statistics [Frühwirth-Schnatter \(2006\)](#). For example, regime-switching models deliver separate likelihood peaks that correspond to distinct combinations of structural parameters and latent states ([Diebold and Inoue \(2001\)](#)). In SVAR models identification of structural parameters could hold locally but not globally depending on identifying restrictions ([Bacchicocchi and Kitagawa \(2025\)](#)). Taken together, these examples show that multimodality is a pervasive feature, making it a natural and important focus of our discussion.

In this section, we analyze a canonical example inspired by [Guan and Krone \(2007\)](#) to illustrate the challenges of sampling from multimodal distributions and the effectiveness of an identification-aware approach. Employing a circular topology, which is boundary-free, circumvents the endpoint treatments of a bounded interval.

Example 2. *The state space Ω is a one-dimensional circle of circumference $4L$, represented as the interval*

$[-2L, 2L]$ with its endpoints identified. The target distribution $\pi(\theta)$ is bimodal:

$$\pi(\theta) \propto \begin{cases} \exp(-\nu|\theta|), & \text{if } \theta \in [-L, L] \\ \exp(-\nu(2L - |\theta|)), & \text{if } \theta \in [-2L, -L) \cup (L, 2L] \end{cases}$$

where $L \gg 1$ and $\nu > 0$. The parameters L and ν control the problem's difficulty: large L increases the separation between modes, while large ν makes each mode sharper and more concentrated.

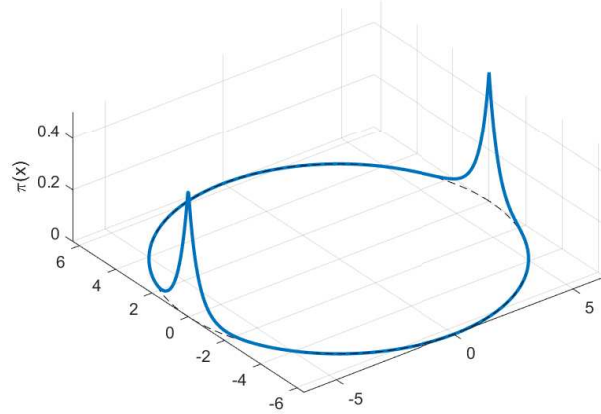


Figure 2: Target π defined on a 1-D circle, with $L = 10, \nu = 2$

A standard Metropolis Hastings sampler with a local δ -ball random walk mixes poorly on this two-mode circle. As shown in Proposition 8, its spectral gap collapses exponentially:

$$\gamma(P) \leq C_1 e^{-\nu(L-\delta)}.$$

This indicates that the sampler becomes prohibitively slow, effectively getting trapped in one mode, whenever the modes are sharp (large ν) or far apart (large L).

The slow mixing is caused by the low-probability barrier between the modes. To break this barrier, we design a proposal that respects the inherent symmetry of the state space. Let

$$s(\theta) = \begin{cases} \theta + 2L, & \theta \in [-2L, 0), \\ \theta - 2L, & \theta \in [0, 2L). \end{cases}$$

be the antipodal shift and define the teleport kernel

$$T(\theta, \cdot) = \frac{1}{2}\delta_\theta(\cdot) + \frac{1}{2}\delta_{s(\theta)}(\cdot), \quad \text{where } \delta_\theta(\cdot) \text{ denotes the Dirac measure at } \theta$$

Let P be one MH step with a symmetric δ -ball proposal. The identification-aware transition is the two-stage composition $\tilde{P} = PT$, i.e., at each iteration first apply T (stay put with probability 1/2 or jump to $s(\theta)$ with probability 1/2), then perform one local MH step from the resulting point. It is worth noting that \tilde{P} is by itself reversible in this specific setting.

This small change to the proposal mechanism has a profound impact on performance. As proven in Proposition 8 in Appendix C, we can obtain a uniform lower bound on the spectral gap:

$$\gamma(\tilde{P}) \geq C_2 \min\{(\nu\delta)^2, 1\},$$

so choosing $\delta \propto \nu^{-1}$ keeps $\gamma(\tilde{P})$ bounded away from zero independently of L and ν .

We now introduce a more general setup. Let π be a probability density on a connected state space $\Omega \subseteq \mathbb{R}^n$. Fix $h > 0$ with $m \geq 2$ modes. We assume that the support of π can be decomposed into m disjoint, open components A_1, \dots, A_m with $\pi(\cup_{i=1}^m A_i) = 1$ such that each π has only one mode in each A_i . Let $w_i := \pi(A_i)$, $\pi_i(\cdot) := \pi(\cdot \cap A_i)/w_i$, $\mu_i \in A_i$ be the mode of π restricted to A_i , and write $d_i := \text{dist}(\mu_i, \partial A_i) = \inf_{z \in \partial A_i} \|\mu_i - z\|_2$, where ∂A_i stands for the boundary of the closure of A_i , and $d_* := \min_i d_i$.

Assumption 1. (i) *There exist constants $c_i \geq 1$ and $\nu_i > 0$ such that, for all $r \in (0, d_i]$,*

$$\pi_i(\{\theta \in A_i : \|\theta - \mu_i\| \geq r\}) \leq c_i e^{-\nu_i r}.$$

Set $c_{\max} := \max_i c_i$, $\nu_{\min} := \min_i \nu_i$, and $\nu_{\max} := \max_i \nu_i$.

(ii) *Fix a step size $\delta > 0$ and define $A_i^{\text{int}} := \{\theta \in A_i : \text{dist}(\theta, \partial A_i) \geq \delta\}$. There exist $\varepsilon_1 \in (0, 1]$, $\varepsilon_2 > 0$, and measurable cores $A_i^\circ \subset A_i$ with $\pi_i(A_i^\circ) \geq \varepsilon_1$ such that, for every $i \neq j$ and all $\theta \in A_i^\circ$,*

$$T(\theta, A_j^{\text{int}}) \geq \varepsilon_2,$$

where $T(\theta, \cdot)$ is a π -reversible teleport kernel used in the composition.

(iii) *For each i there exists a convex set $C_i \subset A_i$ with $\pi_i(C_i) \geq \alpha_i > 0$ and $\delta_0 > 0$ such that $C_i^{\text{int}} :=$*

$\{\theta \in C_i : \text{dist}(\theta, \partial C_i) \geq \delta_0\} \neq \emptyset$, and π is continuous and bounded above/below on C_i^{int} . For some $n_0 \in \mathbb{N}$ and $\eta_0 > 0$,

$$\inf_{\theta \in A_i} P^{n_0}(\theta, \cdot) \geq \eta_0 m_i(\cdot), \quad \text{with } m_i \text{ a probability measure supported on } C_i^{\text{int}}.$$

Assumption 1(i) is a mode-wise concentration condition: within each region A_i it bounds the tail mass away from the mode μ_i up to the radius d_i . It is used to upper-bound the conductance of the RWM by showing that the δ -boundary layer near ∂A_i has exponentially small π_i -mass as d_i grows, hence $\gamma(P)$ is exponentially small in d_i . Assumption 1(ii) states that a single teleport step places a fixed fraction of probability into the interior A_j^{int} of any other mode, uniformly over a core A_i° . This guarantees the inter-mode communication for the composed kernel $\tilde{P} = PT$. Assumption 1(iii) provides a within-mode “small set” $C_i \subset A_i$ on which a Doeblin-type minorization holds for some finite number of MH steps. This yields a uniform positive lower bound on the spectral gap of P restricted to A_i (see [Meyn and Tweedie \(2009, Ch. 16\)](#)).

An alternative condition for Assumptions 1(i) and (iii) is log-concavity: if π_i is log-concave on A_i , Lemma 4 yields the mode-wise exponential tail bound required by 1(i). If there exists a convex $C_i \subset A_i$ on which π is log-concave, then for sufficiently small δ , Lemma 3 gives a positive spectral gap for the δ -ball MH on C_i .

A widely used class of statistical models that meets these conditions is the k -mixture Gaussian $\pi(\theta) = \sum_{i=1}^k w_i \mathcal{N}(\theta; \mu_i, \Sigma_i)$ with well-separated means, take $A_i = \{\theta : w_i \varphi_i(\theta) = \max_j w_j \varphi_j(\theta)\}$. Separation guarantees $d_i > 0$. On each A_i the mixture behaves sub-Gaussian around μ_i , so Assumption 1(i) holds with ν_i comparable to $\lambda_{\max}(\Sigma_i)^{-1/2}$. Choosing $T(\theta, \cdot) = \pi(\cdot | A_j)$ and δ smaller than the interior margin of A_j gives Assumptions 1(ii)–(iii). For Assumption 1(iii), take $C_i = \{(\theta - \mu_i)^\top \Sigma_i^{-1}(\theta - \mu_i) \leq r_i^2\} \subset A_i$ with r_i small. Then, π is bounded above/below on C_i^{int} and the δ -ball MH (with $\delta \leq \delta_0$) satisfies the required minorization.

Proposition 2. *Let π be a probability density on $\Omega \subseteq \mathbb{R}^n$, and suppose Assumption 1 holds with sets A_1, \dots, A_m , modes μ_i , radii d_i , and the teleport kernel T . Let P be the RWM kernel with the uniform δ -ball proposal,*

$$q(\theta, \cdot) = \text{Unif}(B(\theta, \delta)), \quad \delta > 0,$$

and let $\tilde{P} := \frac{1}{2}PT + \frac{1}{2}TP$ denote the reversible composed kernel. Then:

1. For any $\delta > 0$,

$$\gamma(P) \leq 2c_{\max} \exp \{ -\nu_{\min}(d_* - \delta) \}, \quad d_* := \min_{1 \leq i \leq m} d_i.$$

2. There exists a constant $c_0 > 0$, depending only on $(\varepsilon_1, \varepsilon_2, n_0, m, \eta_0)$ (and not on the separations d_i), such that

$$\gamma(\bar{P}) \geq c_0.$$

Refer to Appendix C.2 for a detailed proof.

Proposition 2 shows that the plain δ -ball RWM–MH can mix very slowly: its spectral gap admits an upper bound of order $\exp\{-\nu_{\min}(d_* - \delta)\}$, so it deteriorates exponentially as the modes become farther apart (large d_*) and/or the target is more sharply concentrated (large ν_{\min}). In contrast, the IA–MH composition \bar{P} removes any dependence on inter-mode separation: under Assumption 1 its gap is bounded below by a positive constant that does not involve the d_i . If Assumption 1(i) and (iii) are replaced by log-concavity, the lower bound can depend on the within-mode “condition number” ν_{\min}/ν_{\max} . Choosing $\delta \propto 1/\nu_{\max}$ yields a gap that is uniform in the separations and degrades only as ν_{\max} grows relative to ν_{\min} , not with the distance between modes.

For the Gaussian RWM case, we pursue an alternative set of assumptions: instead of working with Assumption 1, we adopt a log-concavity framework and strengthen it to strong log-concavity. The corresponding result is stated in Proposition 9 in Appendix C.

Proposition 3 establishes that Hamiltonian Monte Carlo (HMC) can also experience significant bottlenecks in multi-modal settings, leading to an exponentially small spectral gap.

Proposition 3 (Hamiltonian Monte Carlo). *Under the same setup as Proposition 2, let L_h decompose into m disjoint open components A_1, \dots, A_m with $\pi(\cup_i A_i) = 1$. For each i , define $w_i = \pi(A_i)$, $\pi_i(\cdot) = \pi(\cdot \cap A_i)/w_i$, and let $\mu_i \in A_i$ be a mode of π_i . Set $d_i := \text{dist}(\mu_i, \partial A_i)$ and $d_* := \min_i d_i$.*

Let Assumption 1(i) hold. In addition, assume the potential $U = -\log \pi$ is L_s -smooth on each A_i :

$$\|\nabla U(x) - \nabla U(y)\| \leq L_s \|x - y\|, \quad \text{for all } x, y \in A_i$$

Let P be the standard HMC kernel with Gaussian momentum $p_0 \sim \mathcal{N}(0, \sigma^2 I_n)$, ℓ leapfrog steps of size η , and the usual Metropolis accept/reject step. Then, for fixed (ℓ, η, σ^2) ,

$$\gamma(P) \leq C \exp \left(- \min \left\{ \frac{1}{2} \nu_{\min} d_*, \frac{c d_*^2}{\sigma^2 (\ell \eta)^2} \right\} \right),$$

for some constants $C, c > 0$ that depend only on $(n, \ell, \eta, \sigma^2, L_s, c_{\max})$ but not on d_* .

The proof is provided in Appendix C. Proposition 3 shows that, in the multi-modal setup considered, HMC admits an exponentially small upper bound on its spectral gap as the inter-mode separation grows. By contrast, as we show in Proposition 2, the spectral gap of IA-RWM is bounded below by a constant independent of inter-mode distances, yielding provably faster mixing than standard HMC.

As for lower bounds, in general multimodal settings (without additional structure on the modes and barriers) there is no known universal, closed-form lower bound for the HMC spectral gap. Explicit lower bounds are available only for specific target families. Consequently, one cannot appeal to a general HMC lower bound to conclude that identification-aware HMC must mix faster than standard HMC.

As for IA-HMC, while a fully general spectral-gap lower bound is not yet available, the teleport mechanism directly targets the bottlenecks that hinder plain HMC, and empirical results indicate the same qualitative advantage. Existing literature highlights the poor performance of HMC in multi-modal settings. For example, [Mangoubi et al. \(2018\)](#) demonstrate that for certain multi-modal targets, HMC can perform even worse than random-walk Metropolis, as it struggles to cross between modes due to the geometry of Hamiltonian trajectories. These results align with the upper-bound analysis in Proposition 3, where transitions between modes are shown to be exponentially unlikely. Similar arguments, such as those adapted from the conductance bounds in [Vishwanath and Tak \(2024\)](#), also support the observation that HMC can be highly inefficient in multi-modal scenarios. We leave establishing a general lower-bound theory for IA-HMC for future work.

2.3.2 Set-identification

Apart from multi-modality, another common source of identification failure in statistical models is set-identification. When the parameter is set-identified, there is typically a continuum of observationally equivalent parameter values forming a manifold in the parameter space.

Specifically, within an arbitrarily small neighborhood of a parameter, there always exists another parameter configuration that produces an identical data-generating process. In what follows, we compare the mixing times of the IA-RWM algorithm with those of the standard RWM in the presence of local unidentifiability. We begin by illustrating the concept with a concrete example.

Example 3. Consider the parameter space

$$\Theta_D = X \times Y_D \subset \mathbb{R}^d,$$

where $d = m + r$. Here, $X \subset \mathbb{R}^m$ is a fixed, bounded set (with $m \geq 1$). Let $Y_D = [-D, D]^r$.

Consider the target distribution π_D on Θ_D such that π_D is flat over the identified set, i.e., π_D factors as

$$\pi_D(\theta_x, \theta_y) = p(\theta_x)u_D(\theta_y), \quad (\theta_x, \theta_y) \in \Theta_D,$$

where $p(\theta_x)$ is a continuous density on X , bounded away from 0 and ∞ . $u_D(\cdot)$ is the uniform density on Y_D .

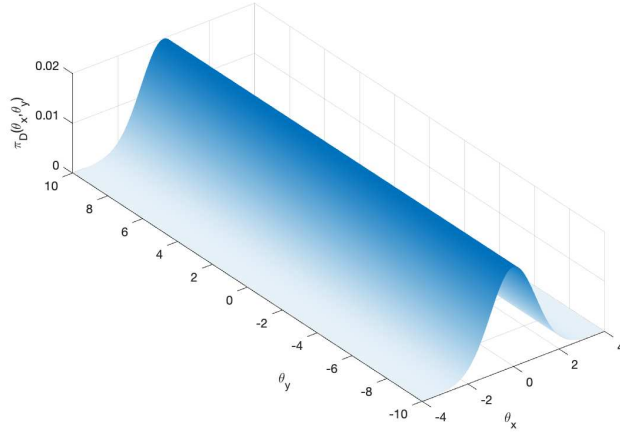


Figure 3: Target density $\pi_D(\theta_x, \theta_y) = p(\theta_x)u_D(\theta_y)$, where $D = 10$. Here, $p(\theta_x) = \frac{1}{\sqrt{2\pi}} \exp\left(-\frac{\theta_x^2}{2}\right)$ is the standard Gaussian restricted to $[-4, 4]$, and $u_D(\theta_y)$ is the uniform density on $[-10, 10]$.

In this model, θ_x is assumed to be identified, while u_D is flat in the θ_y direction, reflecting that θ_y is unidentifiable. As $D \rightarrow \infty$, the size of Y_D grows without bound. For simplicity, we assume $p(\theta_x)$ is the standard Gaussian density and use the standard RWM algorithm as a benchmark. Under the additional assumption that the proposal density q is sufficiently diffuse (so that, for a small number of steps, the transition probability $q^n((\theta_x, \theta_y), (\theta'_x, \theta'_y))$ is uniformly bounded below for all θ_y), one can show that the RWM's spectral gap $\gamma(P)$ tends to 0 as the unidentifiable region expands. In contrast, the IA–RWM algorithm maintains a spectral gap $\gamma(\bar{P})$ that is uniformly bounded away from 0, which ensures faster convergence even as D grows. This result is formalized in Proposition

10 and proved in Appendix C.1.

This idea extends beyond the rectangular setting for Y_D . In differential geometry, one can often represent a family of smooth, compact, connected r -dimensional manifolds (known as the leaves of a foliation, or fibres) as the level sets of a smooth function, provided that certain regularity and topological conditions hold. Intuitively, think of the parameter space as stacked by smoothly curved surfaces rather than straight rectangular blocks. Each point belongs to one surface and one only. The surfaces never cross, and as you move the points, they shift gradually without sharp bends or gaps. Under these mild geometric conditions we can tag every surface with a single coordinate, the density depends only on that tag, and the identification-aware sampler can still update the uninformative directions by drawing a fresh point uniformly on the current surface. This is exactly the same strategy that works in the rectangular case. These assumptions are formalized as below.

Assumption 2. (i) *There exists a C^∞ map $\phi : \Theta \rightarrow \Phi \subset \mathbb{R}^{d-r}$ whose Jacobian $D_\theta \phi$ has constant rank $d-r$ for every $\theta \in \Theta$.*

(ii) *For every $u \in \Phi$, the fiber (i.e. observationally equivalent set)*

$$\mathcal{F}(u) := \{\theta \in \Theta : \phi(\theta) = u\}$$

is compact and connected.

(iii) *For each $u \in \Phi$ there exists a smooth hypersurface $\Sigma(u) \subset \mathcal{F}(u)$ such that $\Sigma(u)$ separates $\mathcal{F}(u)$ into two subsets $\mathcal{F}(u)^-$ and $\mathcal{F}(u)^+$ with $0 < c_1 \leq \text{Vol}_{\mathcal{F}}(\mathcal{F}(u)^-) / \text{Vol}_{\mathcal{F}}(\mathcal{F}(u)) \leq c_2 < 1$, and $\Sigma(u)$ admits a tubular neighborhood of width at least $\varepsilon_{\min} > 0$ inside $\mathcal{F}(u)$, i.e., there is a diffeomorphism $\Sigma(u) \times (-\varepsilon_{\min}, \varepsilon_{\min}) \rightarrow \mathcal{N}_{\varepsilon_{\min}}(\Sigma(u)) \subset \mathcal{F}(u)$.*

(iv) *Assume*

$$\pi(d\theta) = f(u)w_u(\theta)\mu_u(d\theta)du,$$

where $u = \phi(\theta)$, $0 < \underline{f} \leq f(u) \leq \bar{f} < \infty$, and for each u the function $w_u : \mathcal{F}(u) \rightarrow (0, \infty)$ satisfies

$$0 < w_{\min} \leq w_u(\theta) \leq w_{\max} < \infty \quad \text{for } \mu_u\text{-a.e. } \theta \in \mathcal{F}(u),$$

and w_u is locally Lipschitz on $(\mathcal{F}(u), d_{\mathcal{F}})$. That is, for every compact $K \subset \mathcal{F}(u)$ there exists $L_{u,K} <$

∞ such that

$$|w_u(\theta) - w_u(\theta')| \leq L_{u,K} d_{\mathcal{F}}(\theta, \theta') \quad \text{for all } \theta, \theta' \in K,$$

where $d_{\mathcal{F}}(\theta, \theta')$ is the shortest-path distance within $\mathcal{F}(u)$ between θ and θ' .

The conditional μ_u is the normalized r -dimensional Hausdorff measure on the fiber $\mathcal{F}(u)$:

$$\mu_u(A) = \frac{\text{Vol}_{\mathcal{F}}(A)}{\text{Vol}_{\mathcal{F}}(\mathcal{F}(u))}, \quad A \subset \mathcal{F}(u).$$

(v) There exist $\rho > 0$ and constants $0 < c \leq C < \infty$ such that, for every $\theta \in \Theta$, points with $\|u - \phi(\theta)\| + \|s\| \leq \rho$ admit a unique representation

$$\theta = \Psi_{\theta}(u, s), \quad u \in \mathbb{R}^{d-r}, s \in \mathbb{R}^r,$$

satisfying

$$\phi(\Psi_{\theta}(u, s)) = u, \quad \text{and}$$

$$c\|(u, s) - (u', s')\| \leq \|\Psi_{\theta}(u, s) - \Psi_{\theta}(u', s')\| \leq C\|(u, s) - (u', s')\|,$$

and with Jacobian determinant of Ψ_{θ} bounded between c and C .

(vi) The proposal density g is symmetric and translation-invariant, and satisfies: (i) There exist $\delta > 0$ and $c_g > 0$ such that

$$g(z) \geq c_g \quad \text{for all } \|z\| \leq \delta,$$

and (ii) its tail probability $\overline{G}(t) := \int_{\|z\|>t} g(z) dz$ has finite first moment,

$$\int_0^\infty \overline{G}(t) dt < \infty.$$

The parameter vector $\phi(\theta) \in \mathbb{R}^{d-r}$ has a smaller dimension than θ and it corresponds to a vector of reduced-form parameters commonly available in structural econometric models. See, for example, [Giacomini and Kitagawa \(2021\)](#). Assumption 2(i) ensures, by the Regular Level Set Theorem ([Lee, 2012](#), Corollary 5.14), that each fiber $\mathcal{F}(u)$ is a smooth r -dimensional submanifold of Θ .⁸ It ensures that local neighborhoods of fibers behave regularly, avoiding pathological changes

⁸A subset $M \subset \Theta$ is a *smooth r -dimensional submanifold* if for every $x \in M$ there exists a neighborhood $U \subset \mathbb{R}^d$ of x and a smooth map $F : U \rightarrow \mathbb{R}^{d-r}$ such that $M \cap U = \{y \in U : F(y) = 0\}$ and $DF(y)$ has full rank $d - r$ for all $y \in U$.

in fiber geometry. The assumption about the rank of $D_\theta\phi$ requires that the dimension of the ϕ corresponds to the dimension of minimally sufficient reduced-form parameters.

Assumption 2(ii) rules out fibers that wander off to infinity or split into disjoint pieces, both of which can cause improper posteriors or poor mixing. In familiar SVAR settings, the rotation set (e.g., $SO(n)$) is compact, and after an ordering convention it is connected.

In Assumption 2 (iii), every fiber admits a smooth “mid-fiber” slice $\Sigma(u)$ that splits it into two parts of comparable size and has a uniform tubular neighborhood. For MCMC this means a small random-walk step cannot jump from one side of the fiber to the other unless the current point is close to the slice, which is exactly what lets us control crossing probabilities. The uniform neighborhood width is a standard geometric implication of smoothness and is made precise by the tubular neighborhood theorem (Lee, 2012, Thm. 6.24).

When $\pi(\theta) \propto L(y | \theta)p(\theta)$ and the likelihood is flat along each fiber $\mathcal{F}(u)$, Assumption 2(iv) matches the posterior disintegration with $f(u) \propto L(u)p(u)$ and $w_u(\theta) \propto p_u(\theta)$ (the prior’s conditional on $\mathcal{F}(u)$). Thus w_u encodes prior information along the observationally equivalent set: $w_u \equiv 1$ corresponds to a uniform prior, while informative priors yield non-uniform w_u . The bounds on f and w_u imply a uniform acceptance floor for moves that change u ,

$$\alpha(\theta, \theta') \geq \frac{fw_{\min}}{\bar{f}w_{\max}} =: \alpha_0.$$

Assumption 2(v) provides uniform local coordinates (u, s) near any parameter value, with controlled distortion of distances and volumes. In practice, this means we can vary u and the fiber coordinate s in a stable way everywhere in the parameter space, which is what we need for the geometric bounds used later.

Assumption 2(vi) requires the proposal g to place positive mass on a fixed small ball and to have light tails. Both δ -ball and Gaussian random walks satisfy this. These properties let us guarantee short moves occur with non-negligible probability and keep the contribution of very long jumps under control.

Proposition 4. *Let Assumptions 2(i)–(vi) hold. For $u \in \Phi$, let $D(u) := \sup_{\theta, \theta' \in \mathcal{F}(u)} d_{\mathcal{F}}(\theta, \theta')$ and $D_{\max} := \sup_{f(u) > 0} D(u)$. Let P be the standard random-walk Metropolis kernel targeting π (from (iv))*

with proposal g (from (vi)). Define the teleport kernel T by

$$T(\theta, A) := \frac{\int_{A \cap \mathcal{F}(\phi(\theta))} w_{\phi(\theta)}(\xi) \mu_{\phi(\theta)}(d\xi)}{\int_{\mathcal{F}(\phi(\theta))} w_{\phi(\theta)}(\xi) \mu_{\phi(\theta)}(d\xi)},$$

where μ_u is the normalized r -dimensional Hausdorff measure on $\mathcal{F}(u)$ from (iv), and set

$$\bar{P} := \frac{1}{2}(PT) + \frac{1}{2}(TP).$$

Then:

1. There exists $C < \infty$ independent of D_{\max} such that $\gamma(P) \leq C/D_{\max}$. In particular, $\gamma(P) \rightarrow 0$ as $D_{\max} \rightarrow \infty$.
2. There exist $n \in \mathbb{N}$ and $\varepsilon_0 > 0$, independent of D_{\max} , such that for all $\theta \in \Theta$ and measurable $A \subset \Theta$,

$$\bar{P}^n(\theta, A) \geq \varepsilon_0 \frac{\pi(A \cap T_0)}{\pi(T_0)},$$

where $T_0 \subset \Theta$ is a fixed measurable set with $\pi(T_0) > 0$ independent of D_{\max} . Consequently, \bar{P} is uniformly ergodic and its $L_2(\pi)$ spectral gap is bounded below uniformly in D_{\max} . In particular, one may take

$$\gamma(\bar{P}) \geq 1 - (1 - \varepsilon_0)^{1/n} > 0.$$

Proof can be found in Appendix C.2. Proposition 4 formalizes that standard random-walk Metropolis mixes increasingly slowly as the fibers $F(u)$ grow in diameter, while the identification-aware RWM maintains uniformly fast mixing regardless of fiber size, because it refreshes uninformative directions via weighted draws along each fiber. Intuitively, IA-RWM avoids the bottleneck along nearly flat dimensions that traps standard RWM.

3 Sampling Simulation

In this section, we perform two simple simulation exercises to showcase the efficiency gain we achieved from employing the identification-aware step.

Simulation 1 (Mixture Gaussian). *In this simulation exercise, I draw a sample of size 1,000 from the*

mixture Gaussian distribution

$$X \sim p\mathcal{N}(\mu_1, \sigma_1^2) + (1 - p)\mathcal{N}(\mu_2, \sigma_2^2),$$

where the true $(\mu_1, \mu_2, \sigma_1, \sigma_2, p) = (0, 20, 1, 5, 0.3)$. Then, I sample the parameters $(\mu_1, \mu_2, \sigma_1, \sigma_2, p)$ based on the likelihood with 1,000 chains of length 100,000, randomize the initial guess of the parameters in each simulation, and use the random walk Markov chain as the baseline proposal distribution.

Figure 4 plots the sample distribution of one out of the 1,000 chains. identification-aware Gaussian random-walk Metropolis-Hastings (RWM) is able to “teleport” across two modes while standard RWM is stuck in one of the two modes. In fact, based on 1,000 simulation exercises, the RWM consistently ends up trapped in one of the modes almost every time. In contrast, using that $K(\mu_1, \mu_2, \sigma_1, \sigma_2, p) = \{(\mu_1, \mu_2, \sigma_1, \sigma_2, p), (\mu_2, \mu_1, \sigma_2, \sigma_1, 1 - p)\}$, the chain was able to explore both modes. Figure 5b shows that the reported means of (μ_1, σ_1) are clustered near $(10, 3)$ ⁹ more tightly than those in Figure 5a, indicating that the identification-aware MCMC method reliably estimates the posterior means even when scaling varies between modes.

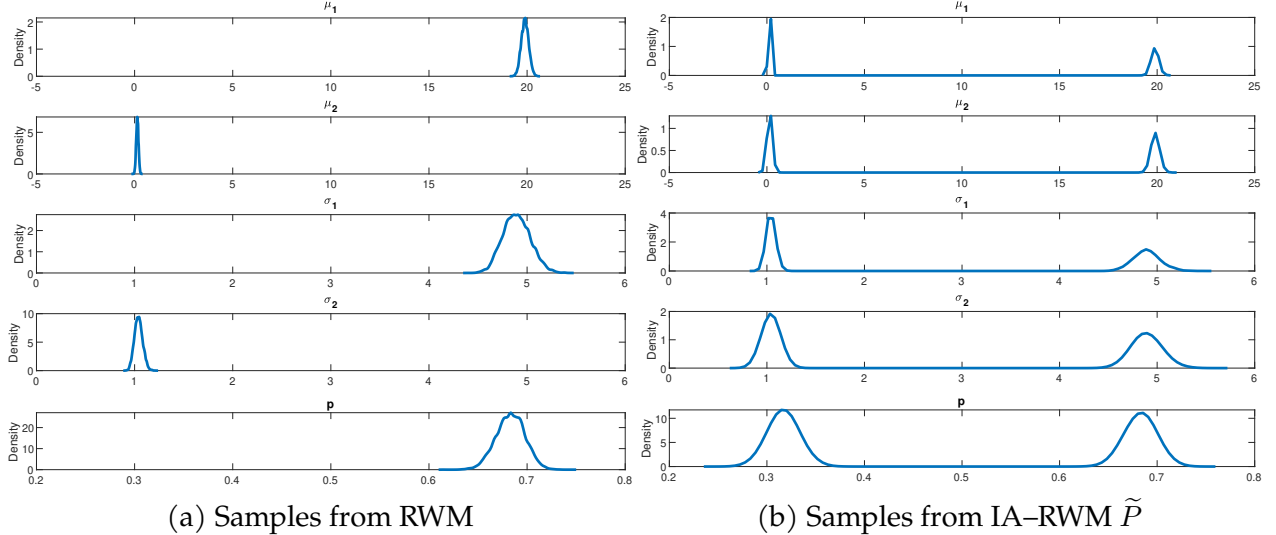


Figure 4: Sampling distributions from a mixture Gaussian likelihood using RWM and IA-RWM \tilde{P}

While our identification-aware MCMC method is highly effective at exploring multi-modal distributions, its gain in efficiency becomes less obvious when local identification fails. Specifi-

⁹Different scaling in the marginal distributions around each mode causes the posterior mean to deviate slightly from $(10, 3)$.

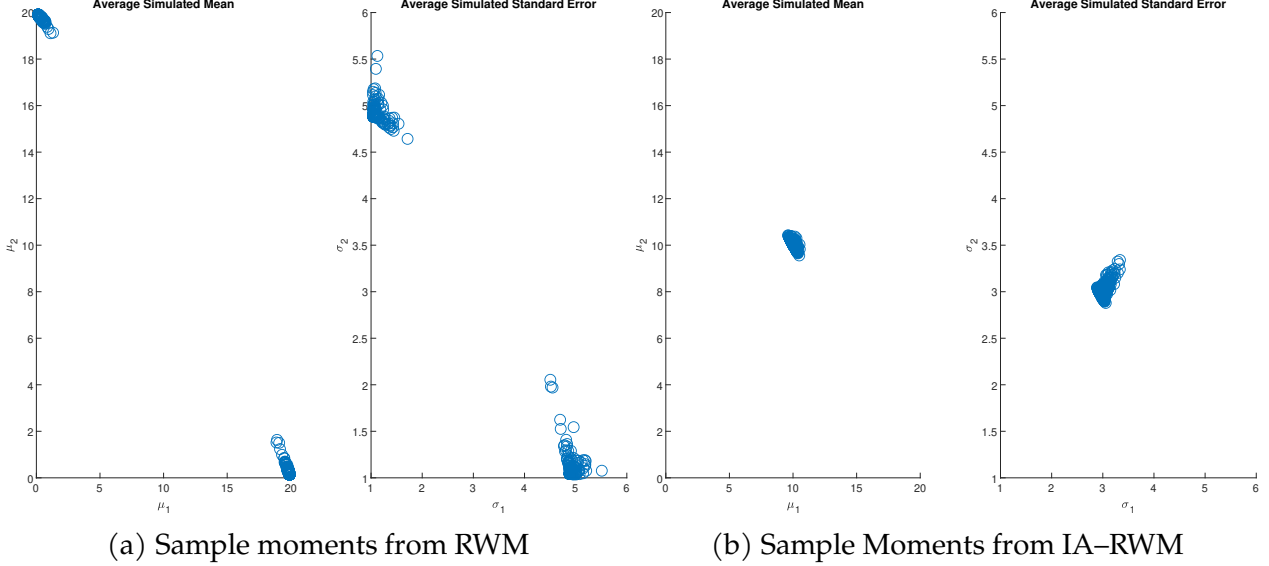


Figure 5: Comparison of sampled moments across 1,000 chains with length $N = 1,000$

cally, in scenarios where maxima are not isolated but instead form continuous manifolds or more complex structures, the method’s ability to thoroughly navigate the distribution is unclear.

Simulation 2 (Conditional Gaussian). *In this simulation exercise, we sample two Gaussian distributions, one with two parameters and the other with seven parameters. They are both of the form*

$$X \sim \mathcal{N}\left(\sum_i^k \mu_i, 1\right),$$

where $k = 2$ and 10 , respectively. Unlike the mixture Gaussian case, the observationally equivalent sets in this example will be $K(\mu_1, \dots, \mu_k) = \{\bar{\mu}_1, \dots, \bar{\mu}_k : \sum_i \bar{\mu}_i = \sum_i \mu_i\}$, an affine subspace with infinite elements.

In both experiments, a uniform prior is used. For $k = 2$, the true parameter values are set to $(\mu_1, \mu_2) = (0, 2)$, and a sample of size 1,000 is generated. The naive Maximum Likelihood Estimator (MLE) is highly sensitive to the choice of initial values. For instance, initializing at $(0, 0)$ yields estimates of $(\hat{\mu}_1, \hat{\mu}_2) = (0, 2)$.¹⁰ To see how well each algorithm explores the support, we bound each μ_i between $[-10, 10]$. The result of one simulation run with 10,000 iterations¹¹ in Figure 6

¹⁰Different starting points lead to varying MLE estimates, which is expected because any (μ_1, μ_2) pair with the same sum results in identical likelihoods. This dependence on initial values arises solely from the implementation of the interior-point optimization method. Similar effects are observed in the movement of particles within SMC.

¹¹For SMC, it has 10,000 particles with 10 iterations.

gives more credit to sequential Monte Carlo. Metropolis Hastings on average (across simulations) performs well, but it tends to be less stable and less evenly distributed on the global maxima.

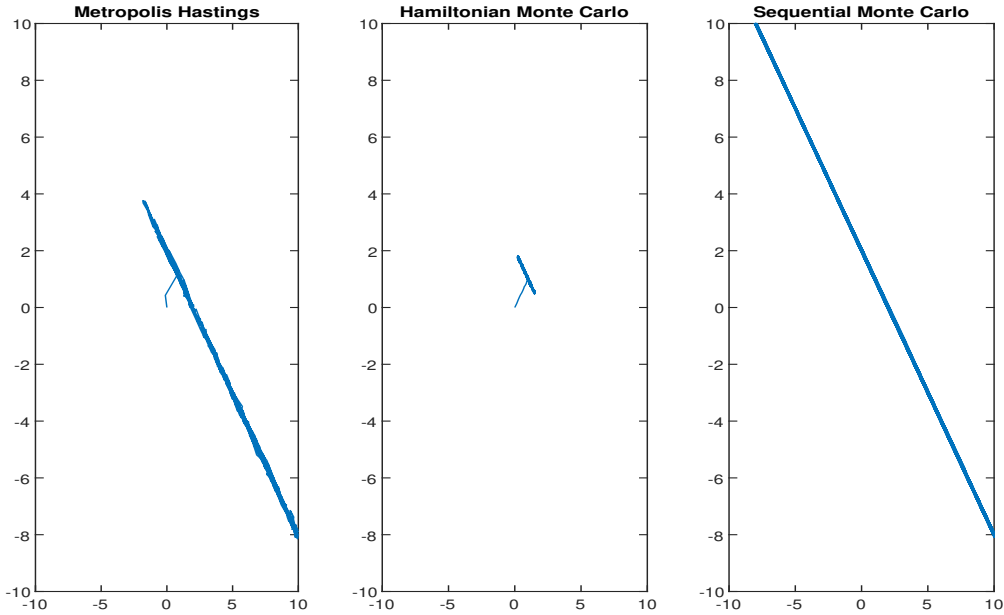


Figure 6: Trace plot of posterior samples for μ_1 and μ_2 of size 10,000, $k = 2$

Since standard SMC outperforms the other two classic algorithms in this example, we expanded the study to a higher dimensional scenario with $k = 10$. This scaling allows for a more comprehensive evaluation of the algorithms' performance in higher-dimensional parameter spaces, where the number of particles and identification-aware MH (IA-RWM) samples remains relatively small compared to the dimensionality, limiting their ability to fully explore the space. In this scaled-up exercise, we compare only the performance of IA-RWM and SMC, utilizing the settings from [Herbst and Schorfheide \(2014\)](#). The true parameter values are set to $\mu_1 = 10$ and $\mu_i = 0$ for $i \neq 1$. Intuitively, when dimension n increases, the number of points needed to explore the full support grows exponentially. We ran SMC with 20 tempering stages and 10^8 particles, effectively approaching the machine's hardware limit. We sample the same amount of points with 10,000 Metropolis-Hastings sample, and 10,000 from $K(\mu_1, \dots, \mu_k)$ for each (μ_1, \dots, μ_k) , using the batch augmentation variant in [B.2](#). Both methods were parallelized in MATLAB. On an Intel Xeon Gold 6246R CPU with 128 GB RAM, the SMC procedure took approximately 1,100 seconds to complete, whereas our method required about 700 seconds.

In Figure 7, the spatial distribution of samples projected to the first two dimensions is depicted. SMC particles exhibit a clear clustering around the point $(10, 0)$, which aligns closely with

the initial particle distribution. This concentration suggests that SMC is strongly influenced by the starting values, potentially limiting its exploration of the parameter space. In contrast, IA–RWM samples are more evenly dispersed in the $[-10, 10]^2$ subspace, demonstrating a more thorough exploration and reduced dependence on initial conditions.

Figure 8 illustrates the marginal kernel density estimates for the parameters μ_1 and μ_2 . The SMC method shows a sharp concentration of μ_1 around 10 and μ_2 around 0, reflecting the clustering observed in the scatter plot. This concentration near the starting values indicates a potential limitation in capturing the full posterior distribution's variability when local identification fails. In contrast, IA–RWM exhibits a more diffuse marginal density, approaching a uniform distribution while still reflecting a slight offset from the origin. This diffuse distribution underscores IA–RWM's capability to explore the parameter space more effectively, capturing a broader range of plausible parameter values.

Overall, the comparative analysis across the spatial distributions, marginal densities, and summary statistics underscores the enhanced performance and robustness of the IA–RWM method over the traditional SMC approach, particularly in scenarios where thorough exploration of high-dimensional, flat regions is essential.

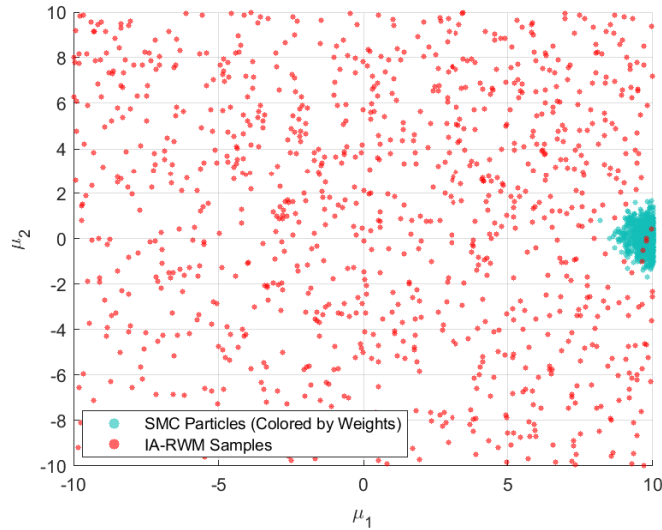


Figure 7: 2D projection of samples: SMC particles vs. IA–RWM samples in (μ_1, μ_2) space

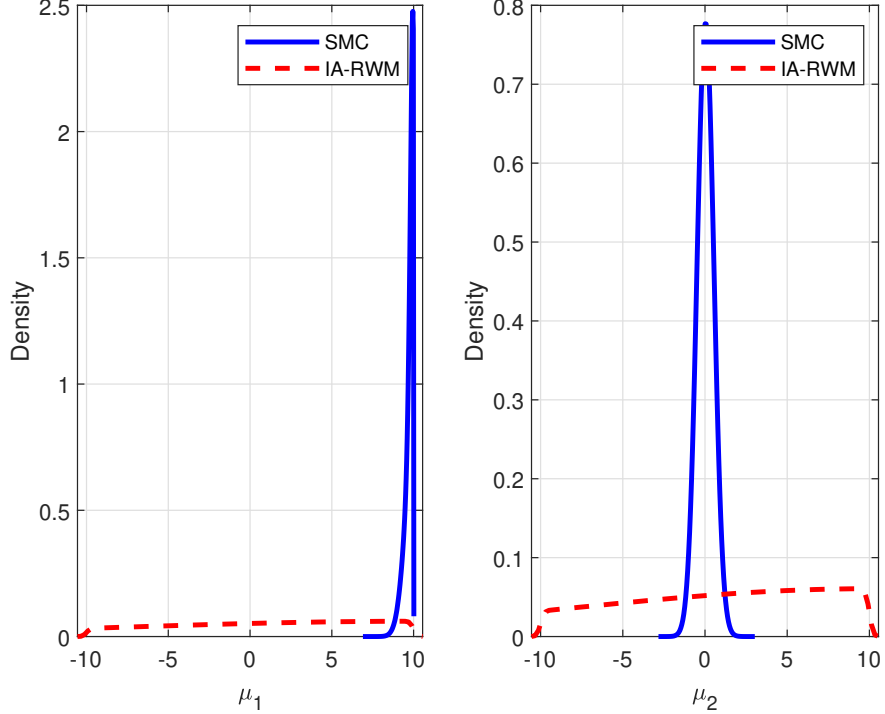


Figure 8: Marginal kernel density estimates for parameters μ_1 and μ_2 : SMC vs. IA-RWM

4 Identification-aware MCMC with informative prior

The target posterior matters for teleportation solely through the prior conditional on the observationally equivalent set. Note that in earlier examples with a uniform prior, all observationally equivalent modes have the same posterior height, making the inferior performance of traditional samplers less apparent in the Bayesian case where the prior over observationally equivalent parameters is informative through the prior specification. In this section, we explicitly incorporate the informative conditional prior into the teleportation step to ensure the resulting Markov chain maintains the posterior as its stationary distribution. We begin with an MA(1) example to show how the teleport step integrates into Bayesian samplers and improves posterior sampling efficiency.

4.1 Moving Average Processes

It is well known that an MA(1) process,

$$y_t = \epsilon_t + \theta \epsilon_{t-1}, \quad \epsilon_t \sim \mathcal{N}(0, \sigma^2),$$

exhibits an observational equivalence between (θ, σ) and $(\theta^{-1}, |\theta|\sigma)$. Throughout we analyze a single dataset generated at $(\theta, \sigma) = (0.5, 1)$. The observationally equivalent point is $(\theta, \sigma) = (2, 0.5)$, which induces the same likelihood.

Following [Plagborg-Møller \(2019\)](#), we consider independent priors on (θ, σ) . The prior places $\theta \sim \mathcal{N}(1, 0.5^2)$ and $\log \sigma \sim \mathcal{N}(0, 0.25^2)$, which favors the vicinity of $(0.5, 1)$ over $(2, 0.5)$. For comparison, we also examine a likelihood-only (uniform prior) specification, in which the prior is effectively flat and the posterior coincides with the likelihood.¹²

We perform posterior inference in the transformed parameterization $(\theta, s = \log \sigma)$ using three samplers, each run for 50,000 iterations: (i) a random-walk Metropolis (RWM; target acceptance 0.234), (ii) the adaptive No-U-Turn Sampler (NUTS; target acceptance 0.80; [Hoffman et al., 2014](#)), and (iii) an identification-aware random-walk Metropolis (IA-RWM) that augments local RWM updates (target 0.234) with a teleport move between observationally equivalent points.

NUTS is a Hamiltonian Monte Carlo method that adaptively adjusts both the leapfrog step size and the trajectory length, so the user need only supply gradients of the log posterior. It is well regarded for efficiently exploring the interior of a single mode, even in moderately high-dimensional settings. However, as noted by [Plagborg-Møller \(2019\)](#), performance can deteriorate under highly diffuse priors when the posterior is multi-modal, as exploration across modes may slow despite adaptation.

To assess sensitivity to the prior and initialization, we consider three setups: a uniform (likelihood-only) prior, an informative prior with the chain initialized at the true value $(0.5, 1)$, and the same informative prior with the chain initialized at the observationally equivalent point $(2, 0.5)$. For each configuration and sampler, we overlay in light gray the true marginal posterior obtained by direct grid integration of the joint log posterior and plot the sampler’s marginal density estimate from the draws.

From Figure 9 and 10 we can see that, under the informative prior, the posterior mass is strongly concentrated near $(0.5, 1)$, with a smaller secondary mode near $(2, 0.5)$. When initialized near the dominant mode (row 2), both RWM and NUTS produce marginals that agree well with the gray truth curves. However, when initialized at the observationally equivalent point (row 3), RWM and NUTS tend to get stuck in that local region for the entire sampling process and can under-represent the dominant mode, yielding marginals that deviate from the gray overlays and masking bimodality. In contrast, IA-RWM, by explicitly traversing the observationally equivalent

¹²In the uniform case, the conditional “fiber” move between (θ, σ) and $(\theta^{-1}, |\theta|\sigma)$ is a simple 1/2 draw.

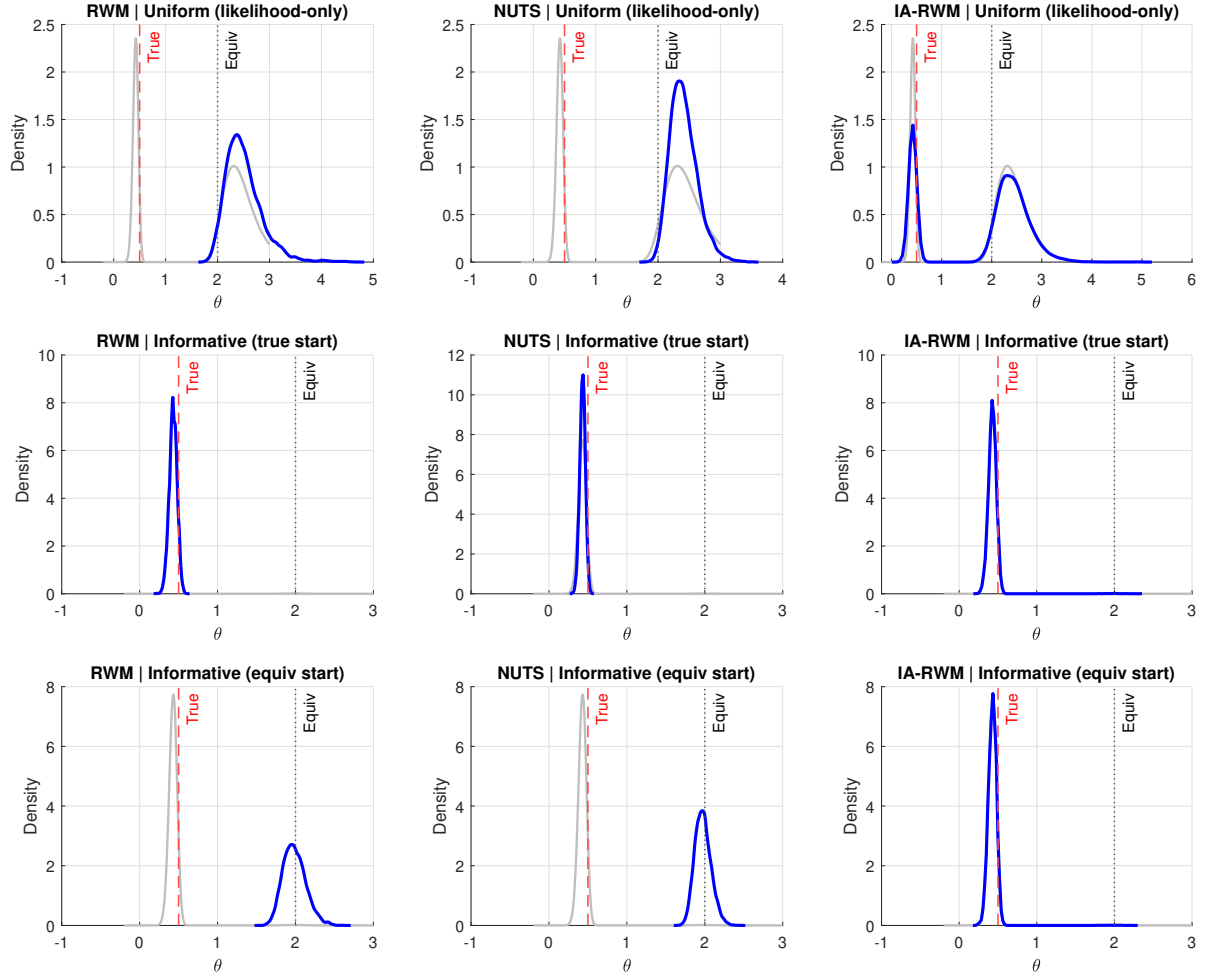


Figure 9: θ posteriors. Light-gray curves are grid-based marginal posteriors; colored curves are KDEs from sampler draws. Vertical lines: true $\theta = 0.5$ (red dashed) and observationally equivalent $\theta = 2$ (black dotted).

points, robustly mixes between the two regions and recovers the correct marginal shapes regardless of initialization.

Under the uniform (likelihood-only) specification (row 1), the mass allocated to the two observationally equivalent regions is more balanced. Here, too, IA-RWM delivers consistent bimodal marginals, while RWM/NUTS are more sensitive to their starting point.

Overall, the results show that set identification and multimodality can hinder standard samplers, whereas exploiting the observational-equivalence structure enables more effective posterior exploration.

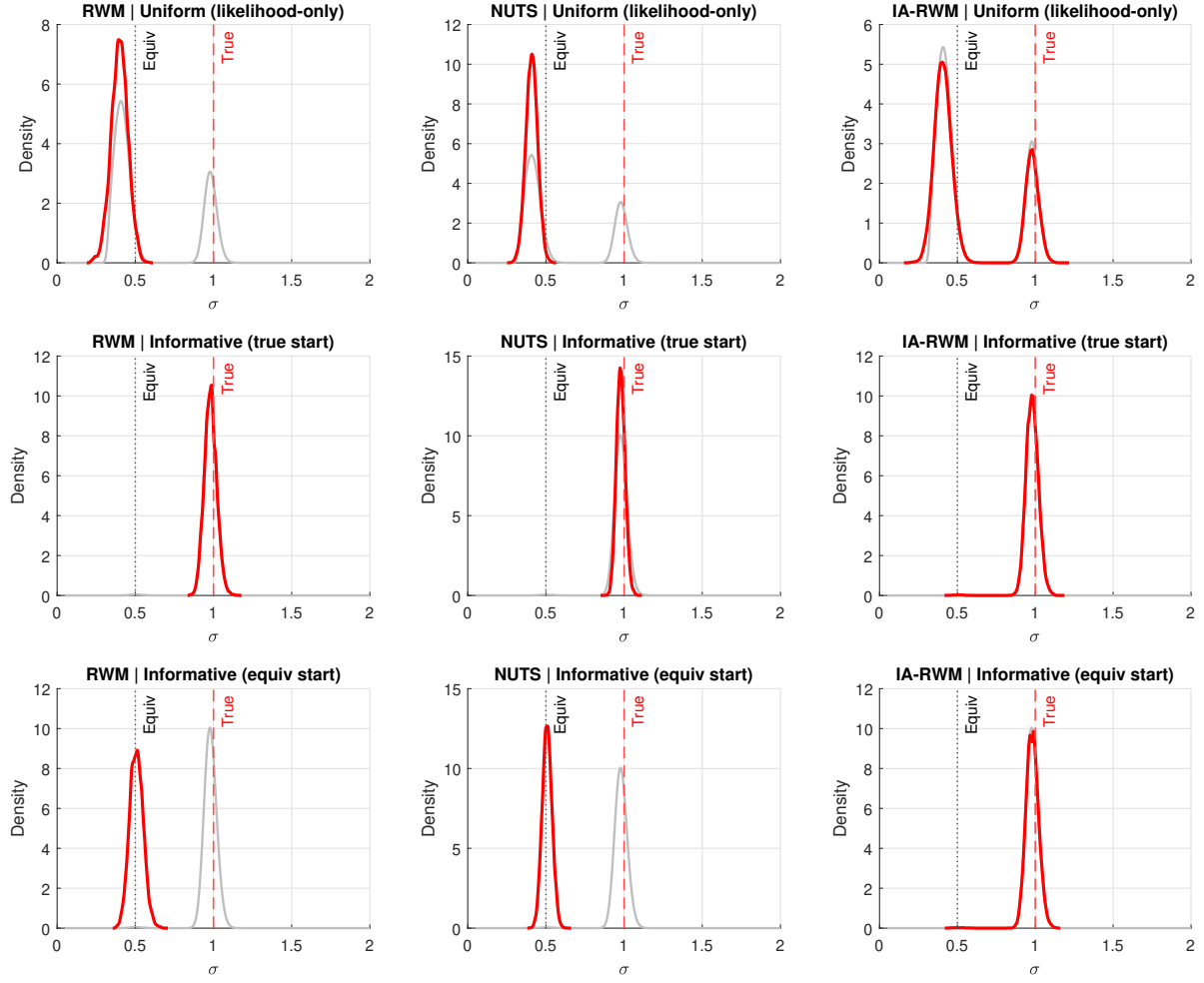


Figure 10: σ posteriors. Light-gray curves are grid-based marginal posteriors; colored curves are KDEs from sampler draws. Vertical lines: $\sigma = 1$ (red dashed) and observationally equivalent $\sigma = 0.5$ (black dotted).

4.2 Application: News Shocks and Business Cycles

In this section we reassess the algorithms using the SVMA setup of [Plagborg-Møller \(2019\)](#). An n variable SVMA writes the data as

$$y_t = \sum_{\ell=0}^q \Theta_{\ell} \varepsilon_{t-\ell}, \quad \varepsilon_t \sim \mathcal{N}(0, \Sigma).$$

We collect impulse responses in $\Theta = \{\Theta_{ij,\ell} : 1 \leq i, j \leq n\}$ and the shocks are assumed i.i.d. Gaussian with covariance matrix $\Sigma = \text{diag}(\sigma_1, \dots, \sigma_n)$. Identification for this model has been studied extensively in [Lippi and Reichlin \(1994\)](#) and [Plagborg-Møller \(2019\)](#), and are briefly revisited in Appendix E. The application uses three quarterly U.S. series: TFP growth, real GDP growth,

and the ex-ante real federal-funds rate, and three latent shocks: an unanticipated productivity shock, a technology news shock, and a monetary-policy shock. The sample spans 1954Q3 – 2007Q4 ($T = 213$). Series are detrended using the Stock–Watson kernel smoother, and the real rate is the effective funds rate minus contemporaneous GDP-deflator inflation. We adopt a finite MA lag $q = 16$: the Akaike Information Criterion suggests $q \approx 13$, while autocorrelation diagnostics support a slightly longer window, so $q = 16$ is chosen to be conservative.

We place a multivariate Gaussian prior on the impulse responses. For each (i, j) and horizon $0 \leq \ell \leq q$,

$$\Theta_{ij,\ell} \sim \mathcal{N}(\mu_{ij,\ell}, \tau_{ij,\ell}^2), \quad \text{Corr}(\Theta_{ij,\ell+k}, \Theta_{ij,\ell}) = \rho_{ij}^k \quad (0 \leq \ell \leq \ell + k \leq q),$$

and the vectors $\{\Theta_{ij,0:q}\}$ are a priori independent across (i, j) . Impact responses are normalized by fixing the own-shock impacts to unity, $\Theta_{jj,0} = 1$, with zero prior variance ($\tau_{jj,0}^2 = 0$). Shock standard deviations $\sigma_1, \dots, \sigma_n$ are mutually independent and independent of the IRFs, with

$$\log \sigma_j \sim \mathcal{N}(\mu_j^\sigma, (\tau_j^\sigma)^2).$$

Priors are centered on the log-linearized sticky-price DSGE model of [Sims \(2012\)](#): $\mu_{ij,\ell}$ equals the DSGE IRF, except for the news shock where the uncertain anticipation horizon is handled by setting the TFP mean to one-half of the DSGE impact and spreading that mass over $\ell = 0, \dots, 6$. Variances $\tau_{ij,\ell}^2$ are calibrated so the DSGE IRFs lie inside 90% prior bands under reasonable parameter perturbations. Bands for news-shock IRFs are deliberately wide (often including zero), whereas monetary-policy IRFs are tighter to reflect stronger beliefs about their qualitative shape. Smoothness parameters use $\rho_{ij} = 0.5$ for TFP responses and $\rho_{ij} = 0.9$ for GDP and the real rate, encoding smoother behavior for output and rates and allowing spikier productivity. Shock-scale priors are deliberately vague, with $\mu_j^\sigma = \log 0.5$ and $\tau_j^\sigma = 2$.

In his paper, [Plagborg-Møller \(2019\)](#) uses a two-step heuristic to provide the No-U-Turn Sampler (NUTS) with a high-density starting value. First, he constructs a rough posterior-mode guess: the sample auto-covariance function of the data is computed, an invertible SVMA representation matching this auto-covariance is obtained, and a greedy search over all root flips of the characteristic polynomial is performed so that the candidate maximizes the Gaussian prior density.¹³ This

¹³This is essentially a discrete search among a subset of observationally equivalent points, as no rotation is performed.

candidate mode is then blended with the prior mean along a convex grid. The weight that yields the highest posterior probability defines the initial parameter vector supplied to the sampler. The procedure ensures numerical stability (by starting from an invertible representation) and avoids low-density regions that would require a long burn-in. On the other hand, it starts in a high-probability region and a local Markov chain may still get trapped there if the target distribution is multi-modal.

We generate posterior samples of size 10,000 (thinned from 100,000, which is ten times the number in [Plagborg-Møller \(2019\)](#)) with NUTS, IA-RWM (block-wise), and IA-NUTS separately, first using his original prior, and then with a bounded uniform prior. The identification-aware variant used here is the reversibilized teleport-local composition $\bar{P} = \frac{1}{2}(PT + TP)$ for both IA-RWM and IA-NUTS. Implementation details are provided in [Appendix E](#).

[Figure 11](#) reports posterior results for $\log \sigma_i$ (marginal plots of Θ are in the Appendix) under the tighter prior. All samplers are initialized at the same point obtained by a greedy mode search. Because visualizing the full “true” posterior, let alone its marginals, is infeasible in this setting, we diagnose behavior using summary statistics and local mode analyses. On the trace plots and marginal densities, NUTS and IA-NUTS are more stable than IA-RWM and deliver very similar marginal shapes. Relative to NUTS, however, IA-NUTS yields (in our sample) a lower posterior mean, similar average log-posterior, a larger posterior mode, and greater variance ([Table 1](#)). The marginal for $\log \sigma_1$ and $\log \sigma_2$ suggests that IA-NUTS locates a distinct mode that coincides with the mode visited by IA-RWM. While the numerical values should not be read too literally, the table indicates that IA-RWM may have traversed a broader region of support, and that the target is at least bimodal (and possibly multimodal).

As an additional piece of evidence, IA-RWM’s draws frequently achieve high log-posterior values with non-trivial step sizes and the chain spends sustained time in a region that NUTS visits rarely (if at all). This persistent occupancy, together with relatively large log-posterior values, points to an alternative high-density region with non-negligible mass that is more readily uncovered by the IA-based procedures.

To further investigate, we performed a sample-based mode search that draws candidate seeds from each sampler and then conducts brief, box-constrained local optimization from condensed seed sets. This exercise consistently returned higher log-posterior maximizers from IA-NUTS or IA-RWM than from NUTS, and the top IA-NUTS modes were well separated from those reached by NUTS.

However, there are two caveats that could temper the interpretation of mode-search. First, none of the polished modes reproduces the prominent visual marginal mode of NUTS with very small $\log \sigma_2$ (below -2), and the optimizers can be sensitive to tuning parameters. The apparent marginal peak need not correspond to a distinct high-posterior maximizer in the full parameter space. It may reflect projection of a broader ridge or a different basin whose summit lies elsewhere in Θ . Second, larger peak log-posterior values do not imply larger posterior mass. Our mode search certifies the existence of alternative high-density basins but does not quantify their volume.

Taken together, the evidence supports the practical advantage of IA-NUTS over standard NUTS in this problem: IA-NUTS more reliably discovers alternative basins with higher attained log-posterior than those found by NUTS under the same computational budget. At the same time, without being able to quantify the posterior mass of the explored regions, the extent of IA-RWM and IA-NUTS's mixing remains unknown.

Table 1: Summary statistics of 10,000 posterior draws

	NUTS	IA-RWM	IA-NUTS
Log-posterior at mean	75.82	-312.66	-582.326
Avg log-posterior	2.08	6.18	1.14
Sum per-param SD	23.70	25.98	36.49
Highest log-posterior	36.14	59.57	67.88

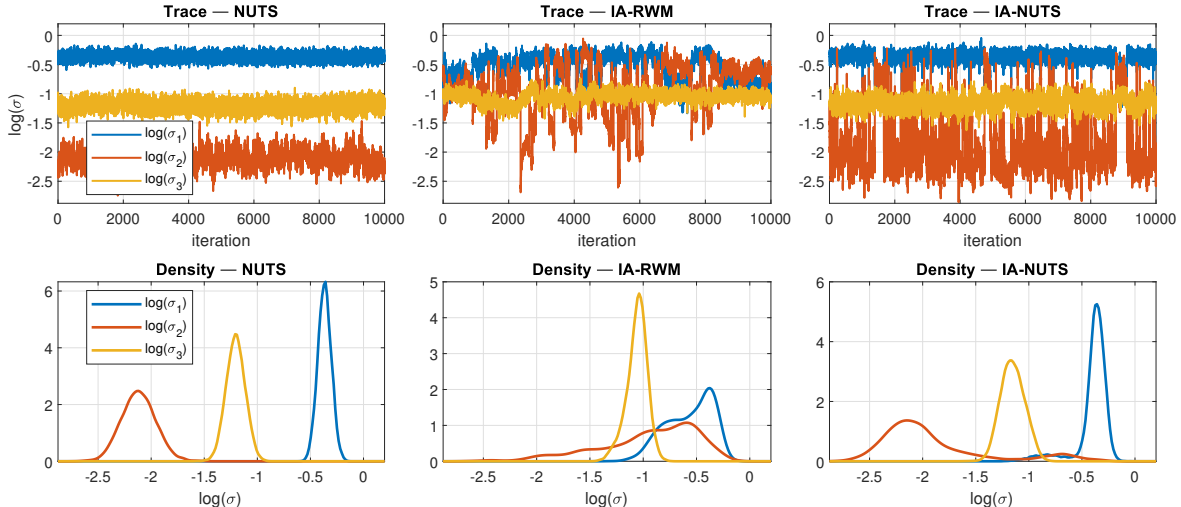


Figure 11: Trace and kernel-density plots of 10,000 posterior $\log \sigma$ draws, obtained by retaining every 10th sample after thinning.

Next, we replace the informative Gaussian prior with an independent, uniform prior on (Θ, ϕ) ,

where $\Theta = \{\Theta_{ij,\ell}\}$ and $\phi = (\phi_1, \dots, \phi_n)$ with $\phi_j = \log \sigma_j$. Specifically, $\Theta_{ij,\ell} \sim \text{Unif}[a_{ij,\ell}, b_{ij,\ell}]$ and $\phi_j \sim \text{Unif}[L_j, U_j]$ independently across all indices (i.e., uniform on a hyper-rectangle), where $a_{ij} = b_{ij} = 100$, $L_j = -8$, $U_j = 5$ for all i, j . The sampler enforces these bound constraints via specular reflection at the boundaries.

Given the 153-dimensional parameter space and the flat directions created by set identification, and exacerbated under a uniform prior, the goal is to find a sampler that balances numerical stability with genuine state-space coverage. From Figure 12, and Figure 19 - 24 in the Appendix, the IA-NUTS achieves that balance. Its trace plots are stationary yet display sustained movement across the support without prolonged residence near the parameter bounds, and its kernel densities are sharply peaked with credible shoulders and tails. Such shapes are expected when information is weak: many IRFs are locally close to zero under the normalization, the likelihood changes very little along broad manifolds, and the marginal projections of these manifolds concentrate probability near the origin while retaining non-negligible mass in the wings. IA-NUTS's occasional global refresh moves reposition the chain across observationally equivalent regions, which helps prevent persistent max-depth saturation and reduces the artificial broadening that repeated boundary reflections can induce.

Baseline NUTS performs noticeably worse in this environment. The traces experience long excursions and show pronounced swings, and the corresponding marginals look overly broad and uneven across panels, suggesting the sampler is not settling into a stable geometry. In fact, baseline NUTS turns out to cost 3 times more gradient evaluations than IA-NUTS, suggesting frequent hits of maximum depth. By contrast, IA-RWM produces very persistent traces with tiny step-to-step movement, and its marginals collapse into narrow spikes near zero—patterns consistent with an overly conservative proposal that fails to traverse the flat directions. IA-NUTS strikes the better balance: its traces remain stable without sticking, and its marginals are tight where the data are informative yet still display believable shoulders and tails, indicating more faithful exploration of the weakly identified posterior.

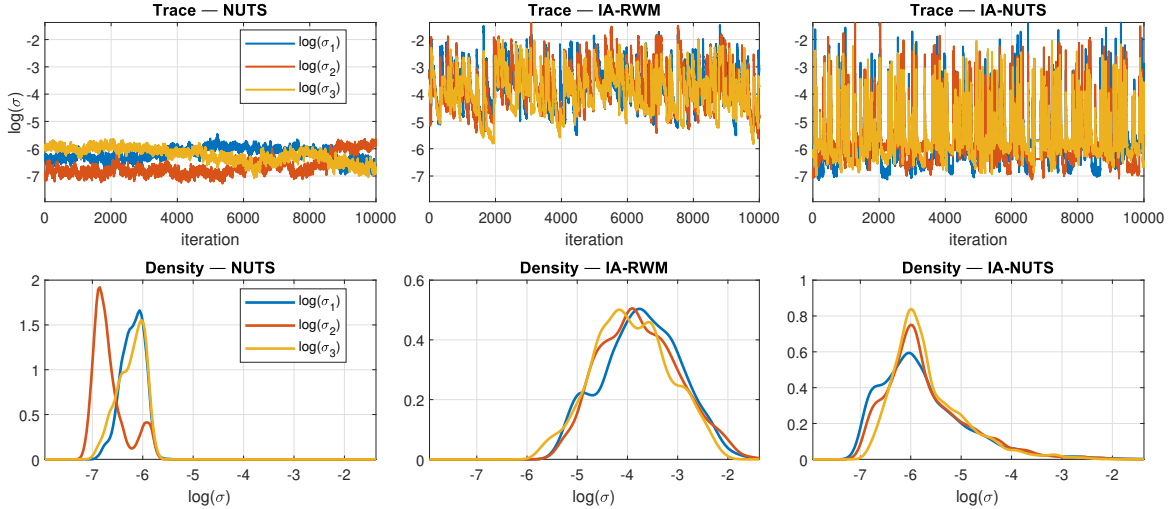


Figure 12: Trace and density plots of 10,000 posterior $\log \sigma$ draws, obtained by retaining every 10th sample after thinning under the uniform prior.

5 Conclusions and discussion

We proposed identification-aware sampling schemes and showed that they outperform the conventional RWM and HMC in terms of the speed of convergence. The key idea of exploiting identified sets and introducing global moves along them in sampling algorithms readily extends to a broad class of Markov chain based methods, thereby expanding both their applicability and practical efficiency.

Moreover, although our exposition focuses on $K(\theta)$ as the set of parameters sharing the same data generating process (i.e., an observationally equivalent set) or likelihood, this assumption can be relaxed. In practice, one may define $K(\theta)$ as any subset of parameters yielding nearly identical or approximated likelihood (e.g., using Whittle approximations). When exact equivalence is replaced by approximate equivalence, one can introduce a suitable weighting or correction step to ensure that the sampler still targets the correct posterior distribution. This generalization is especially valuable in models or data scenarios where strict observational equivalences are difficult to characterize, but approximate regions of high posterior density can be identified. We leave the thorough treatment of this issue for future work.

A Supplemental Figures and Tables

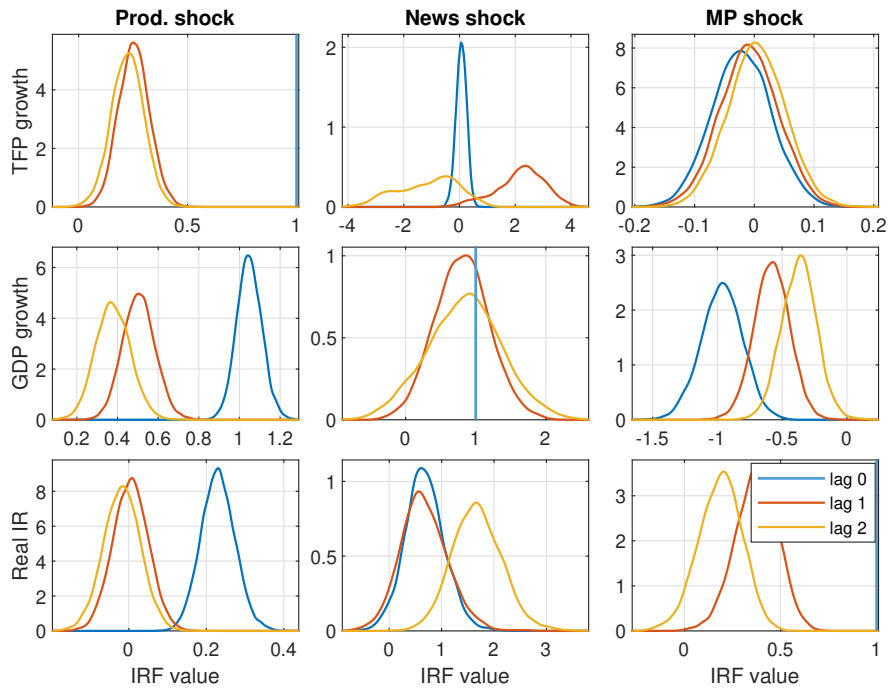


Figure 13: Kernel-density plots of IRF draws obtained by NUTS.

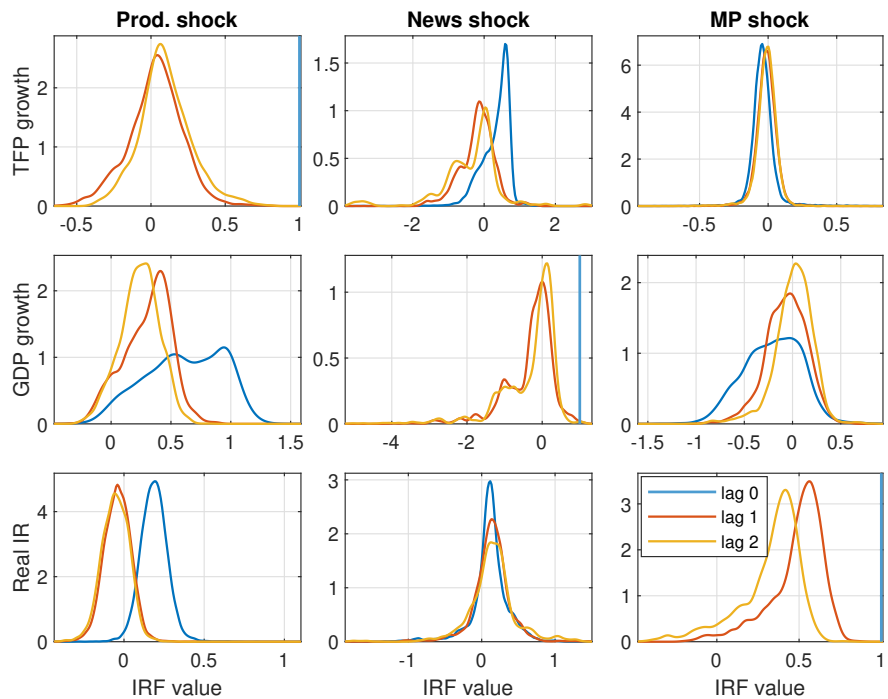


Figure 14: Kernel-density plots of IRF draws obtained by IA-RWM.

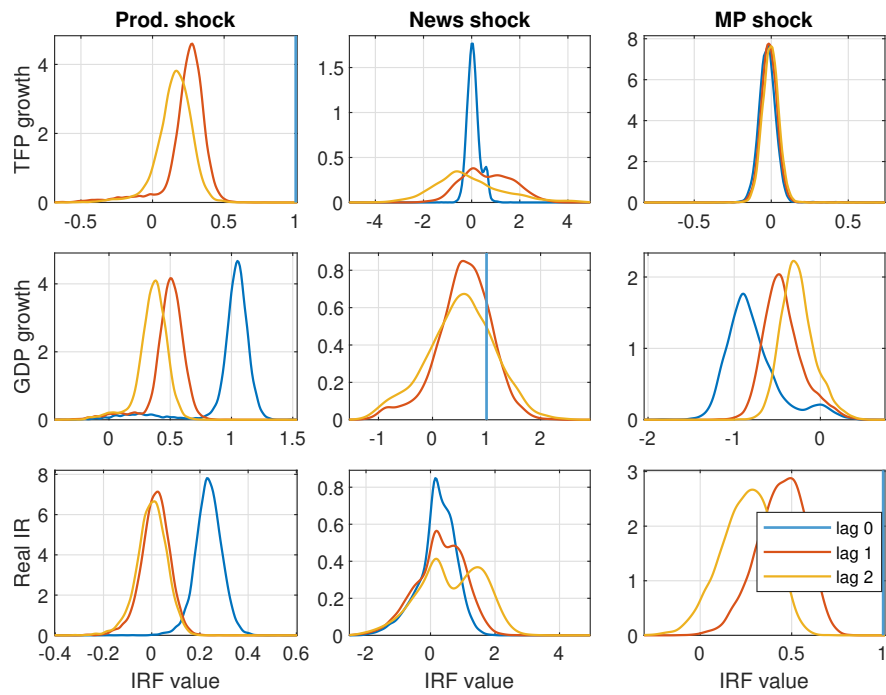


Figure 15: Kernel-density plots of IRF draws obtained by IA-NUTS.

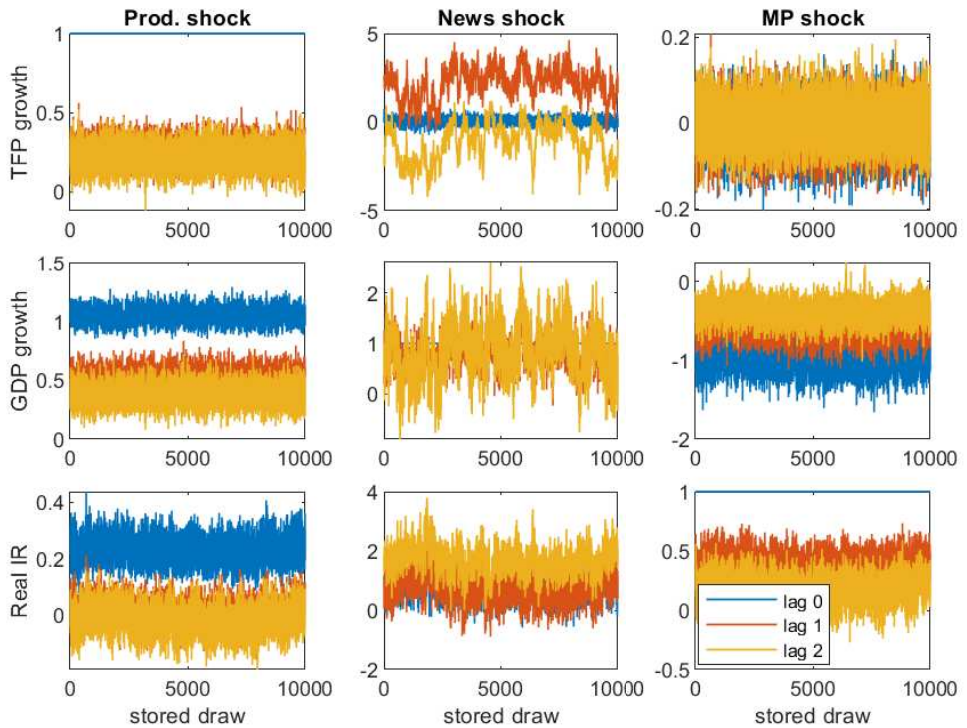


Figure 16: Trace plots of IRF draws obtained by NUTS.

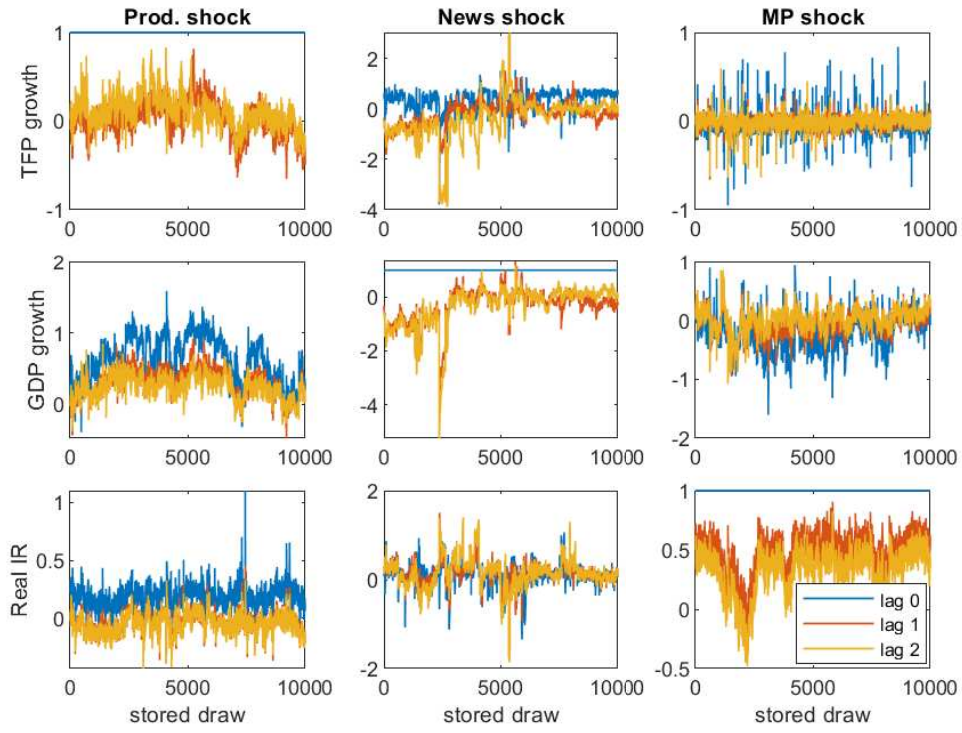


Figure 17: Trace plots of IRF draws obtained by IA–RWM.

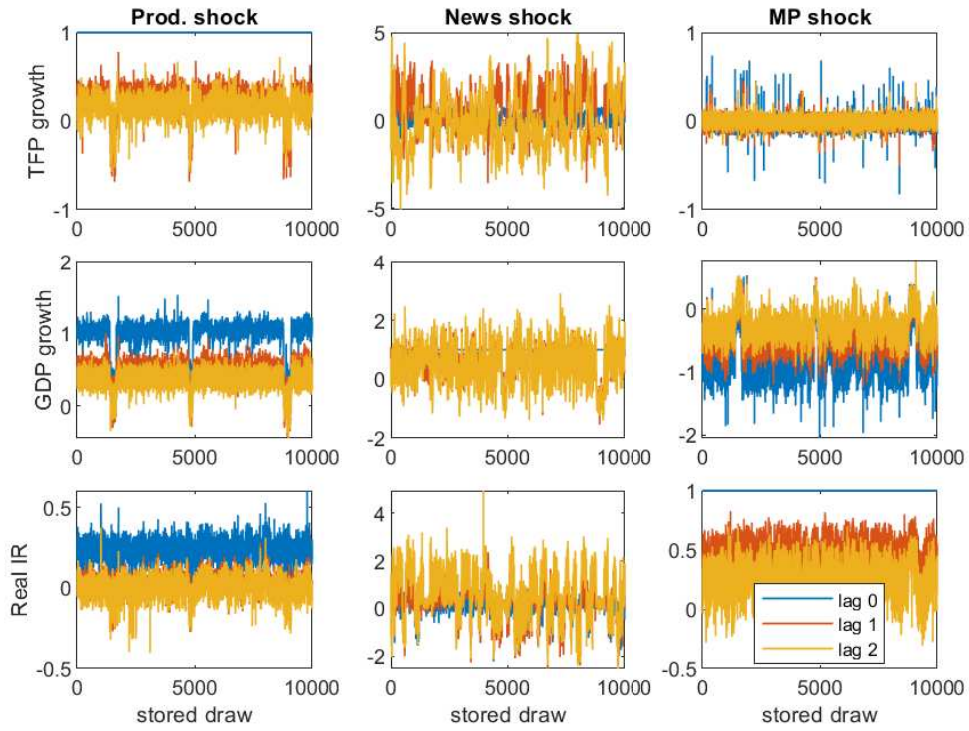


Figure 18: Trace plots of the posterior draws of IRF obtained with IA–NUTS.

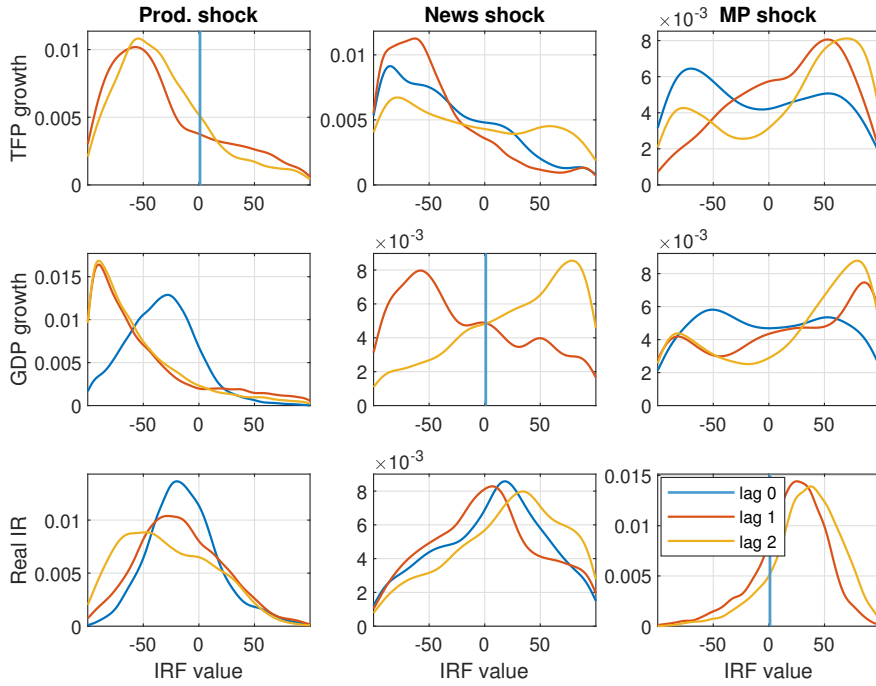


Figure 19: Kernel-density plots of IRF draws obtained by NUTS under the uniform prior.

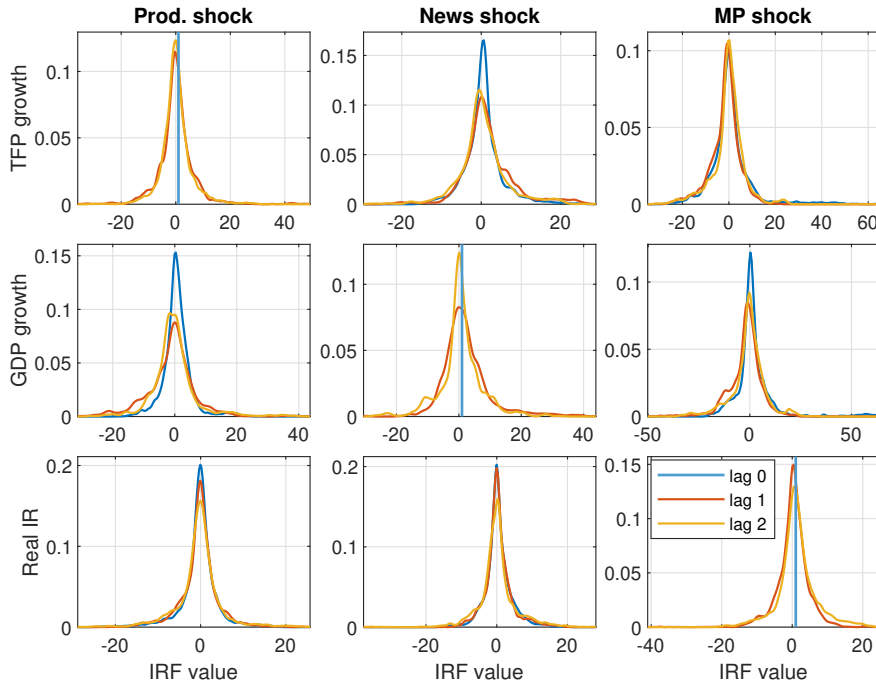


Figure 20: Kernel-density plots of IRF draws obtained by IA-RWM under the uniform prior.

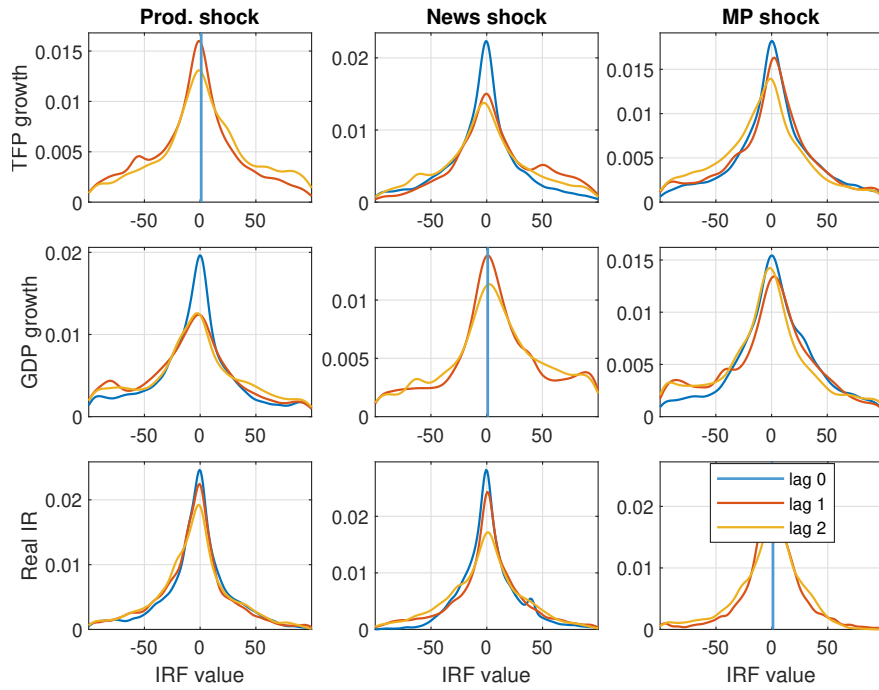


Figure 21: Kernel-density plots of IRF draws obtained by IA-NUTS under the uniform prior.

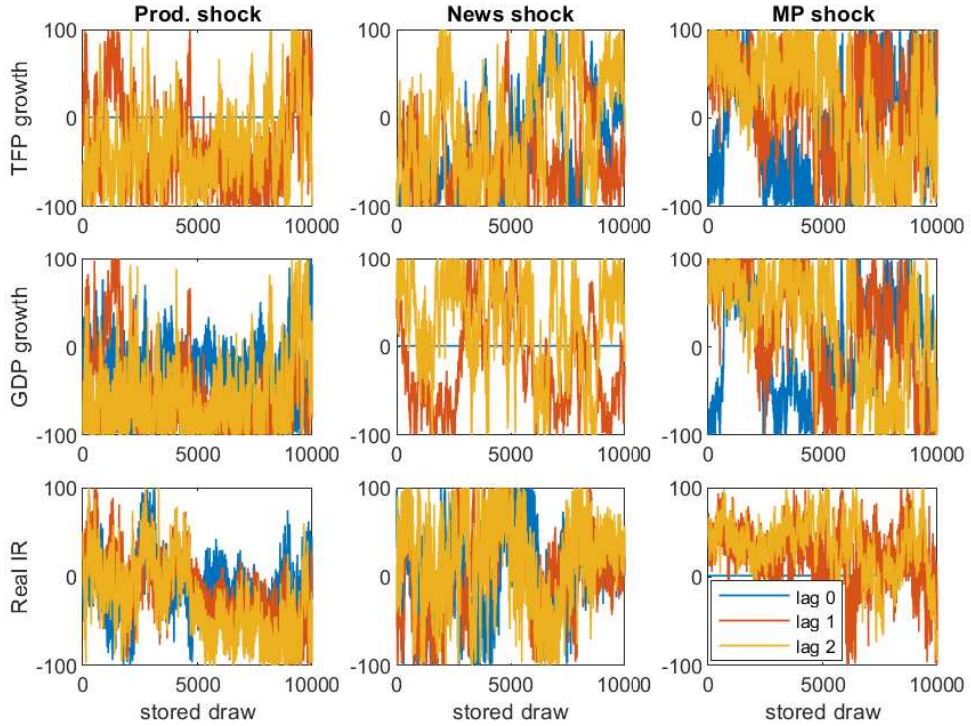


Figure 22: Trace plots of IRF draws obtained by NUTS under the uniform prior.

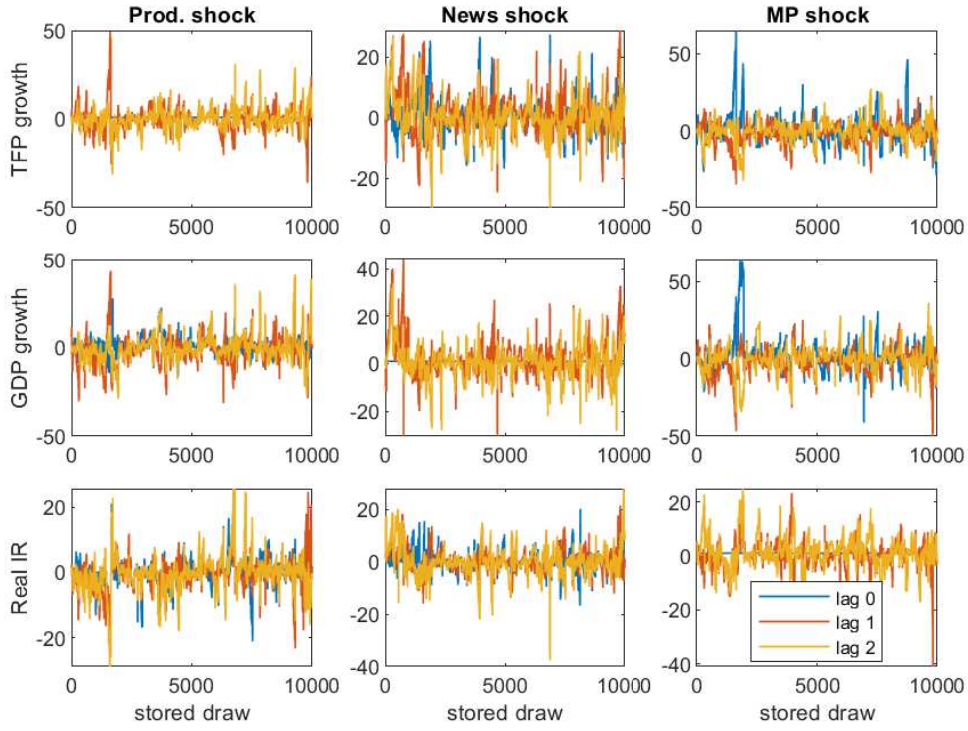


Figure 23: Trace plots of IRF draws obtained by IA–RWM under the uniform prior.

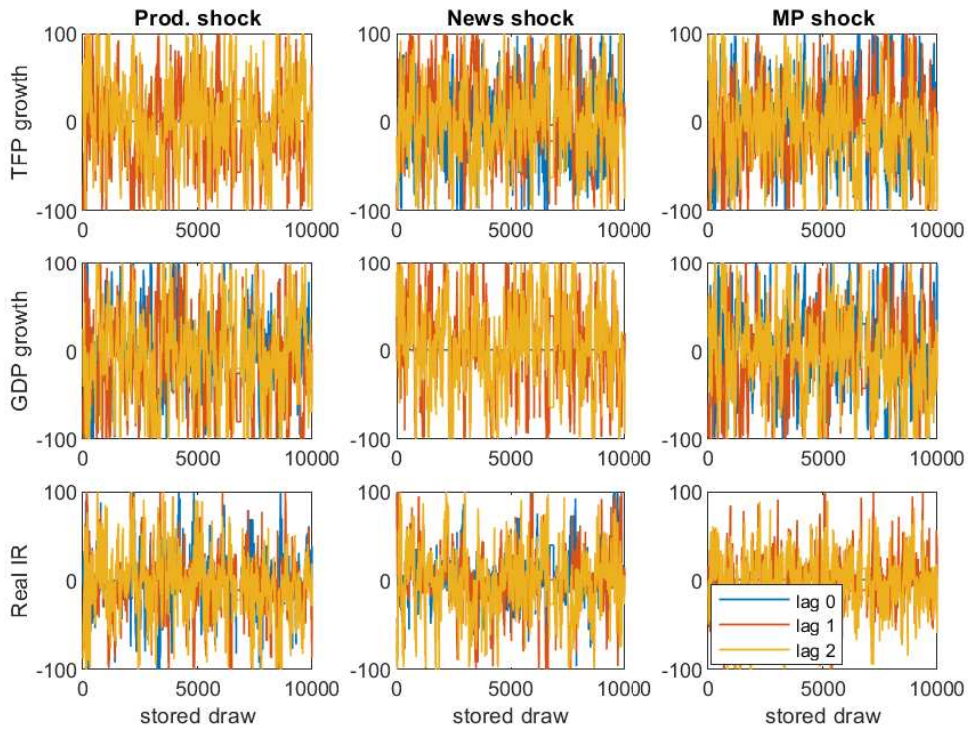


Figure 24: Trace plots of the posterior draws of IRF obtained with IA-NUTS under the uniform prior.

B Algorithms

B.1 Sequential Monte Carlo

Sequential Monte Carlo (SMC) methods operate with a population of weighted particles that evolve through resampling and mutation steps, providing a flexible approach to approximating posterior distributions. Unlike single-chain MCMC methods, SMC can explore multiple regions of the parameter space simultaneously, which helps mitigate the risk of being trapped in local modes. Algorithm 4 follows the setup of [Herbst and Schorfheide \(2014\)](#).

Algorithm 4 (SMC). 1. *Setup*:

- (a) Let $\pi_0(\theta)$ be the prior and $\pi_1(\theta) \propto \pi_0(\theta)L(y|\theta)$ be the posterior.
- (b) Define a sequence of intermediate distributions:

$$\pi_t(\theta) \propto \pi_0(\theta)L(y|\theta)^{\lambda_t}, \quad t = 0, 1, \dots, T,$$

where $0 = \lambda_0 < \lambda_1 < \dots < \lambda_T = 1$ is a tempered path from the prior to the posterior.

- (c) Choose the initial number of particles N and the sequence $\{\lambda_t\}_{t=0}^T$.
- (d) Initialize particle set $\{\theta_0^i\}_{i=1}^N$ by sampling from $\pi_0(\theta)$. Assign equal weights $w_0^i = 1/N$.

2. For $t = 1$ to T :

- (a) **Reweighting**: Update the importance weights from $\{\theta_{t-1}^i, w_{t-1}^i\}$ to reflect λ_t :

$$w_t^i \propto w_{t-1}^i \times [L(y|\theta_{t-1}^i)]^{(\lambda_t - \lambda_{t-1})}.$$

Normalize the weights so that $\sum_i w_t^i = 1$.

- (b) **Resample**: If the effective sample size $ESS = 1 / \sum_i (w_t^i)^2$ falls below a threshold, resample the particles $\{\theta_t^i\}_{i=1}^N$ according to $\{w_t^i\}_{i=1}^N$. Reset weights to $w_t^i = 1/N$ for all i .

- (c) **Mutate**:

- i. Perform one or more MCMC updates (e.g., a Metropolis-Hastings step) on each particle θ_t^i , using $\pi_t(\theta)$ as the target distribution.
- ii. Update the weights if needed (in adaptive SMC, this might be integrated into the MCMC acceptance or proposal adjustments).

3. **Output**: At $t = T$, the particles $\{\theta_T^i\}$ (with weights $\{w_T^i\}$) approximate the posterior $\pi_1(\theta)$.

Because of its efficiency, SMC methods are amongst the most widely used computational techniques in statistics, engineering, physics, finance and many other disciplines. However, it also faces

a few practical limitations. First, selecting the tempering schedule $\{\lambda_t\}$ can be challenging: if increments in λ_t are too large, the particle weights may collapse rapidly (the particle set degenerates), while overly small increments lead to high computational cost. Second, each stage involves both a resampling step and MCMC mutation, which can be computationally expensive, particularly in high-dimensional parameter spaces or when the underlying model is highly non-linear. Moreover, while SMC is often more robust than a single, fixed MCMC chain, it can still suffer if the distribution is strongly multi-modal and the chosen path through the parameter space fails to adequately explore all modes. Careful tuning (e.g., adaptive proposal strategies in MCMC moves or adaptive schedules for λ_t) is usually necessary for SMC to achieve both broad coverage of the parameter space and efficient computational performance.

B.2 Identification-aware Variants

In this section, we list three schemes whose marginal transition kernel $\tilde{P}(\theta, d\theta'')$ satisfies detailed balance $\pi(d\theta)\tilde{P}(\theta, d\theta'') = \pi(d\theta'')\tilde{P}(\theta'', d\theta)$, and a batch augmentation scheme. A symmetric local proposal $q(\theta'|\theta) = q(\theta|\theta')$ is always assumed.

B.2.1 Random Order

The two-step, random order composition $\bar{P} = \frac{1}{2}TP + \frac{1}{2}PT$ suggests that, each transition operates in two stages. In the first stage, we flip a coin, and with $\frac{1}{2}$ chance we run either TP or PT . This idea is based on Algorithm 3 in the main text, but has our desired reversibility. However, when direct sampling from $T(\theta, \cdot)$ is infeasible (e.g., in the SVMA application), we can use a within-class multiple-try Metropolis (MTM) step as per [Liu et al. \(2000\)](#) that targets $T(\theta, \cdot)$ on $K(\theta)$:

1. Forward draws on the class: sample $u_1, \dots, u_M \stackrel{\text{i.i.d.}}{\sim} r(\cdot|\theta)$ supported on $K(\theta)$.
2. Weights: compute $w_m = \frac{\pi(u_m)}{r(u_m|\theta)}$, $m = 1, \dots, M$.
3. Candidate selection: pick index m^* with probability $w_{m^*} / \sum_{j=1}^M w_j$ and set $u^* := u_{m^*}$.
4. Reverse draws: draw $u'_1, \dots, u'_M \stackrel{\text{i.i.d.}}{\sim} r(\cdot|u^*)$ on $K(\theta)$, force inclusion of the current point by setting $u'_1 = \theta$, and compute $w'_j = \frac{\pi(u'_j)}{r(u'_j|u^*)}$.
5. Accept/reject on the class: accept $\theta \rightarrow u^*$ with

$$\alpha_T(\theta, u^*) = \min \left\{ 1, \frac{\sum_{j=1}^M w'_j}{\sum_{m=1}^M w_m} \right\};$$

otherwise stay at θ .

We formalize this as Lemma 5 in the Appendix C.1.

Lemma 5 states that, for fixed θ , the within-class MTM transition S_θ is reversible with respect to the conditional target $T(\theta, \cdot)$ on $K(\theta)$. Hence $T(\theta, \cdot)$ is its stationary law. Define the Stage-1 kernel on Θ by $S(\theta, A) = S_\theta(\theta, A \cap K(\theta))$. Because π disintegrates along the partition $\{K(\theta)\}$ and each S_θ leaves $T(\theta, \cdot)$ invariant on its class, S preserves π :

$$\int_{\Theta} S(\theta, A) \pi(d\theta) = \pi(A) \quad \text{for all measurable } A \subset \Theta.$$

Remarks. (i) The support/mutual absolute continuity condition $r(u|\cdot) > 0$ whenever $\pi(u) > 0$ on $K(\theta)$ ensures the MTM weights and sums are well defined. (ii) Repeating the MTM update a few times within Stage 1 moves the intermediate law toward $T(\theta, \cdot)$ without changing π -invariance of the overall two-stage kernel.

B.2.2 MH Composition

Given a teleport kernel T in Equation (1), define the mixed proposal

$$\tilde{q}(\theta''|\theta) = \int T(\theta, d\theta') q(\theta''|\theta'),$$

which averages the local proposal q over the observationally equivalent set $K(\theta)$. The corresponding Metropolis–Hastings acceptance is

$$\tilde{\alpha}(\theta, \theta'') = \min\left\{1, \frac{\pi(\theta'')\tilde{q}(\theta|\theta'')}{\pi(\theta)\tilde{q}(\theta''|\theta)}\right\}.$$

Let \tilde{P}_P denote the resulting transition kernel. If T is the teleport in (1), then \tilde{P}_P is π -reversible. In general \tilde{P}_P is different from the sequential compositions PT and TP . They coincide only under additional symmetry.

A practical limitation is that $\tilde{q}(\theta''|\theta)$ requires integrating $q(\cdot|\theta')$ over $K(\theta)$ for each θ'' , which is typically intractable unless $K(\theta)$ is finite or very low dimensional. One way to work around this is to use exact auxiliary–variable realization. Use a within-class Multiple–Try Metropolis construction on $K(\theta)$: draw a forward set $u_1, \dots, u_M \sim T(\theta, \cdot)$, propose $\theta''_m \sim q(\cdot|u_m)$, select a candidate with the standard MTM weights, and mirror this with a reverse set drawn from $T(\theta'', \cdot)$. With the usual MTM acceptance based on the sums of forward and reverse weights, the resulting kernel is π -reversible and does not require evaluating \tilde{q} explicitly (see Appendix B.2.1). This targets π exactly (though it is not, for finite M , identical to \tilde{P}_P).

While exact and π -reversible, in general this variant can be either too restrictive or computationally burdensome. Using exact auxiliary variables requires multiple draws from T and q plus a matched reverse set at each iteration, and it scales poorly when $K(\theta)$ is large or high dimensional. Accordingly, we do not use it in our empirical applications and include it here for completeness.

B.2.3 Mixture Chain

Combine the local kernel P and the teleport kernel T from (1) into

$$\tilde{P}_H = (1 - \varepsilon)P + \varepsilon T, \quad \varepsilon \in [0, 1].$$

If both P and T are π -reversible, then \tilde{P}_H is π -reversible. A direct implementation is a coin flip at each iteration: with probability ε draw $\theta' \sim T(\theta, \cdot)$ and accept automatically; with probability $1 - \varepsilon$ perform the usual P -update (e.g., a Metropolis–Hastings step with symmetric proposal q).

Another alternative is to view the move as a single MH step with proposal

$$q_{\text{mix}}(\theta, \theta') = (1 - \varepsilon)q(\theta, \theta') + \varepsilon t(\theta, \theta'),$$

where t is a density representation of T . This requires a common dominating measure for q and t ; when $K(\theta)$ is lower dimensional, t is naturally defined with respect to an r -dimensional Hausdorff measure and a direct density mixture on the ambient space is not available unless one augments the state or reparametrizes. In practice, the coin-flip implementation above is preferred. It realizes \tilde{P}_H exactly and avoids measure-theoretic complications.

B.2.4 Batch Augmentation

This is the scheme used in Simulation 2. When sampling on $K(\theta_t)$ is significantly cheaper than running another local step of P , augmenting the exist Markov chain lead to much faster mixing without altering the invariant target. Let $\{\theta_t\}_{t \geq 1}$ be an ergodic Markov chain with invariant distribution π (e.g. a local MH/HMC kernel). At each iteration t with state θ_t , draw an auxiliary batch

$$U_{t,1}, \dots, U_{t,M} \stackrel{\text{i.i.d.}}{\sim} T(\theta_t, \cdot),$$

where $T(\theta, \cdot)$ is the teleport kernel in (1).

Under stationarity of $\{\theta_t\}$, each batch point $U_{t,j}$ is marginally π :

$$P(U_{t,j} \in A) = \int T(\theta, A)\pi(d\theta) = \pi(A), \quad A \subset \Theta \text{ measurable.}$$

Equivalently, the augmented pair has joint law $\tilde{\pi}(d\theta, du) = \pi(d\theta)T(\theta, du)$, whose θ -marginal is π . Therefore any Monte Carlo average built from the $U_{t,j}$'s targets the same π -expectations as the base chain.

If the per-iteration batch size is fixed ($M_t \equiv M$), one may stack all auxiliary draws and use the pooled empirical measure

$$\hat{\Pi}_{\text{stack}} = \frac{1}{NM} \sum_{t=1}^N \sum_{j=1}^M \delta_{U_{t,j}}$$

to approximate π and to compute π -averages $\int g d\hat{\Pi}_{\text{stack}}$. If M_t varies with t , a simple robust choice is the block average

$$\frac{1}{N} \sum_{t=1}^N \left(\frac{1}{M_t} \sum_{j=1}^{M_t} g(U_{t,j}) \right),$$

which remains consistent for $\int g(\theta) \pi(d\theta)$ and avoids unintended reweighting when M_t depends on θ_t .¹⁴

C Technical Details

First we state a few lemmas that are going to be used throughout most of the proofs.

C.1 Supplementary Results

Lemma 1 (Cheeger's Inequality). *Let P be a reversible Markov transition kernel with invariant measure π . Denote $\gamma(P)$ the spectral gap of P , and the conductance of P is defined as*

$$\mathbf{h}_P = \inf_{S \subseteq \Omega, 0 < \pi(S) \leq 1/2} \frac{\int_S P(\theta, S^c) \pi(d\theta)}{\pi(S)}.$$

Then

$$\frac{\mathbf{h}_P^2}{2} \leq \gamma(P) \leq 2\mathbf{h}_P.$$

Proof of this Lemma can be found in [Lawler and Sokal \(1988\)](#) or [Diaconis and Stroock \(1991\)](#).

Lemma 2 (State Decomposition Theorem). *Let $\{A_1, \dots, A_m\}$ be a partition of Ω . The transition kernel P_{A_i} of the restricted Markov chain is given by*

$$P_{A_i}(\theta, B) = P(\theta, B) + 1_B(\theta)P(\theta, A_i^c) \quad \text{for } \theta \in A_i, B \subset A_i$$

The “component” Markov chain with state space $\{1, \dots, m\}$ and transition probabilities is defined as:

$$P_H(i, j) = \frac{1}{2\pi(A_i)} \int_{A_i} P(\theta, A_j) \pi(d\theta) \quad \text{for } i \neq j$$

and $P_H(i, i) = 1 - \sum_{j \neq i} P_H(i, j)$. Then we have

$$\gamma(P) \geq \frac{1}{2} \gamma(P_H) \left(\min_{i=1, \dots, m} \gamma(P_{A_i}) \right).$$

A proof can be found in [Madras and Randall \(2002\)](#).

¹⁴Naively pooling $\sum_{t,j} g(U_{t,j}) / \sum_t M_t$ is also consistent if $\{M_t\}$ is independent of $\{\theta_t\}$. When M_t correlates with θ_t , block averaging is safer.

Lemma 3 (Lower Bound for δ -ball Random Walk). *Let π be a log-concave probability distribution on a convex set $A \subseteq \mathbb{R}^n$, and let its concentration be characterized by the parameter ν . Let P be the Metropolis-Hastings kernel on A with a δ -ball random walk proposal. For a universal constant $a > 0$, if the step size is chosen such that $\nu\delta \leq a$, the spectral gap γ of this kernel is bounded below by:*

$$\gamma \geq C \frac{(\nu\delta)^2}{n}$$

for a universal constant $C > 0$.

Proof can be found in [Kannan et al. \(1997\)](#).

Lemma 4 (Local Concentration of Log-Concave Measures). *Let π be a log-concave probability measure on \mathbb{R}^d with density*

$$\pi(\theta) \propto e^{-U(\theta)}, \quad U : \mathbb{R}^d \rightarrow (-\infty, \infty] \text{ convex.}$$

Let $\beta = \int \theta \pi(d\theta)$ be the mean, and let $\mu \in \arg \max_\theta \pi(\theta)$ be any mode. Then there exist constants $C \geq 1$ and $\nu > 0$ (depending on π) such that, for all $r > 0$,

$$\pi(\{\theta : \|\theta - \beta\| \geq r\}) \leq Ce^{-\nu r} \quad \text{and} \quad \pi(\{\theta : \|\theta - \mu\| \geq r\}) \leq Ce^{-\nu r}.$$

In particular, log-concavity implies exponentially decaying tails about both the mean and the mode, possibly with different constants.

Proof can be found in [Borell \(1974\)](#).

Lemma 5. *For fixed θ , the within-class MTM transition S_θ on $K(\theta)$ is reversible with respect to $T(\theta, \cdot)$; in particular, $T(\theta, \cdot)$ is a stationary distribution for S_θ .*

Proof. This is the detailed-balance result of Multiple-Try Metropolis in [Liu et al. \(2000, Theorem 1\)](#).

Proposition 1 (Stationary Distribution of the Composite Kernel).

Proof. By Equation(1),

$$T(\theta, A) = \frac{\int_{A \cap K(\theta)} \pi(u) \nu(du)}{\int_{K(\theta)} \pi(u) \nu(du)},$$

where $\pi(\cdot)$ denotes the ν -density of the target and ν is the reference (Lebesgue/Hausdorff/counting) measure.

For any measurable $A \subset \Theta$,

$$\int T(\theta, A) \pi(d\theta) = \int \frac{\int_{A \cap K(\theta)} \pi(u) \nu(du)}{\int_{K(\theta)} \pi(v) \nu(dv)} \pi(d\theta) = \int_{u \in A} \pi(u) \left[\int \frac{\mathbf{1}_{K(\theta)}(u)}{\int_{K(\theta)} \pi(v) \nu(dv)} \pi(d\theta) \right] \nu(du).$$

Fix u . If $\mathbf{1}_{K(\theta)}(u) = 1$ then $K(\theta) = K(u)$, so the denominator equals $\int_{K(u)} \pi(v)\nu(dv)$, which is also $\int_{K(u)} \pi(d\theta)$ since $\pi(d\theta) = \pi(\theta)\nu(d\theta)$ on $K(u)$. Hence

$$\int \frac{\mathbf{1}_{K(\theta)}(u)}{\int_{K(\theta)} \pi(v)\nu(dv)} \pi(d\theta) = \frac{\int_{K(u)} \pi(d\theta)}{\int_{K(u)} \pi(v)\nu(dv)} = 1,$$

and therefore

$$\int T(\theta, A)\pi(d\theta) = \int_{u \in A} \pi(u)\nu(du) = \pi(A).$$

By Fubini and the previous identity,

$$\int \tilde{P}(\theta, A)\pi(d\theta) = \int \left(\int P(z, A)T(\theta, dz) \right) \pi(d\theta) = \int P(z, A) \left(\int T(\theta, dz)\pi(d\theta) \right) = \int P(z, A)\pi(dz) = \pi(A),$$

because P is π -invariant. This proves \tilde{P} is π -invariant. \square

Proposition 5 (Reversibility). *Let T be the teleport kernel in Equation (1) with $Z(\theta) := \int_{K(\theta)} \pi(u)\nu(du) \in (0, \infty)$ for π -a.e. θ . Let P be any π -reversible Markov kernel on Θ . Define*

$$\bar{P} := \frac{1}{2}(PT) + \frac{1}{2}(TP), \quad \tilde{P}_H := (1 - \varepsilon)P + \varepsilon T, \quad \varepsilon \in [0, 1].$$

Then T , \bar{P} , and \tilde{P}_H are π -reversible.

Now assume in addition that P is a Metropolis–Hastings kernel with a symmetric local proposal $q(\cdot|\cdot)$, and define the fiber-averaged proposal

$$\tilde{q}(\theta''|\theta) := \int T(\theta, d\theta')q(\theta''|\theta').$$

Let \tilde{P}_P be the one-step MH kernel with proposal \tilde{q} and

$$\tilde{P}_P(\theta, d\theta'') := \tilde{q}(\theta''|\theta) \left[\tilde{\alpha}(\theta, \theta'')d\theta'' + (1 - \tilde{\alpha}(\theta, \theta''))\delta_\theta(d\theta'') \right], \quad \tilde{\alpha}(\theta, \theta'') = \min \left\{ 1, \frac{\pi(\theta'')\tilde{q}(\theta|\theta'')}{\pi(\theta)\tilde{q}(\theta''|\theta)} \right\}.$$

Then \tilde{P}_P is π -reversible.

In general \bar{P} , \tilde{P}_H , and \tilde{P}_P need not coincide. If, however, π is constant on each set $K(\theta)$ and

$$\tilde{q}(\theta''|\theta) = \tilde{q}(\theta|\theta'') \quad \text{for all } \theta, \theta'', \tag{3}$$

then

$$PT = TP = \tilde{P}_P, \quad \text{and hence} \quad \bar{P} = PT = \tilde{P}_P.$$

Proof. Reversibility of T . For any θ , write $Z(\theta) := \int_{K(\theta)} \pi(u)\nu(du) \in (0, \infty)$. By (1), if $B \subset \Theta$ is measurable then

$$T(\theta, B) = \frac{\pi(B \cap K(\theta))}{Z(\theta)}.$$

Hence, for measurable $A, B \subset \Theta$,

$$\begin{aligned} \int_A T(\theta, B) \pi(d\theta) &= \int_A \frac{\pi(B \cap K(\theta))}{Z(\theta)} \pi(d\theta) = \int_A \frac{\int_{K(\theta)} \mathbf{1}_B(u) \pi(u) \nu(du)}{Z(\theta)} \pi(d\theta) \\ &= \int_{\Theta} \int_{\Theta} \mathbf{1}_A(\theta) \mathbf{1}_B(u) \mathbf{1}_{\{u \in K(\theta)\}} \frac{\pi(u)}{Z(\theta)} \nu(du) \pi(d\theta). \end{aligned}$$

If $u \in K(\theta)$ then $K(u) = K(\theta)$ and $Z(u) = Z(\theta)$. Using this, switch the order of integration and integrate first in θ :

$$\begin{aligned} \int_A T(\theta, B) \pi(d\theta) &= \int_{\Theta} \mathbf{1}_B(u) \frac{\pi(u)}{Z(u)} \left[\int_{\Theta} \mathbf{1}_A(\theta) \mathbf{1}_{\{\theta \in K(u)\}} \pi(d\theta) \right] \nu(du) \\ &= \int_{\Theta} \mathbf{1}_B(u) \frac{\pi(u)}{Z(u)} \pi(A \cap K(u)) \nu(du). \end{aligned}$$

Now group this outer integral by the partition $\{K(u)\}$: for any fixed class $K(u)$ the factor $\pi(A \cap K(u))/Z(u)$ is constant over that class, so integrating $\mathbf{1}_B(u)\pi(u)$ over $u \in K(u)$ yields $\pi(B \cap K(u))$. Therefore

$$\int_A T(\theta, B) \pi(d\theta) = \int_{\Theta} \frac{\pi(A \cap K(u)) \pi(B \cap K(u))}{Z(u)} \nu(du),$$

and the right-hand side is symmetric in A and B . Hence it also equals $\int_B T(\theta, A) \pi(d\theta)$, proving that T is π -reversible.

Reversibility of \bar{P} . For bounded measurable $f, g \geq 0$,

$$\int f(\theta) (PT)g(\theta) \pi(d\theta) = \int (Tf)(\theta) Pg(\theta) \pi(d\theta) = \int (PTf)(\theta) g(\theta) \pi(d\theta),$$

using detailed balance for P and T . With $f = \mathbf{1}_A$, $g = \mathbf{1}_B$ this yields $\int_A (PT)(\theta, B) \pi(d\theta) = \int_B (TP)(\theta, A) \pi(d\theta)$. Therefore

$$\int_A \bar{P}(\theta, B) \pi(d\theta) = \frac{1}{2} \int_A (PT)(\theta, B) \pi(d\theta) + \frac{1}{2} \int_A (TP)(\theta, B) \pi(d\theta) = \int_B \bar{P}(\theta, A) \pi(d\theta),$$

so \bar{P} is π -reversible.

Reversibility of \tilde{P}_H . A convex combination of π -reversible kernels is π -reversible:

$$\int_A \tilde{P}_H(\theta, B) \pi(d\theta) = (1 - \varepsilon) \int_A P(\theta, B) \pi(d\theta) + \varepsilon \int_A T(\theta, B) \pi(d\theta) = \int_B \tilde{P}_H(\theta, A) \pi(d\theta).$$

Reversibility of \tilde{P}_P . This is the standard Metropolis–Hastings detailed balance identity with proposal \tilde{q} and acceptance $\tilde{\alpha}$.

Equality Assume π is constant on each $K(\theta)$. Write the MH acceptance in P as $\alpha(\theta', \theta'') =$

$\min\{1, \pi(\theta'')/\pi(\theta')\}$ with symmetric q . If $\theta' \in K(\theta)$, then $\pi(\theta') = \pi(\theta)$, so $\alpha(\theta', \theta'') = \min\{1, \pi(\theta'')/\pi(\theta)\}$ is constant in θ' . Hence, for measurable A ,

$$\begin{aligned} (PT)(\theta, A) &= \int_{K(\theta)} T(\theta, d\theta') \left[\int_A q(\theta''|\theta') \alpha(\theta', \theta'') d\theta'' + \mathbf{1}_A(\theta') \int (1 - \alpha(\theta', z)) q(z|\theta') dz \right] \\ &= \int_A \min \left\{ 1, \frac{\pi(\theta'')}{\pi(\theta)} \right\} \underbrace{\left(\int_{K(\theta)} q(\theta''|\theta') T(\theta, d\theta') \right) d\theta''}_{= \tilde{q}(\theta''|\theta)} \\ &\quad + \mathbf{1}_A(\theta) \int \left(1 - \min \left\{ 1, \frac{\pi(z)}{\pi(\theta)} \right\} \right) \tilde{q}(z|\theta) dz. \end{aligned}$$

If, in addition, (3) holds, then $\tilde{q}(\theta''|\theta) = \tilde{q}(\theta|\theta'')$, so the one-step MH acceptance reduces to $\tilde{\alpha}(\theta, \theta'') = \min\{1, \pi(\theta'')/\pi(\theta)\}$ and the last two displays coincide with

$$\tilde{P}_P(\theta, A) = \int_A \tilde{q}(\theta''|\theta) \tilde{\alpha}(\theta, \theta'') d\theta'' + \mathbf{1}_A(\theta) \int (1 - \tilde{\alpha}(\theta, z)) \tilde{q}(z|\theta) dz.$$

Therefore $PT = \tilde{P}_P$. By the same symmetry, TP yields the same transition law, so $TP = PT = \tilde{P}_P$, and consequently $\bar{P} = PT$. \square

Proposition 6 (Spectral Bounds). *Let P and T be π -reversible Markov kernels and define the reversibilized two-step kernel*

$$\bar{P} = \frac{1}{2}(PT + TP).$$

For $\varepsilon \in [0, 1]$ set the hybrid kernel $\tilde{P}_H = (1 - \varepsilon)P + \varepsilon T$. Let q be a proposal density and define the teleported proposal

$$\tilde{q}(y|x) = \int T(x, d\eta) q(y|\eta),$$

and let \tilde{P}_P be the Metropolis–Hastings kernel with target π and proposal \tilde{q} . Assume there exists a version $\bar{p}(x, y)$ of the density of $\bar{P}(x, dy)$ w.r.t. a reference measure such that, for some $m \in (0, 1]$,

$$\tilde{q}(y|x) \geq m\bar{p}(x, y) \quad \text{for } \pi\text{-a.e. } (x, y).$$

Then:

$$\gamma(\tilde{P}_H) \geq \varepsilon(1 - \varepsilon)\gamma(\bar{P}), \quad \gamma(\tilde{P}_P) \geq m\gamma(\bar{P}).$$

In particular, with $\varepsilon = \frac{1}{2}$ one has $\gamma(\frac{1}{2}P + \frac{1}{2}T) \geq \frac{1}{4}\gamma(\bar{P})$.

Proof. Fix $f \in L_2^0(\pi)$ with $\|f\| = 1$ and put $a := 1 - \langle Pf, f \rangle \geq 0$, $b := 1 - \langle Tf, f \rangle \geq 0$. Then

$$1 - |\langle \tilde{P}_H f, f \rangle| \geq 1 - \langle \tilde{P}_H f, f \rangle = (1 - \varepsilon)a + \varepsilon b.$$

Further, using $Tf = f - (I - T)f$ and $Pf = f - (I - P)f$,

$$\langle \bar{P}f, f \rangle = \langle Tf, Pf \rangle = 1 - a - b + \langle (I - T)f, (I - P)f \rangle \leq 1 - a - b + \|(I - T)f\| \|(I - P)f\|.$$

Since $\|(I - P)f\|^2 \leq 2a$ and $\|(I - T)f\|^2 \leq 2b$, we get

$$\langle \bar{P}f, f \rangle \leq 1 - a - b + 2\sqrt{ab}, \quad \text{hence} \quad 1 - |\langle \bar{P}f, f \rangle| \geq (\sqrt{a} - \sqrt{b})^2.$$

By the elementary inequality

$$(1 - \varepsilon)a + \varepsilon b \geq \varepsilon(1 - \varepsilon)(\sqrt{a} - \sqrt{b})^2 \quad (\varepsilon \in [0, 1], a, b \geq 0),$$

we conclude

$$1 - |\langle \tilde{P}_H f, f \rangle| \geq \varepsilon(1 - \varepsilon)(1 - |\langle \bar{P}f, f \rangle|).$$

Taking the supremum over unit $f \in L_2^0(\pi)$ yields $\gamma(\tilde{P}_H) \geq \varepsilon(1 - \varepsilon)\gamma(\bar{P})$.

For MH with proposal \tilde{q} ,

$$1 - \langle \tilde{P}_P f, f \rangle = \frac{1}{2} \iint (f(y) - f(x))^2 \min\{\pi(x)\tilde{q}(y | x), \pi(y)\tilde{q}(x | y)\} dxdy.$$

By the coverage assumption and detailed balance of \bar{P} ,

$$\min\{\pi(x)\tilde{q}(y | x), \pi(y)\tilde{q}(x | y)\} \geq m\pi(x)\bar{p}(x, y),$$

hence

$$1 - \langle \tilde{P}_P f, f \rangle \geq m\frac{1}{2} \iint (f(y) - f(x))^2 \pi(x)\bar{p}(x, y) dxdy = m(1 - \langle \bar{P}f, f \rangle).$$

Thus $1 - |\langle \tilde{P}_P f, f \rangle| \geq m(1 - |\langle \bar{P}f, f \rangle|)$ for all unit $f \in L_2^0(\pi)$, and taking suprema gives $\gamma(\tilde{P}_P) \geq m\gamma(\bar{P})$. \square

Proposition 7 (Two parameters, finite states). *Let $\Omega = \{1, \dots, m\}^2$ and define*

$$\pi(\theta_1, \theta_2) = \begin{cases} a, & \text{if } \theta_1 = \theta_2, \\ b, & \text{if } \theta_1 \neq \theta_2, \end{cases} \quad 0 < b < a, \quad ma + m(m-1)b = 1.$$

Let $D := \{(\theta, \theta) : \theta = 1, \dots, m\}$ (the diagonal) and $O := \Omega \setminus D$. Let P be the random-scan single-site Gibbs kernel. Define a teleport kernel T by

$$T(x, y) = \begin{cases} \frac{1}{m}, & x \in D, y \in D, \\ \mathbf{1}_{\{y=x\}}, & x \in O, \\ 0, & \text{otherwise.} \end{cases}$$

Then T is π -reversible, and with

$$\bar{P} := \frac{1}{2}(PT) + \frac{1}{2}(TP),$$

we have, in the limit $b \rightarrow 0$ (equivalently $a \rightarrow 1/m$),

$$\gamma(P) \rightarrow 0 \quad \text{and} \quad \gamma(\bar{P}) \rightarrow 1.$$

Proof. Define U_D to be the uniform distribution on D , i.e.

$$U_D(y) = \begin{cases} 1/m, & y \in D, \\ 0, & y \in O. \end{cases}$$

(i) *Standard Gibbs P .* Let the conductance of P be

$$\mathbf{h}_P := \min_{\substack{S \subset \Omega \\ \pi(S) \leq 1/2}} \frac{\sum_{x \in S} \pi(x) P(x, S^c)}{\pi(S)}.$$

By Cheeger's inequality, $\gamma(P) \leq 2\mathbf{h}_P$. Fix $S \subset D$ with $\pi(S) \approx 1/2$ (this is possible since $\pi(D) \rightarrow 1$ as $b \rightarrow 0$). For any $x \in D$, the random-scan single-site Gibbs update changes exactly one coordinate, so it cannot jump from (i, i) to (j, j) with $j \neq i$ in one step. Hence from $x \in D$,

$$P(x, S^c) = P(x, O).$$

By symmetry of the model,

$$P(x, O) = \frac{(m-1)b}{a + (m-1)b} \quad \text{for every } x \in D.$$

Therefore

$$\sum_{x \in S} \pi(x) P(x, S^c) = \sum_{x \in S} \pi(x) P(x, O) = \frac{(m-1)b}{a + (m-1)b} \sum_{x \in S} \pi(x) = \frac{(m-1)b}{a + (m-1)b} \pi(S),$$

so

$$\Phi_P(S) = \frac{\sum_{x \in S} \pi(x) P(x, S^c)}{\pi(S)} = \frac{(m-1)b}{a + (m-1)b} \xrightarrow{b \rightarrow 0} 0.$$

Hence $\mathbf{h}_P \rightarrow 0$ and thus $\gamma(P) \rightarrow 0$.

(ii) *Identification-aware \bar{P} .*

Fix $x \in D$ and $y \in D$. A direct one-step computation gives

$$(PT)(x, y) = \frac{a}{a + (m-1)b} \cdot \frac{1}{m}, \quad (TP)(x, y) = \frac{a}{a + (m-1)b} \cdot \frac{1}{m},$$

because from any diagonal state a single Gibbs update stays on the same diagonal with probability

$a/(a + (m-1)b)$, and T uniformizes on D (or, in the TP term, T first puts U_D and then P can only remain on the same diagonal). Therefore, for all $x \in D$ and $y \in D$,

$$\bar{P}(x, y) = \frac{1}{2}(PT)(x, y) + \frac{1}{2}(TP)(x, y) = \frac{a}{a + (m-1)b} \cdot \frac{1}{m}.$$

Summing over $y \in D$ yields

$$\bar{P}(x, D) = \frac{a}{a + (m-1)b} \xrightarrow[b \rightarrow 0]{} 1, \quad \bar{P}(x, O) = 1 - \bar{P}(x, D) \xrightarrow[b \rightarrow 0]{} 0.$$

Thus, entrywise for $x \in D$ and $y \in D$,

$$\bar{P}(x, y) \xrightarrow[b \rightarrow 0]{} U_D(y),$$

and the restriction of \bar{P} to D converges to the rank-one kernel with all rows equal to U_D . Since $\pi(D) \rightarrow 1$ and $\bar{P}(x, O) \rightarrow 0$ for $x \in D$, the second-largest eigenvalue of \bar{P} (in $L_2(\pi)$) satisfies $\lambda_2(\bar{P}) \rightarrow 0$, hence $\gamma(\bar{P}) = 1 - \lambda_2(\bar{P}) \rightarrow 1$. \square

Proposition 8 (1-D two modes). *Let the state space be a one-dimensional circle Ω of circumference $4L$, represented by $[-2L, 2L]$ with endpoints connected. The target π is bimodal:*

$$\pi(\theta) \propto \begin{cases} e^{-\nu|\theta|}, & \theta \in [-L, L], \\ e^{-\nu(2L-|\theta|)}, & \theta \in [-2L, -L) \cup (L, 2L], \end{cases}$$

with $\nu > 0$.

1. *Standard sampler.* Let P be Metropolis–Hastings with a symmetric δ -ball random walk. Then there is $C_1 > 0$ such that

$$\gamma(P) \leq C_1 e^{-\nu(L-\delta)}.$$

2. *Identification-aware RWM.* Let

$$s(\theta) = \begin{cases} \theta + 2L, & \theta \in [-2L, 0), \\ \theta - 2L, & \theta \in [0, 2L). \end{cases}$$

and define the teleport kernel

$$T(\theta, \cdot) = \frac{1}{2}\delta_\theta(\cdot) + \frac{1}{2}\delta_{s(\theta)}(\cdot), \quad \delta_\theta(\cdot) \text{ denotes the Dirac measure at } \theta$$

Let $\tilde{P} := PT$. There exist constants $c_0, C_2 > 0$ such that if $\delta \leq c_0/\nu$, then

$$\gamma(\tilde{P}) \geq C_2,$$

uniformly in L and ν .

Proof. (1) δ -ball RWM. Write $A = [-L, L]$ and $A^c = \Omega \setminus A$. By symmetry, $\pi(A) = \pi(A^c) = 1/2$. A move from A to A^c can occur only from the boundary strips $[L - \delta, L]$ and $[-L, -L + \delta]$. Hence

$$\mathbf{h}_P(A) = \frac{1}{\pi(A)} \int_A P(\theta, A^c) \pi(d\theta) \leq \frac{1}{\pi(A)} \int_{A \cap \partial_\delta A} \pi(\theta) d\theta = \frac{2}{\pi(A)} \int_{L-\delta}^L c e^{-\nu\theta} d\theta = \frac{4c}{\nu} (e^{-\nu(L-\delta)} - e^{-\nu L}),$$

where c is the normalizing constant inside A and $\partial_\delta A$ is the δ -neighborhood of the boundary. Thus $\mathbf{h}_P(A) \leq C e^{-\nu(L-\delta)}$, and Cheeger's inequality gives $\gamma(P) \leq 2\mathbf{h}_P \leq C_1 e^{-\nu(L-\delta)}$ for a possibly different constant C_1 .

(2) Identification-aware RWM.

For any $\theta \in A$,

$$\tilde{P}(\theta, A^c) = \frac{1}{2} P(\theta, A^c) + \frac{1}{2} P(s(\theta), A^c).$$

By translation invariance of the δ -ball proposal and the symmetry $\pi(s(\cdot)) = \pi(\cdot)$,

$$P(s(\theta), A) = P(\theta, A^c), \quad P(s(\theta), A^c) = 1 - P(\theta, A^c),$$

hence for every $\theta \in A$,

$$\tilde{P}(\theta, A^c) = \frac{1}{2}.$$

Averaging over $\theta \in A$ gives the across-component conductance exactly:

$$\mathbf{h}_{\tilde{P}}(A) = \frac{1}{\pi(A)} \int_A \tilde{P}(\theta, A^c) \pi(d\theta) = \frac{1}{2}.$$

The induced two-state chain on $\{A, A^c\}$ has off-diagonal probability $1/2$, so $\gamma(\tilde{P}_H) = 1$.

Let P_A be the MH kernel on A targeting $\pi_A(\theta) \propto e^{-\nu|\theta|}$ with the same symmetric δ -ball proposal (and similarly P_{A^c} on A^c). From Lemma 3, there exist constants $C' > 0$ and $c_0 > 0$ such that

$$\gamma(P_A) \geq C'(\nu\delta)^2, \quad \gamma(P_{A^c}) \geq C'(\nu\delta)^2, \quad \text{whenever } \nu\delta \leq c_0.$$

The restriction of $\tilde{P} = PT$ to A is

$$(\tilde{P})_A = \frac{1}{2} I_A + \frac{1}{2} P_A,$$

because the branch $T(\theta, \cdot) = \delta_{s(\theta)}$ starts outside A and contributes a self-loop under restriction, while the branch $T(\theta, \cdot) = \delta_\theta$ followed by P gives P_A . For reversible kernels, $\gamma(\frac{1}{2}I + \frac{1}{2}K) = \frac{1}{2}\gamma(K)$, hence

$$\gamma((\tilde{P})_A) \geq \frac{1}{2}\gamma(P_A) \geq \frac{C'}{2}(\nu\delta)^2, \quad \gamma((\tilde{P})_{A^c}) \geq \frac{C'}{2}(\nu\delta)^2.$$

By the bound in Lemma 2,

$$\gamma(\tilde{P}) \geq \frac{1}{2}\gamma(\tilde{P}_H) \min \left\{ \gamma((\tilde{P})_A), \gamma((\tilde{P})_{A^c}) \right\} \geq \frac{1}{2} \cdot 1 \cdot \frac{C'}{2}(\nu\delta)^2 = C_2(\nu\delta)^2,$$

for $C_2 = C'/4$ and any $\nu\delta \leq c_0$. Choosing $\delta \propto 1/\nu$ makes the lower bound a positive constant independent of L , as claimed. \square

Proposition 9 (Gaussian RWM). *Let π be a probability density on a connected $\Omega \subset \mathbb{R}^n$. Suppose the support decomposes into m disjoint open connected components A_1, \dots, A_m with $\pi(\cup_i A_i) = 1$. For each i , set $w_i = \pi(A_i)$, define $\pi_i(B) = \pi(B \cap A_i)/w_i$, pick a mode $\mu_i \in A_i$ of π restricted to A_i , and write $d_i = \text{dist}(\mu_i, \partial A_i)$ and $d_* = \min_i d_i$.*

Assume:

(SLC) *Strong log-concavity: For each i , $\pi_i(\theta) \propto e^{-U_i(\theta)}$ on A_i with*

$$\nabla^2 U_i(\theta) \succeq m_i I_n \quad \text{for all } \theta \in A_i, \quad m_{\min} := \min_i m_i > 0.$$

Moreover, there exists $\delta > 0$ such that $A_i^{\text{int}} := \{\theta \in A_i : \text{dist}(\theta, \partial A_i) \geq \delta\} \neq \emptyset$, and on A_i^{int} the Hessian is bounded above:

$$\nabla^2 U_i(\theta) \preceq L_i I_n \quad \text{for all } \theta \in A_i^{\text{int}}, \quad L_{\max} := \max_i L_i < \infty.$$

In particular, for all $r \in (0, d_i]$ there exist $c_i \geq 1$ and $\nu_i > 0$ with

$$\pi_i(\{\theta \in A_i : \|\theta - \mu_i\| \geq r\}) \leq c_i e^{-\nu_i r}.$$

Write $c_{\max} = \max_i c_i$, $\nu_{\min} = \min_i \nu_i$, and $\nu_{\max} = \max_i \nu_i$.

(TEL) *Teleport kernel: T is π -reversible and there exist $\varepsilon_1 \in (0, 1]$, $\varepsilon_2 > 0$, $\varepsilon_0 > 0$, and measurable cores $A_i^\circ \subset A_i$ with $\pi_i(A_i^\circ) \geq \varepsilon_1$ such that for all $i \neq j$ and all $\theta \in A_i^\circ$,*

$$T(\theta, A_j^{\text{int}}) \geq \varepsilon_2 \quad \text{and} \quad T(\theta, A_i^{\text{int}}) \geq \varepsilon_0.$$

Let P be the Metropolis–Hastings kernel with Gaussian random-walk proposal $q(\theta, \cdot) = \mathcal{N}(\theta, \sigma^2 I_n)$ ($\sigma > 0$) and let

$$\bar{P} := \frac{1}{2}(PT) + \frac{1}{2}(TP).$$

Then:

1. *For any $\sigma > 0$,*

$$\gamma(P) \leq 2c_{\max} \exp\left(-\frac{1}{2}\nu_{\min} d_*\right).$$

2. *There exists $c_0 > 0$ (independent of $\{d_i\}$ and all inter-mode separations) such that*

$$\gamma(\bar{P}) \geq c_0.$$

Proof. Part (1): Gaussian RWM. Fix i with $\pi(A_i) \leq 1/2$ and set $C_i = \{\theta \in A_i : \|\theta - \mu_i\| \leq d_i/2\}$ and $S_i = A_i \setminus C_i$. By strong log-concavity concentration, $\pi(S_i) = \pi(A_i)\pi_i(S_i) \leq \pi(A_i)c_i e^{-\nu_i d_i/2}$. If $\theta \in C_i$, a one-step exit requires a jump of length at least $d_i/2$, so with $Z \sim \mathcal{N}(0, \sigma^2 I_n)$,

$$P(\theta, A_i^c) \leq \Pr(\|Z\| \geq d_i/2) \leq C_n \exp\left(-\frac{d_i^2}{8\sigma^2}\right),$$

for a constant C_n depending only on n . Therefore

$$\begin{aligned} Q(A_i, A_i^c) &= \int_{A_i} P(\theta, A_i^c) \pi(d\theta) \\ &\leq \int_{C_i} P(\theta, A_i^c) \pi(d\theta) + \int_{S_i} \pi(d\theta) \leq \pi(A_i) \left[C_n e^{-d_i^2/(8\sigma^2)} + c_i e^{-\nu_i d_i/2} \right]. \end{aligned}$$

Thus $\mathbf{h}_P(A_i) := Q(A_i, A_i^c)/\pi(A_i) \leq C_n e^{-d_i^2/(8\sigma^2)} + c_i e^{-\nu_i d_i/2}$. Pick i with $d_i = d_*$. Then $\mathbf{h}_P \leq \mathbf{h}_P(A_i)$ and Cheeger's inequality (Lemma 1) gives

$$\gamma(P) \leq 2\mathbf{h}_P \leq 2C_n e^{-d_*^2/(8\sigma^2)} + 2c_{\max} e^{-\nu_{\min} d_*/2},$$

which implies the stated bound.

Part (2): IA-RWM $\bar{P} = \frac{1}{2}(PT) + \frac{1}{2}(TP)$. Apply the state-decomposition bound (Lemma 2) to \bar{P} :

$$\gamma(\bar{P}) \geq \frac{1}{2}\gamma_H \min_{1 \leq i \leq m} \gamma_i,$$

where γ_H is the spectral gap of the aggregated chain \bar{P}_H on $\{1, \dots, m\}$ with stationary weights $w_i = \pi(A_i)$, and γ_i is the spectral gap of the restriction of \bar{P} to A_i .

Fix $i \neq j$ and $\theta \in A_i^\circ$. By (TEL), $T(\theta, A_j^{\text{int}}) \geq \varepsilon_2$. For $z \in A_j^{\text{int}}$, choose any $\rho \in (0, \delta]$ such that $B(z, \rho) \subset A_j$. The Gaussian proposal places mass $\Pr(\|Z\| \leq \rho) > 0$ there, and on A_j^{int} the L_{\max} -smoothness implies, for $u \in B(z, \rho)$,

$$\frac{\pi(u)}{\pi(z)} = e^{-(U(u) - U(z))} \geq e^{-\frac{1}{2}L_{\max}\rho^2}.$$

Hence

$$\inf_{z \in A_j^{\text{int}}} P(z, A_j) \geq p_s := \Pr(\|Z\| \leq \rho) e^{-\frac{1}{2}L_{\max}\rho^2} > 0.$$

Therefore $(PT)(\theta, A_j) \geq \varepsilon_2 p_s$ and, since $\bar{P} = \frac{1}{2}(PT) + \frac{1}{2}(TP)$,

$$\bar{P}(\theta, A_j) \geq \frac{1}{2}\varepsilon_2 p_s.$$

Integrating over $\theta \in A_i$ and using $\pi_i(A_i^\circ) \geq \varepsilon_1$,

$$\bar{P}_H(i, j) = \frac{1}{\pi(A_i)} \int_{A_i} \bar{P}(\theta, A_j) \pi(d\theta) \geq \frac{1}{2} \varepsilon_1 \varepsilon_2 p_s,$$

and a standard comparison with the complete-graph random walk yields

$$\gamma_H \geq \frac{1}{2} \min \left\{ 1, \frac{1}{2} m \varepsilon_1 \varepsilon_2 p_s \right\}.$$

Consider the restriction of \bar{P} to a fixed A_i . Using (TEL), for any $\theta \in A_i^\circ$,

$$\bar{P}(\theta, \cdot) \geq \frac{1}{2} (TP)(\theta, \cdot) \geq \frac{1}{2} \int_{A_i^{\text{int}}} T(\theta, dz) P(z, \cdot).$$

Fix $\rho \in (0, \delta]$ and choose an arbitrary ball $B_i \subset A_i^{\text{int}}$ of radius ρ . As above, for any $z \in A_i^{\text{int}}$ the Gaussian RWM step has

$$P(z, B_i) \geq \Pr(\|Z\| \leq \rho) e^{-\frac{1}{2} L_{\max} \rho^2} \cdot \frac{\lambda(B_i)}{\lambda(B(0, \rho))} =: a_0 > 0,$$

where λ is Lebesgue measure (the last factor is the conditional probability that a proposal inside $B(z, \rho)$ lands in the fixed B_i , which is positive by overlap of balls of the same radius in a connected interior). Consequently, for all $\theta \in A_i^\circ$,

$$\bar{P}(\theta, \cdot) \geq \frac{1}{2} \varepsilon_0 a_0 \cdot \text{Unif}(B_i)(\cdot) =: \eta_* m_i(\cdot),$$

with $\eta_* = \frac{1}{2} \varepsilon_0 a_0 > 0$ and m_i the uniform law on B_i . This one-step Doeblin minorization on a set of positive π_i -mass implies a strictly positive spectral gap for the restriction (e.g., by standard minorization \Rightarrow uniform ergodicity on the small set and aperiodicity), and the elementary bound

$$\gamma_i \geq 1 - \sqrt{1 - \eta_*} \geq \frac{1}{2} \eta_*,$$

using $1 - \sqrt{1 - x} \geq x/2$ for $x \in [0, 1]$. Taking the minimum over i gives the displayed lower bound for $\min_i \gamma_i$.

Combining the inter- and within-mode bounds in the decomposition inequality yields the stated $c_0 > 0$, with dependence only on $(\varepsilon_1, \varepsilon_2, \varepsilon_0, \delta, n, \sigma, L_{\max}, m)$ and, in particular, independent of $\{d_i\}$. \square

Proposition 10. *Let the parameter space be*

$$\Theta_D = X \times Y_D \subset \mathbb{R}^{m+r}, \quad d = m + r,$$

where $X \subset \mathbb{R}^m$ is bounded and convex with nonempty interior, and

$$Y_D = D \cdot G_0, \quad G_0 \subset \mathbb{R}^r,$$

with G_0 bounded and satisfying the tube condition: there exists $C_G < \infty$ such that for all $\eta \in (0, 1]$, $|\{y \in G_0 : \text{dist}(y, \partial G_0) \leq \eta\}| \leq C_G \eta$. Then $|Y_D| = |G_0|D^r$.

Let the target density factor as $\pi_D(\theta_x, \theta_y) = p(\theta_x)u_D(\theta_y)$, where u_D is the uniform density on Y_D and p is continuous on X with

$$0 < p_{\min} \leq p(\theta_x) \leq p_{\max} < \infty \quad \forall \theta_x \in X.$$

Let the Random Walk Metropolis proposal be translation-invariant and symmetric,

$$q(\theta, \theta') = g(\theta' - \theta),$$

where g satisfies: (i) there exist $\delta > 0$ and $c_g > 0$ such that $g(z) \geq c_g$ for all $\|z\| \leq \delta$; and (ii) with $\overline{G}(t) := \int_{\|z\| > t} g(z)dz$ one has

$$\int_0^\infty \overline{G}(t)dt \leq T_g < \infty.$$
¹⁵

Consider two Markov kernels. First, P denotes the local RWM on Θ_D using proposal g and standard Metropolis–Hastings acceptance. Second, define the teleport kernel T by

$$T((\theta_x, \theta_y), (\theta'_x, \theta'_y)) = \mathbf{1}_{\{\theta'_x = \theta_x\}} \frac{\mathbf{1}_{\{\theta'_y \in Y_D\}}}{|Y_D|},$$

and set the IA–RWM kernel

$$\bar{P} := \frac{1}{2}(PT) + \frac{1}{2}(TP).$$

Then:

1. There exists a constant $C_1 < \infty$, independent of D , such that the spectral gap of P satisfies

$$\gamma(P) \leq \frac{C_1}{D}.$$

In particular, $\gamma(P) \rightarrow 0$ at least at rate D^{-1} as $D \rightarrow \infty$.

2. There exist $n \in \mathbb{N}$, $\varepsilon_0 > 0$, and a probability measure ν on Θ_D (all independent of D) such that, for all sufficiently large D and all $\theta \in \Theta_D$,

$$\bar{P}^n(\theta, \cdot) \geq \varepsilon_0 \nu(\cdot).$$

¹⁵These conditions hold, for example, for Gaussian proposals and for proposals with exponentially decaying tails, and also for compact-support proposals.

Hence \bar{P} is uniformly ergodic for all large D , and its spectral gap is bounded below by a positive constant independent of D .

Proposition 10 (Cylinder Space)

Proof. We prove (1) and (2) in turn.

(1) *Upper bound for P .* Fix a hyperplane cut along the growing block: choose $t \in \mathbb{R}$ so that

$$|\{y \in G_0 : y_1 \leq t\}| = \frac{1}{2}|G_0|$$

and define

$$A := X \times \{y \in Y_D : y_1 \leq Dt\}.$$

Then $|A| = \frac{1}{2}|X||Y_D|$ and, because $\pi_D(\theta) = p(\theta_x)/|Y_D|$, we have $\pi_D(A) = 1/2$.

For $\eta > 0$, define the η -tube around the cut in Y_D :

$$S_{D,\eta} := \{y \in Y_D : |y_1 - Dt| \leq \eta\}.$$

By the tube condition on G_0 and scaling, the tube volume scales linearly in η :

$$|S_{D,\eta}| \leq C_G D^{r-1} \eta$$

for some C_G depending only on G_0 . Hence

$$\frac{|X||S_{D,\eta}|}{|X||Y_D|} = \frac{|S_{D,\eta}|}{|Y_D|} \leq \frac{C_G}{|G_0|} \frac{\eta}{D}.$$

Write $Z \sim g$ and $\bar{G}(t) = \Pr(\|Z\| > t)$. For $\theta \in A$, decompose

$$P(\theta, A^c) \leq \Pr(\text{cross the cut with } \|Z\| \leq \delta) + \Pr(\|Z\| > \text{dist}(y, \text{cut})).$$

Integrating over $\theta \in A$ against π_D , the first term is supported on $X \times S_{D,\delta}$ and is bounded by

$$\int_A \pi_D(\theta) \mathbf{1}_{\{y \in S_{D,\delta}\}} d\theta \leq p_{\max} \frac{|S_{D,\delta}|}{|Y_D|} \leq p_{\max} \frac{C_G}{|G_0|} \frac{\delta}{D}.$$

For the long-jump term, the distance $S := |y_1 - Dt|$ along the growing coordinate has density under u_D bounded by C_a/D , where C_a depends only on G_0 . Hence, by Fubini and monotonicity of \bar{G} ,

$$\int_A \pi_D(\theta) \Pr(\|Z\| > S) d\theta \leq p_{\max} \frac{C'}{D} \int_0^\infty \bar{G}(s) ds \leq p_{\max} \frac{C'T_g}{D}.$$

Combining these and using $\pi_D(A) = 1/2$, the conductance of A satisfies

$$\Phi(A) = \frac{\int_A \pi_D(\theta) P(\theta, A^c) d\theta}{\pi_D(A)} \leq \frac{2p_{\max}}{D} \left(\frac{C_G}{|G_0|} \delta + C' T_g \right) = \frac{C_\Phi}{D}.$$

For reversible P , Cheeger's inequality yields $\gamma(P) \leq 2\mathbf{h}(P) \leq 2\Phi(A) \leq 2C_\Phi/D$. This proves (1).

(2) *Doeblin minorization for \bar{P}^n , uniform in D .* Let

$$Y_{\text{int}} := \{y \in Y_D : \text{dist}(y, \partial Y_D) \geq \delta/2\}.$$

By the tube estimate, there is a constant C_Y (depending only on G_0) such that $u_D(Y_{\text{int}}) \geq 1 - C_Y \delta/D$. Because X is bounded and convex with nonempty interior, pick a closed ball

$$R_x := \overline{B}(x^*, \rho) \subset \text{int}(X), \quad 0 < \rho \leq \delta/4.$$

Define the product set and reference measure

$$T := R_x \times Y_{\text{int}} \subset \Theta_D, \quad \nu(\cdot) := \frac{\pi_D(\cdot \cap T)}{\pi_D(T)}.$$

Note that $\pi_D(T) \geq \mu_x(R_x) p_{\min} (1 - C_Y \delta/D)$, so $\pi_D(T)$ is bounded below uniformly in D for all large D .

Consider the kernel (PT) (teleport in y to u_D , then one local RWM step). Fix any starting state $\theta = (x, y) \in \Theta_D$. After applying T we are at (x, \tilde{y}) with $\tilde{y} \sim u_D$. Conditional on $\tilde{y} \in Y_{\text{int}}$, connect x to x^* by a polygonal chain inside X with steps of length at most $\delta/4$ and cover it by closed d -balls of radius $\delta/8$. The number of steps is bounded by $n_0 \leq C_{\text{path}}$, where C_{path} depends only on $\text{diam}(X)$ and δ (hence independent of D). At each local RWM step, the proposal density satisfies $g \geq c_g$ on $B(0, \delta)$, so the probability to land in the next $\delta/8$ -ball is at least

$$\underline{q} := c_g \text{vol}(B_d(0, \delta/8)) > 0,$$

and the Metropolis acceptance probability is at least

$$\alpha_0 := p_{\min}/p_{\max} > 0,$$

since the y -marginal is uniform and only $p(\cdot)$ changes in the x -block. Because $\|\Delta y\| \leq \delta/8$ and $\tilde{y} \in Y_{\text{int}}$ (clearance $\geq \delta/2$), the proposed state remains in Y_D at each step. Therefore, in $n := C_{\text{path}}$ applications of PT ,

$$(PT)^n(\theta, T) \geq (1 - C_Y \delta/D) \eta, \quad \eta := (\underline{q} \alpha_0)^{C_{\text{path}}} > 0,$$

uniformly over θ and D .

Since $\bar{P} = \frac{1}{2}(PT) + \frac{1}{2}(TP)$ is a mixture, for any $n \in \mathbb{N}$

$$\bar{P}^n \geq 2^{-n}(PT)^n \quad (\text{entrywise as kernels}).$$

Hence, for all large D and all $\theta \in \Theta_D$,

$$\bar{P}^n(\theta, T) \geq 2^{-n}(PT)^n(\theta, T) \geq 2^{-n}(1 - C_Y\delta/D)\eta.$$

Finally, for any measurable $A \subset \Theta_D$,

$$\bar{P}^n(\theta, A) \geq \bar{P}^n(\theta, T) \frac{\pi_D(A \cap T)}{\pi_D(T)} \geq 2^{-n}\left(1 - C_Y\frac{\delta}{D}\right)\eta \nu(A).$$

Choose D_0 so that $1 - C_Y\delta/D \geq 1/2$ for all $D \geq D_0$, and set

$$\varepsilon_0 := 2^{-n}\frac{1}{2}\eta > 0.$$

Then, for all $D \geq D_0$ and all $\theta \in \Theta_D$,

$$\bar{P}^n(\theta, \cdot) \geq \varepsilon_0 \nu(\cdot),$$

which is a Doeblin minorization uniform in D . Uniform ergodicity and a spectral gap bounded away from 0 (uniformly in D) follow from standard results for reversible Markov chains with a small set minorization (e.g. [Meyn and Tweedie \(2009, Chapter 16.2\)](#), [Roberts and Rosenthal \(2004\)](#)). \square

C.2 Proofs of Main Results

Proposition 2

Proof. Write $Q_P(S, S^c) := \int_S P(\theta, S^c)\pi(d\theta)$, $\Phi_P(S) := Q_P(S, S^c)/\pi(S)$, and $\mathbf{h}_P := \inf_{\pi(S) \leq 1/2} \Phi_P(S)$. By Cheeger's inequality (Lemma 1),

$$\gamma(P) \leq 2\mathbf{h}_P.$$

Fix i with $\pi(A_i) \leq 1/2$ and let $S := A_i$. If $\theta \in A_i$ satisfies $\text{dist}(\theta, \partial A_i) > \delta$, then $B(\theta, \delta) \subset A_i$ and the uniform δ -ball proposal never leaves A_i in one step, hence $P(\theta, A_i^c) = 0$. Therefore

$$Q_P(A_i, A_i^c) = \int_{A_i} P(\theta, A_i^c)\pi(d\theta) \leq \pi(\{\theta \in A_i : \text{dist}(\theta, \partial A_i) \leq \delta\}).$$

Every $\theta \in A_i$ with $\text{dist}(\theta, \partial A_i) \leq \delta$ satisfies $\|\theta - \mu_i\| \geq d_i - \delta$, so by Assumption 1(i),

$$\pi(A_i \cap \{\text{dist}(\cdot, \partial A_i) \leq \delta\}) = w_i \pi_i(\|\theta - \mu_i\| \geq d_i - \delta) \leq w_i c_i e^{-\nu_i(d_i - \delta)}.$$

Hence $\Phi_P(A_i) \leq c_i e^{-\nu_i(d_i - \delta)}$. Minimizing over i with $\pi(A_i) \leq 1/2$ gives $\mathbf{h}_P \leq c_{\max} e^{-\nu_{\min}(d_* - \delta)}$, and Cheeger's inequality yields

$$\gamma(P) \leq 2c_{\max} \exp\{-\nu_{\min}(d_* - \delta)\}.$$

Now consider the reversible kernel $\bar{P} = \frac{1}{2}(PT) + \frac{1}{2}(TP)$. By the state-space decomposition lemma for reversible chains (Lemma 2),

$$\gamma(\bar{P}) \geq \frac{1}{2}\gamma_H \min_{1 \leq i \leq m} \gamma_i,$$

where γ_i is the spectral gap of the restriction of \bar{P} to A_i , and γ_H is the spectral gap of the aggregated chain \bar{P}_H on $\{1, \dots, m\}$ with stationary vector $w_i = \pi(A_i)$.

Assumption 1(iii) gives a Doeblin minorization for P on A_i : there exist $n_0 \in \mathbb{N}$, $\eta_0 > 0$, and a probability m_i supported on $C_i^{\text{int}} \subset A_i$ such that

$$\inf_{\theta \in A_i} P^{n_0}(\theta, \cdot) \geq \eta_0 m_i(\cdot).$$

Because $\bar{P} = \frac{1}{2}(PT) + \frac{1}{2}(TP)$ includes the PT move with probability $1/2$ at each step, the n_0 -step restricted chain of \bar{P} inherits a minorization with constant reduced by at most 2^{-n_0} . Consequently,

$$\gamma_i \geq 1 - (1 - 2^{-n_0} \eta_0)^{1/n_0} \geq \frac{\eta_0}{2n_0} \quad (1 \leq i \leq m),$$

where we used $1 - (1 - x)^{1/n} \geq x/(2n)$ for $x \in (0, 1]$.

For $i \neq j$ and $\theta \in A_i^\circ$, Assumption 1(ii) gives $T(\theta, A_j^{\text{int}}) \geq \varepsilon_2$. If $z \in A_j^{\text{int}}$, then $B(z, \delta) \subset A_j$, so the subsequent δ -ball MH step satisfies $P(z, A_j) = 1$. Hence

$$(PT)(\theta, A_j) \geq \varepsilon_2 \Rightarrow \bar{P}(\theta, A_j) = \frac{1}{2}(PT)(\theta, A_j) + \frac{1}{2}(TP)(\theta, A_j) \geq \frac{1}{2}\varepsilon_2.$$

Integrating over $\theta \in A_i$ and using $\pi_i(A_i^\circ) \geq \varepsilon_1$,

$$\bar{P}_H(i, j) = \frac{1}{\pi(A_i)} \int_{A_i} \bar{P}(\theta, A_j) \pi(d\theta) \geq \frac{1}{\pi(A_i)} \int_{A_i^\circ} \frac{1}{2}\varepsilon_2 \pi(d\theta) = \frac{1}{2}\varepsilon_1\varepsilon_2.$$

Thus all off-diagonal entries of \bar{P}_H are bounded below by $\frac{1}{2}\varepsilon_1\varepsilon_2$, which implies

$$\gamma_H \geq \frac{1}{2} \min \left\{ 1, m \cdot \frac{1}{2}\varepsilon_1\varepsilon_2 \right\} =: c_H(\varepsilon_1, \frac{\varepsilon_2}{2}, m) > 0.$$

Combining the bounds,

$$\gamma(\bar{P}) \geq \frac{1}{2}\gamma_H \min_i \gamma_i \geq \frac{1}{2}c_H(\varepsilon_1, \frac{\varepsilon_2}{2}, m) \cdot \frac{\eta_0}{2n_0} =: c_0 > 0,$$

where c_0 depends only on $(\varepsilon_1, \varepsilon_2, n_0, \eta_0, m)$ and is independent of the separations d_i . \square

Proposition 3

Proof. By Cheeger's inequality, $\gamma(P) \leq 2\mathbf{h}_P$, where $\mathbf{h}_P := \inf_{S: \pi(S) \leq 1/2} \frac{\int_S P(\theta, S^c) \pi(d\theta)}{\pi(S)}$. Fix an index i with $\pi(A_i) \leq 1/2$. Write $d_i = \text{dist}(\mu_i, \partial A_i)$ and, for some $R \in (0, d_i)$ to be chosen later, split

$$C_R := \{\theta \in A_i : \|\theta - \mu_i\| < R\}, \quad S_R := A_i \setminus C_R.$$

Then

$$\int_{A_i} P(\theta, A_i^c) \pi(d\theta) = \int_{C_R} P(\theta, A_i^c) \pi(d\theta) + \int_{S_R} P(\theta, A_i^c) \pi(d\theta) =: I_{\text{core}} + I_{\text{shell}}.$$

By the exponential tail decay,

$$I_{\text{shell}} \leq \pi(S_R) \leq w_i c_i e^{-\nu_i R} \leq c_{\max} e^{-\nu_{\min} R} \pi(A_i).$$

For $\theta \in C_R$, any move into A_i^c must be at least $\Delta_i := d_i - R$ in Euclidean norm to reach the boundary. Let (θ_k, p_k) denote the leapfrog path with step size η , and let θ_ℓ be the proposal after ℓ steps. Standard leapfrog stability on a region with L_s -Lipschitz gradient implies there exists a constant $\kappa = \kappa(L_s, \ell, \eta) \geq 1$ such that

$$\|\theta_\ell - \theta_0\| \leq \kappa \eta \sum_{k=0}^{\ell-1} \|p_{k+1/2}\|.$$

Moreover, $p_{k+1/2}$ remains within a K -factor of p_0 in norm (depending on L_s, ℓ, η). Consequently, there exists $a = a(L_s, \ell, \eta) \in (0, \infty)$ such that

$$\|\theta_\ell - \theta_0\| \leq a \ell \eta \|p_0\|.$$

Therefore, to achieve $\|\theta_\ell - \theta_0\| \geq \Delta_i$ it is necessary that $\|p_0\| \geq \Delta_i / (a \ell \eta)$. Since $p_0 \sim \mathcal{N}(0, \sigma^2 I_n)$,

$$P\left(\|p_0\| \geq \frac{\Delta_i}{a \ell \eta}\right) \leq C_1 \exp\left(-\frac{c_1 \Delta_i^2}{\sigma^2 (\ell \eta)^2}\right),$$

for some $C_1, c_1 > 0$ depending only on n, a . The Metropolis acceptance is ≤ 1 , so

$$P(\theta, A_i^c) \leq C_1 \exp\left(-\frac{c_1 (d_i - R)^2}{\sigma^2 (\ell \eta)^2}\right), \quad \theta \in C_R.$$

Integrating over C_R gives

$$I_{\text{core}} \leq C_1 \exp\left(-\frac{c_1 (d_i - R)^2}{\sigma^2 (\ell \eta)^2}\right) \pi(A_i).$$

Combining the two bounds,

$$\frac{\int_{A_i} P(\theta, A_i^c) \pi(d\theta)}{\pi(A_i)} \leq c_{\max} e^{-\nu_{\min} R} + C_1 \exp\left(-\frac{c_1(d_i - R)^2}{\sigma^2(\ell\eta)^2}\right).$$

Choose $R = d_i/2$. Then

$$\mathbf{h}_P(A_i) \leq c_{\max} \exp\left(-\frac{1}{2}\nu_{\min} d_i\right) + C_1 \exp\left(-\frac{c_1 d_i^2}{4\sigma^2(\ell\eta)^2}\right).$$

Since $\mathbf{h}_P \leq \mathbf{h}_P(A_i)$ for the minimizing i and $d_i \geq d_*$,

$$\mathbf{h}_P \leq C \exp\left(-\min\left\{\frac{1}{2}\nu_{\min} d_*, \frac{cd_*^2}{\sigma^2(\ell\eta)^2}\right\}\right),$$

for suitable $C, c > 0$. Cheeger's inequality yields the stated spectral gap bound. \square

Proposition 4

Proof. (1) Fix $\delta \in (0, \varepsilon_{\min}]$. For each u , let $\Sigma(u) \subset \mathcal{F}(u)$ be the separator from Assumption 2(iii), and write $\mathcal{F}(u)^\pm$ for the two sides. Set $S := \bigcup_{u \in \Phi} \mathcal{F}(u)^-$. By the balance in Assumption 2(iii) and the factorization (iv), $0 < \pi(S) < 1$.

For $\theta \in \Theta$, let $s(\theta) := d_{\mathcal{F}}(\theta, \Sigma(\phi(\theta)))$ be the intrinsic distance to the cut along the fiber. By the uniform coordinates in Assumption 2(v), there exists $a \in (0, \infty)$ such that if $\|z\| \leq as(\theta)$ then the local move $\theta \mapsto \theta + z$ cannot cross $\Sigma(\phi(\theta))$ inside the fiber; equivalently,

$$P(\theta, S^c) \leq \overline{G}(as(\theta)), \quad \theta \in \mathcal{F}(\phi(\theta))^-,$$

where $\overline{G}(t) = \int_{\|z\| > t} g(z) dz$. Average over the minus side with respect to $w_u \mu_u$ and split into the intrinsic δ -collar $\mathcal{N}_\delta(\Sigma(u)) := \{\theta : s(\theta) < \delta\}$ and its complement:

$$\int_{\mathcal{F}(u)^-} P(\theta, S^c) w_u(\theta) \mu_u(d\theta) \leq w_{\max} \mu_u(\mathcal{N}_\delta(\Sigma(u)) \cap \mathcal{F}(u)^-) + \overline{G}(a\delta) w_{\max} \mu_u(\mathcal{F}(u)^- \setminus \mathcal{N}_\delta(\Sigma(u))).$$

By the tubular neighborhood in Assumption 2(iii) and the uniform charts/Jacobian bounds in (v), there exists $C_1 < \infty$ such that

$$\text{Vol}_{\mathcal{F}}(\mathcal{N}_\delta(\Sigma(u))) \leq C_1 \delta \text{Vol}_{\mathcal{F}}(\Sigma(u)), \quad 0 < \delta \leq \varepsilon_{\min}.$$

Since μ_u is the normalized surface measure on $\mathcal{F}(u)$ (Assumption 2(iv)),

$$\mu_u(\mathcal{N}_\delta(\Sigma(u)) \cap \mathcal{F}(u)^-) \leq C_1 \delta \frac{\text{Vol}_{\mathcal{F}}(\Sigma(u))}{\text{Vol}_{\mathcal{F}}(\mathcal{F}(u))}.$$

Again by Assumption 2(v), the normal coordinate spans length comparable to $D(u)$ across the

fiber; a standard tube/coarea estimate yields a constant $C_2 < \infty$ with

$$\frac{\text{Vol}_{\mathcal{F}}(\Sigma(u))}{\text{Vol}_{\mathcal{F}}(\mathcal{F}(u))} \leq \frac{C_2}{D(u)}.$$

Combining,

$$\mu_u(\mathcal{N}_\delta(\Sigma(u)) \cap \mathcal{F}(u)^-) \leq \frac{C_1 C_2}{D(u)} \delta.$$

For the complement, $\mu_u(\mathcal{F}(u)^- \setminus \mathcal{N}_\delta) \leq 1$. Hence there exists $C_3 < \infty$ (absorbing $\overline{G}(a\delta)$ and w_{\max}) such that

$$\int_{\mathcal{F}(u)^-} P(\theta, S^c) w_u(\theta) \mu_u(d\theta) \leq \frac{C_3}{D(u)}.$$

Averaging over u with respect to π and recalling $\pi(S) \in (0, 1)$,

$$h_P := \inf_{A: 0 < \pi(A) \leq 1/2} \frac{1}{\pi(A)} \int_A P(\theta, A^c) \pi(d\theta) \leq \frac{2}{\pi(S)} \int_S P(\theta, S^c) \pi(d\theta) \leq \frac{C_4}{D_{\max}},$$

for a constant $C_4 < \infty$ independent of D_{\max} . By Cheeger's inequality for reversible P , $\gamma(P) \leq 2h_P \leq C/D_{\max}$, proving (1).

(2) Fix a measurable $U_0 \subset \Phi$ with positive Lebesgue measure contained in a compact subset of Φ , and pick $\rho \in (0, \delta/4]$ from Assumption 2(v). Choose $\theta^\dagger \in \Theta$ with $\phi(\theta^\dagger) \in U_0$, and define

$$S := \overline{B}(\theta^\dagger, \rho/8) \subset \phi^{-1}(U_0), \quad \nu(\cdot) := \frac{\text{vol}(\cdot \cap S)}{\text{vol}(S)}.$$

By the small-ball condition in (vi) and the acceptance bound

$$\alpha_0 := \frac{\overline{f} w_{\min}}{\overline{f} w_{\max}}$$

from (iv), there is

$$\kappa_S := c_g \text{vol}(B_d(0, \rho/8)) \alpha_0 > 0$$

such that, for any $\zeta \in S$ and measurable $A \subset \Theta$,

$$P(\zeta, A) \geq \kappa_S \nu(A). \tag{4}$$

From any starting θ , connect $\phi(\theta)$ to $\phi(\theta^\dagger)$ by a straight segment in Φ and cover it by coordinate balls (from (v)) with center spacing at most $\rho/4$. Let n_0 be the number of balls (depending only on ρ and a compact diameter for U_0). At each local RWM step, the probability to reach the next ball is at least

$$q_0 := c_g \text{vol}(B_d(0, \rho/4)),$$

and the Metropolis acceptance is at least α_0 . Hence after n_0 applications of the pair (T, P) , i.e., for

$(PT)^{n_0}$, we have

$$(PT)^{n_0}(\theta, \phi^{-1}(U_0)) \geq \eta_0, \quad \eta_0 := (q_0 \alpha_0)^{n_0} > 0,$$

since each T refresh leaves $u = \phi(\cdot)$ unchanged.

Apply one more pair (T, P) . The refresh T redistributes along the current fiber $\mathcal{F}(u)$ according to w_u ; by the bounds in (iv) and the uniform chart radius ρ in (v), there exists $\kappa_T > 0$ such that, whenever $u \in U_0$,

$$T(\cdot, B_{\mathcal{F}}(\theta^\dagger, \rho/8) \cap \mathcal{F}(u)) \geq \frac{w_{\min}}{w_{\max}} \mu_u(B_{\mathcal{F}}(\theta^\dagger, \rho/8) \cap \mathcal{F}(u)) \geq \kappa_T.$$

From any point in S , the subsequent P -step satisfies (4). Therefore, with $n := n_0 + 1$,

$$(PT)^n(\theta, A) \geq \eta_0 \kappa_T \kappa_S \nu(A).$$

Finally, pass from (PT) to the mixture \bar{P} : since $\bar{P} = \frac{1}{2}(PT) + \frac{1}{2}(TP)$ is a mixture, for any $n \in \mathbb{N}$,

$$\bar{P}^n \geq 2^{-n}(PT)^n \quad (\text{entrywise as kernels}).$$

Hence,

$$\bar{P}^n(\theta, A) \geq 2^{-n}(PT)^n(\theta, A) \geq \underbrace{2^{-n} \eta_0 \kappa_T \kappa_S}_{\varepsilon_0} \nu(A).$$

Since ν is supported on the fixed set $S \subset T_0 := \phi^{-1}(U_0)$ and $\pi(T_0) > 0$, this gives the claimed Doeblin minorization. Uniform ergodicity follows, and for the reversible \bar{P} we obtain

$$\gamma(\bar{P}) \geq 1 - (1 - \varepsilon_0)^{1/n},$$

which is strictly positive and independent of D_{\max} . □

D Example 1 Details

Consider the state space $\{(0,0), (0,1), (1,0), (1,1)\}$ with target

$$\pi(0,0) = \pi(1,1) = a, \quad \pi(0,1) = \pi(1,0) = \frac{1-2a}{2}, \quad a \in (0, \frac{1}{2}).$$

Let P_1 update $\theta_1 \mid \theta_2$ and P_2 update $\theta_2 \mid \theta_1$:

$$P_1 = \begin{pmatrix} 2a & 0 & 1-2a & 0 \\ 0 & 1-2a & 0 & 2a \\ 2a & 0 & 1-2a & 0 \\ 0 & 1-2a & 0 & 2a \end{pmatrix}, \quad P_2 = \begin{pmatrix} 2a & 1-2a & 0 & 0 \\ 2a & 1-2a & 0 & 0 \\ 0 & 0 & 1-2a & 2a \\ 0 & 0 & 1-2a & 2a \end{pmatrix}.$$

The systematic Gibbs kernel, as illustrated in the main text, updates both coordinates each iteration is

$$P_{\text{sys}} = P_1 P_2.$$

This kernel is not π -reversible, so the standard Dirichlet-form characterization of the spectral gap does not apply.

The random-scan Gibbs kernel that updates a single, uniformly chosen coordinate is

$$P_{\text{RS}} = \frac{1}{2}P_1 + \frac{1}{2}P_2,$$

which is π -reversible as a convex combination of π -reversible single-site updates.

Introduce the teleport kernel

$$T = \begin{pmatrix} \frac{1}{2} & 0 & 0 & \frac{1}{2} \\ 0 & 1 & 0 & 0 \\ 0 & 0 & 1 & 0 \\ \frac{1}{2} & 0 & 0 & \frac{1}{2} \end{pmatrix},$$

which swaps $(0, 0)$ and $(1, 1)$ and leaves $(0, 1)$ and $(1, 0)$ fixed. T is π -reversible. Given any base P , define the randomized-order composition

$$\bar{P} = \frac{1}{2}(PT) + \frac{1}{2}(TP).$$

We consider two variants: \bar{P}_{RS} with $P = P_{\text{RS}}$ and \bar{P}_{sys} with $P = P_{\text{sys}}$.

Figure 25 plots the spectral gap γ as a function of a for the three kernels. The random-scan Gibbs gap (black) shrinks toward zero as $a \rightarrow \frac{1}{2}$, reflecting poor movement between the two high-mass corners. Both randomized-order variants (blue for \bar{P}_{RS} , red dashed for \bar{P}_{sys}) substantially enlarge the gap, because the teleport step explicitly bridges the two modes. The reversible \bar{P}_{RS} provides a clean, principled improvement, while \bar{P}_{sys} also accelerates mixing in this toy example.

The proof can be found in the Appendix C.

E Empirical Implementation Details

In our application, we estimate a structural VMA with unit-impact normalization on lag 1. The parameter vector stacks $\Theta = \{\Theta_\ell\}_{\ell=0}^q \in \mathbb{R}^{n \times n \times (q+1)}$ and $\log \sigma \in \mathbb{R}^n$, where $n = 3$ and $q = 16$. This yields a total of 153 free parameters under the unit-impact restriction.

Identification is most transparent in the frequency domain. Let $H(z) = \sum_{\ell=0}^q \Theta_\ell z^\ell$, set $\Psi(z) = H(z) \text{diag}(\sigma)$, and write the spectral density as

$$f_{yy}(\omega) = \Psi(e^{-i\omega}) \Psi(e^{-i\omega})^*.$$

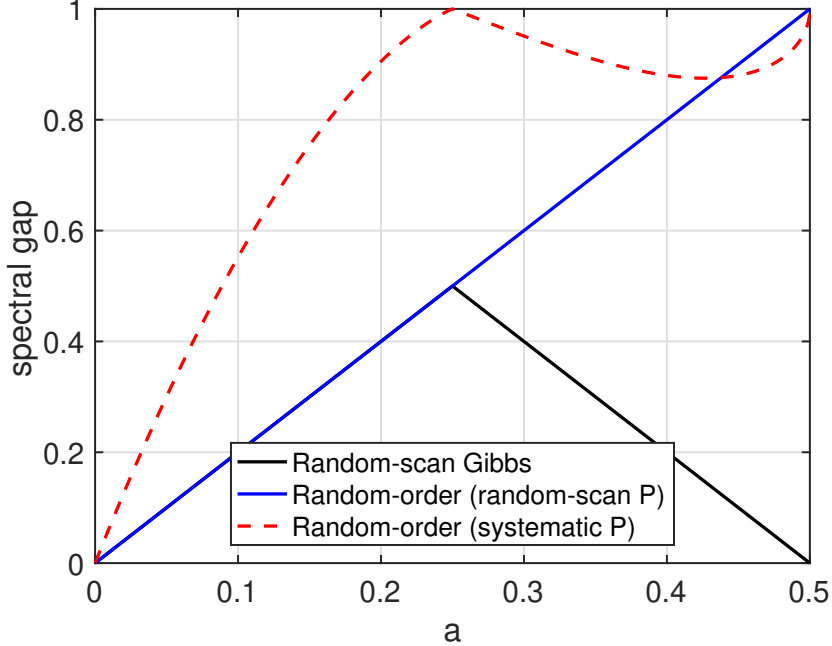


Figure 25: Spectral gap for Random-scan Gibbs, randomized-order with random-scan base, and randomized-order with systematic base.

Two parameterizations $\theta = (\Theta, \sigma)$ and $\theta' = (\Theta', \sigma')$ are observationally equivalent if and only if $f_{yy}(\omega) = f'_{yy}(\omega)$ for all $\omega \in [-\pi, \pi]$. A constructive characterization is: (Θ', σ') lies in the identified set of (Θ, σ) if and only if there exist an orthogonal matrix $Q \in \mathcal{O}(n)$ and a finite sequence of matrix Blaschke factors $R(\gamma_k, z)$ such that

$$\Psi'(z) = \Psi(z) Q R(\gamma_1, z)^{-1} \cdots R(\gamma_b, z)^{-1}, \quad R(\gamma, e^{-i\omega}) R(\gamma, e^{-i\omega})^* = I_n \quad \forall \omega,$$

which preserves f_{yy} pointwise in frequency. Conversely, any two observationally equivalent parameterizations can be connected by such a finite sequence of orthogonal rotations and Blaschke flips; see [Plagborg-Møller \(2019, Prop. 2\)](#), building on [Lippi and Reichlin \(1994\)](#).

Initialization follows [Plagborg-Møller \(2019\)](#). We compute the sample ACF up to lag q , obtain (B, V) by the innovations algorithm, form $\Psi(z) = B(z)V^{1/2}$, and map to (Θ, σ) under the unit-impact normalization. Among observationally equivalent representatives we select the one maximizing the prior density; when the prior is flat along $K(\theta)$ this reduces to choosing an arbitrary representative. With an informative prior we optionally perform a short convex-combination sweep toward the prior mean and keep the posterior maximizer.

Sampling proceeds with a mixture identification-aware kernel as discussed in [Appendix B.2.3](#):

$$\tilde{P}_H = \varepsilon T + (1 - \varepsilon) P,$$

where P is a baseline local kernel (RWM or NUTS) and $T(\theta, \cdot)$ is the conditional teleport on $K(\theta)$

as in (1). Since both P and T are π -reversible, the mixture \tilde{P}_H is also π -reversible.

Direct draws from T are infeasible when the prior is not flat on $K(\theta)$, so we implement T via a multiple-try Metropolis (MTM, see Appendix B.2.1) move restricted to the observationally equivalent set. With probability $\varepsilon = \frac{1}{501}$ ¹⁶ a teleport is attempted. Forward candidates are generated by Haar orthogonal rotations (including signed permutations), weighted by their prior density (the likelihood cancels on $K(\theta)$). One candidate is selected proportional to its weight. A reverse candidate set is drawn around the selected point, and the move is accepted using the standard MTM ratio (sum of backward weights over sum of forward weights). This yields an exact T -invariant refresh and hence a valid π -reversible mixture \tilde{P}_H .

As discussed in Section 2.2, our teleportation kernel T only needs to be supported on a π -preserving partition of the state space, i.e., teleport moves can be restricted to any nontrivial subset $K'(\theta)$ of the identified set $K(\theta)$ for a valid identification-aware kernel. In our SVMA application, we restrict teleportation to Haar orthogonal rotations and do not implement Blaschke flips in the empirical sampler. While Blaschke flips are part of the full characterization of $K(\theta)$, in high-dimensional SVMA they require repeated root-finding and re-normalization across lags and tend to push parameters toward the unit circle, which degrades numerical conditioning of the objective and its gradients. By contrast, Haar rotations alone already generate a rich family of observationally equivalent parameterizations and satisfy the theoretical conditions for a valid T on a subset $K'(\theta) \subseteq K(\theta)$. Local moves in the baseline kernel P may still cross invertibility boundaries when supported by the posterior, but the identification-aware refresh focuses computational effort on numerically stable regions of the identified set.

For the baseline NUTS we use a consistent diagonal mass matrix M in both the leapfrog integrator and the no-U-turn stopping rule: we draw $p \sim \mathcal{N}(0, M)$, set the kinetic energy to $\frac{1}{2}p^\top M^{-1}p$, update $\theta \leftarrow \theta + \varepsilon M^{-1}p$, and optionally adapt M using running variances with mild shrinkage and upper/lower caps. IA-RWM uses blocked Gaussian proposals for (Θ, σ) with Robbins-Monro scale adaptation. IA-NUTS augments NUTS with periodic teleports: after accepted refreshes we briefly re-tune the step size and blend a locally estimated diagonal mass back into M .

References

An, Sungbae and Frank Schorfheide, “Bayesian analysis of DSGE models,” *Econometric reviews*, 2007, 26 (2-4), 113–172.

Bacchicocchi, Emanuele and Toru Kitagawa, “Locally-but not globally-identified SVARs,” *arXiv preprint arXiv:2504.01441*, 2025.

¹⁶This corresponds to an average frequency of one teleportation for every 500 local updates, balancing the cost of global moves with mixing efficiency.

Baumeister, Christiane and James D Hamilton, "Sign restrictions, structural vector autoregressions, and useful prior information," *Econometrica*, 2015, 83 (5), 1963–1999.

Betancourt, Michael, "A conceptual introduction to Hamiltonian Monte Carlo," *arXiv preprint arXiv:1701.02434*, 2017.

Borell, Christer, "Convex measures on locally convex spaces," *Arkiv för matematik*, 1974, 12 (1), 239–252.

Chen, Xiaohong, Timothy M Christensen, and Elie Tamer, "Monte Carlo confidence sets for identified sets," *Econometrica*, 2018, 86 (6), 1965–2018.

Chernozhukov, Victor and Han Hong, "An MCMC approach to classical estimation," *Journal of econometrics*, 2003, 115 (2), 293–346.

Chib, Siddhartha and Edward Greenberg, "Markov chain Monte Carlo simulation methods in econometrics," *Econometric theory*, 1996, 12 (3), 409–431.

Chopin, Nicolas, "Central Limit Theorem for Sequential Monte Carlo Methods and Its Application to Bayesian Inference," *Annals of Statistics*, 2004, pp. 2385–2411.

Diaconis, Persi and Daniel Stroock, "Geometric bounds for eigenvalues of Markov chains," *The Annals of Applied Probability*, 1991, pp. 36–61.

Diebold, Francis X and Atsushi Inoue, "Long memory and regime switching," *Journal of econometrics*, 2001, 105 (1), 131–159.

Durham, Garland and John Geweke, "Adaptive sequential posterior simulators for massively parallel computing environments," in "Bayesian model comparison," Emerald Group Publishing Limited, 2014, pp. 1–44.

Durmus, Alain, Eric Moulines, and Eero Saksman, "On the convergence of hamiltonian monte carlo," *arXiv preprint arXiv:1705.00166*, 2017.

—, **Éric Moulines, and Eero Saksman**, "Irreducibility and geometric ergodicity of Hamiltonian Monte Carlo," *The Annals of Statistics*, 2020, 48 (6), 3545–3564.

Flury, Thomas and Neil Shephard, "Bayesian inference based only on simulated likelihood: particle filter analysis of dynamic economic models," *Econometric Theory*, 2011, 27 (5), 933–956.

Frühwirth-Schnatter, Sylvia, *Finite mixture and Markov switching models*, Vol. 425, Springer, 2006.

Gelman, Andrew, "What do I think about identifiability in Bayesian inference?," 2014.

—, **Walter R Gilks, and Gareth O Roberts**, “Weak convergence and optimal scaling of random walk Metropolis algorithms,” *The Annals of Applied Probability*, 1997, 7 (1), 110–120.

Geweke, John, “Interpretation and inference in mixture models: Simple MCMC works,” *Computational Statistics & Data Analysis*, 2007, 51 (7), 3529–3550.

Giacomini, Raffaella and Toru Kitagawa, “Robust Bayesian inference for set-identified models,” *Econometrica*, 2021, 89 (4), 1519–1556.

Guan, Yongtao and Stephen M Krone, “Small-world MCMC and convergence to multi-modal distributions: From slow mixing to fast mixing,” *Ann. Appl. Probab.*, 2007, 17 (1), 284–304.

Herbst, Edward and Frank Schorfheide, “Sequential Monte Carlo sampling for DSGE models,” *Journal of Applied Econometrics*, 2014, 29 (7), 1073–1098.

Hoffman, Matthew D, Andrew Gelman et al., “The No-U-Turn sampler: adaptively setting path lengths in Hamiltonian Monte Carlo.,” *J. Mach. Learn. Res.*, 2014, 15 (1), 1593–1623.

Huggins, Jonathan H and Daniel M Roy, “Convergence of sequential Monte Carlo based sampling methods,” *arXiv preprint arXiv:1503.00966*, 2015.

Jones, Galin L, “On the Markov chain central limit theorem,” *Probability Surveys*, 2004, 1, 299–320.

Kannan, Ravi, László Lovász, and Miklós Simonovits, “Random walks and an $o^*(n^5)$ volume algorithm for convex bodies,” *Random Structures & Algorithms*, 1997, 11 (1), 1–50.

Kline, Brendan and Elie Tamer, “Bayesian inference in a class of partially identified models,” *Quantitative Economics*, 2016, 7 (2), 329–366.

Kuang, Yizhou, “Bayesian Sensitivity Analysis for Set-identified Structural Models,” 2025.

Lawler, Gregory F and Alan D Sokal, “Bounds on the L^2 spectrum for Markov chains and Markov processes: a generalization of Cheeger’s inequality,” *Transactions of the American mathematical society*, 1988, 309 (2), 557–580.

Lee, J., *Introduction to Smooth Manifolds* Graduate Texts in Mathematics, Springer New York, 2012.

Lindley, Dennis Victor, *Bayesian statistics: A review*, SIAM, 1972.

Lippi, Marco and Lucrezia Reichlin, “VAR analysis, nonfundamental representations, Blaschke matrices,” *Journal of Econometrics*, 1994, 63 (1), 307–325.

Liu, Jun S, Faming Liang, and Wing Hung Wong, “The multiple-try method and local optimization in Metropolis sampling,” *Journal of the American Statistical Association*, 2000, 95 (449), 121–134.

Madras, Neal and Dana Randall, "Markov chain decomposition for convergence rate analysis," *Annals of Applied Probability*, 2002, pp. 581–606.

Mangoubi, Oren and Aaron Smith, "Mixing of Hamiltonian Monte Carlo on strongly log-concave distributions: Continuous dynamics," *The Annals of Applied Probability*, 2021, 31 (5), 2019–2045.

—, **Natesh S Pillai, and Aaron Smith**, "Does Hamiltonian Monte Carlo mix faster than a random walk on multimodal densities?," *arXiv preprint arXiv:1808.03230*, 2018.

Meager, Rachael, "Aggregating distributional treatment effects: A Bayesian hierarchical analysis of the microcredit literature," *American Economic Review*, 2022, 112 (6), 1818–1847.

Mengersen, Kerrie L and Richard L Tweedie, "Rates of convergence of the Hastings and Metropolis algorithms," *The Annals of Statistics*, 1996, 24 (1), 101–121.

Meyn, Sean P and Richard L Tweedie, *Markov chains and stochastic stability*, Springer Science & Business Media, 2009.

Moral, Pierre Del, Arnaud Doucet, and Ajay Jasra, "An adaptive sequential Monte Carlo method for approximate Bayesian computation," *Statistics and computing*, 2012, 22, 1009–1020.

Müller, Ulrich and Andriy Norets, "Locally Robust Efficient Bayesian Inference," Technical Report 2023.

Neal, Radford M, "MCMC using Hamiltonian dynamics," *Handbook of markov chain monte carlo*, 2011, 2 (11), 2.

Plagborg-Møller, Mikkel, "Bayesian inference on structural impulse response functions," *Quantitative Economics*, 2019, 10 (1), 145–184.

Pompe, Emilia, Chris Holmes, and Krzysztof Łatuszyński, "A FRAMEWORK FOR ADAPTIVE MCMC TARGETING MULTIMODAL DISTRIBUTIONS," *The Annals of Statistics*, 2020, 48 (5), 2930–2952.

Roberts, Gareth O and Jeffrey S Rosenthal, "General state space Markov chains and MCMC algorithms," *Probability Surveys*, 2004, 1, 20–71.

— and **Richard L Tweedie**, "Geometric convergence and central limit theorems for multidimensional Hastings and Metropolis algorithms," *Biometrika*, 1996, 83 (1), 95–110.

Rubio-Ramirez, Juan F, Daniel F Waggoner, and Tao Zha, "Structural vector autoregressions: Theory of identification and algorithms for inference," *The Review of Economic Studies*, 2010, 77 (2), 665–696.

Sims, Eric R, "News, non-invertibility, and structural VARs," in "DSGE Models in Macroeconomics: Estimation, Evaluation, and New Developments," Emerald Group Publishing Limited, 2012, pp. 81–135.

Uhlig, Harald, "What are the effects of monetary policy on output? Results from an agnostic identification procedure," *Journal of Monetary Economics*, 2005, 52 (2), 381–419.

Vishwanath, Siddharth and Hyungsuk Tak, "Repelling-Attracting Hamiltonian Monte Carlo," *arXiv preprint arXiv:2403.04607*, 2024.

Woodard, Dawn B, Scott C Schmidler, and Mark Huber, "Sufficient conditions for torpid mixing of parallel and simulated tempering," *Electronic Journal of Probability [electronic only]*, 2009, 14, 780–804.

Zhou, Qing, "Multi-domain sampling with applications to structural inference of Bayesian networks," *Journal of the American Statistical Association*, 2011, 106 (496), 1317–1330.